NUREG/CR–6249
ORNL/TM–12777

Unirradiated Material Properties of Midland Weld WF–70

Prepared by
D. E. McCabe, R. K. Nanstad, S. K. Iskander, R. L. Swain

Oak Ridge National Laboratory

Prepared for
U.S. Nuclear Regulatory Commission

NUREG/CR-6249
ORNL/TM-12777

Unirradiated Material Properties of Midland Weld WF-70

Manuscript Completed: June 1994
Date Published: October 1994

Prepared by
D. E. McCabe, R. K. Nanstad, S. K. Iskander, R. L. Swain

Oak Ridge National Laboratory
Managed by Martin Marietta Energy Systems, Inc.

Oak Ridge National Laboratory
Oak Ridge, TN 37831

Prepared for
Division of Engineering
Office of Nuclear Regulatory Research
U.S. Nuclear Regulatory Commission
Washington, DC 20555-0001
NRC FIN L1098
Under Contract No. DE-AC05-84OR21400

Abstract

Weld metal, designated WF-70, taken from the nozzle course and beltline welds of the Midland Reactor, Unit 1, has been given a preliminary evaluation using the conventional Charpy V-notch (CVN), drop-weight (DWT), and chemical analyses. These tests indicated essentially identical fracture toughness at both locations, but there was a significant difference in copper content, nominally 0.25% versus 0.40%. Because the objective of this study was to evaluate the before-and-after irradiation properties, these are regarded as different materials.

This report summarizes material characterization results and presents the results of fracture mechanics tests on the unirradiated material to establish baseline transition temperature and J-R curves. Tensile properties were also determined.

The fracture mechanics transition temperature by K_{JC} evaluations indicated that the nozzle course weld had a 27°C (49°F) higher transition temperature than the betline weld. The DWT nil-ductility temperature (NDT) was essentially the same for both: -50 ± 10°C (-58 ± 18°F). CVN transition temperature curves, although quite variable among various positions along the girth and through the thickness of the Midland vessel, covered about the same range for both nozzle and beltline welds. The upper-shelf energy (USE) was 89 J (65 ft-lb) in both cases.

Reference nil-ductility temperatures, RT_{NDT}, determined from CVN transition curves [RT_{NDT} method specific to low USE materials] varied from -20 to +37°C (-4 to 99°F) at various locations in the beltline weld. Reference temperatures using a fracture mechanics-based transition temperature model were -60°C (-76°F) for the beltline weld and -33°C (-27°F) for the nozzle weld.

Tensile tests indicated the nozzle weld had higher strength than the beltline weld.

J-R curves were developed at 21, 150, and 288°C (70, 302, and 550°F). The J-R curve toughness decreased with increased test temperature, as expected. A multivariable model of Eason et al. was used to predict J-R curves from CVN USE. The predicted J-R curves matched the experimental J-R curves reasonably well. The test temperature effect between 288 and 150°C (550 and 302°C) was effectively predicted. However, room-temperature J-R curve prediction was not very good. Despite the fact that the nozzle and beltline weld had similar CVN USEs, the nozzle course weld had consistently lower J-R curve toughness than the beltline weld.

Crack-arrest tests were conducted, but the specimens failed to develop American Society for Testing and Materials valid data in all but one test. Insufficient remaining ligament at crack arrest was almost always the problem. The invalid K_a values were all above the American Society of Mechanical Engineers (ASME) K_{IR} curve if the CVN determined range of RT_{NDT} values from -20 to 37°C (-4 to 98.6°F) are used to position the curve. The K_{Ia} data are exactly bounded if the DWT NDT of -50°C (-58°F) is used to position the curve. A proposed method of establishing a mean K_{Ia} curve on data obtained from instrumented CVN test records was tried. This method suggested a 10°C (18°F) transition temperature difference (at the 100-MPa$\sqrt{x}$m toughness level) between static and dynamic tests. The experimental (invalid) K_a data indicated a 50°C (90°F) difference. The ASME K_{IC}/K_{Ia} lower bound curves suggest that there should be approximately a 35°C (63°F) difference. More experimentation and test method development are recommended.

Five experimental objectives to be accomplished from the testing of irradiated materials were identified. One of the more important objectives is to improve the precision of transition temperature shift and to identify any curve shape changes after irradiation, concentrating on utilizing data from small surveillance capsule size specimens.

Contents

Figures

Tables

Acknowledgments

The authors gratefully acknowledge the contributions of J. J. Henry, Jr., for specimen sampling and machining and J. L. Bishop for preparation of the draft manuscript; S. M. Wilson and S. E. Humphrey for final report preparation; K. Spence for editing; and G. R. Carter for quality assurance review. The technical reviews by F. M. Haggag and W. R. Corwin are also appreciated.

Previous Reports in Series

The work here was performed at Oak Ridge National Laboratory under the Heavy-Section Steel Irradiation (HSSI) Program, W. R. Corwin, Program Manager. The HSSI Program is sponsored by the Office of Nuclear Regulatory Research of the U.S. Nuclear Regulatory Commission. The technical monitor is M. E. Mayfield.

This report is designated HSSI Report 10. Reports in this series are listed below:

1. F. M. Haggag, W. R. Corwin, and R. K. Nanstad, Martin Marietta Energy Systems, Inc., Oak Ridge Natl. Lab., Oak Ridge, Tenn., *Irradiation Effects on Strength and Toughness of Three-Wire Series-Arc Stainless Steel Weld Overlay Cladding*, NUREG/CR-5511 (ORNL/TM-11439), February 1990.

2. L. F. Miller, C. A. Baldwin, F. W. Stallman, and F. B. K. Kam, Martin Marietta Energy Systems, Inc., Oak Ridge Natl. Lab., Oak Ridge, Tenn., *Neutron Exposure Parameters for the Metallurgical Test Specimens in the Sixth Heavy-Section Steel Irradiation Series*, NUREG/CR-5409 (ORNL/TM-11267), March 1990.

3. S. K. Iskander, W. R. Corwin, and R. K. Nanstad, Martin Marietta Energy Systems, Inc., Oak Ridge Natl. Lab., Oak Ridge, Tenn., *Results of Crack-Arrest Tests on Two Irradiated High-Copper Welds*, NUREG/CR-5584 (ORNL/TM-11575), December 1990.

4. R. K. Nanstad and R. G. Berggren, Martin Marietta Energy Systems, Inc., Oak Ridge Natl. Lab., *Irradiation Effects on Charpy Impact and Tensile Properties of Low Upper-Shelf Welds, HSSI Series 2 and 3*, USNRC Report NUREG/CR-5696 (ORNL/TM-11804), August 1991.

5. R. E. Stoller, Martin Marietta Energy Systems, Inc., Oak Ridge Natl. Lab., *Modeling the Influence of Irradiation Temperature and Displacement Rate on Radiation-Induced Hardening in Ferritic Steels*, USNRC Report NUREG/CR-5859 (ORNL/TM-12073), August 1992.

6. R. K. Nanstad, D. E. McCabe, and R. L. Swain, Martin Marietta Energy Systems, Inc., Oak Ridge Natl. Lab., *Chemical Composition and RT_{NDT} Determinations For Midland Weld WF-70*, USNRC Report NUREG/CR-5914 (ORNL/TM-12157), to be published.

7. R. K. Nanstad, F. M. Haggag, D. E. McCabe, S. K. Iskander, K. O. Bowman, and B. H. Menke, Martin Marietta Energy Systems, Inc., Oak Ridge Natl. Lab., *Irradiation Effects on Fracture Toughness of Two High-Copper Submerged-Arc Welds, HSSI Series 5*, USNRC Report NUREG/CR-5913 (ORNL/TM-12156/V1), October 1992.

8. S. K. Iskander, W. R. Corwin, and R. K. Nanstad, Martin Marietta Energy Systems, Inc., Oak Ridge Natl. Lab., *Crack-Arrest Tests on Two Irradiated High-Copper Welds*, USNRC Report NUREG/CR-6139 (ORNL/TM-12513), March 1994.

9. R. E. Stoller, Martin Marietta Energy Systems, Inc., Oak Ridge Natl. Lab., *A Comparison of the Relative Importance of Copper Precipitates and Point Defect Clusters in Reactor Pressure Vessel Embrittlement*, USNRC Report NUREG/CR-6231 (ORNL-6811), June 1994.

10. This report.

The HSSI Program includes both follow-on and the direct continuation of work that was performed under the Heavy-Section Steel Technology (HSST) Program. The HSST reports related to irradiation effects in pressure vessel materials and those containing unirradiated properties of materials used in HSSI and HSST irradiation programs are tabulated below as a convenience to the reader.

C. E. Childress, Union Carbide Corp. Nuclear Div., Oak Ridge Natl. Lab., Oak Ridge, Tenn., *Fabrication History of the First Two 12-in.-Thick A-533 Grade B, Class 1 Steel Plates of the Heavy Section Steel Technology Program*, ORNL-4313, February 1969.

T. R. Mager and F. O. Thomas, Westinghouse Electric Corporation, PWR Systems Division, Pittsburgh, Pa., *Evaluation by Linear Elastic Fracture Mechanics of Radiation Damage to Pressure Vessel Steels*, WCAP-7328 (Rev.), October 1969.

P. N. Randall, TRW Systems Group, Redondo Beach, Calif., *Gross Strain Measure of Fracture Toughness of Steels*, HSSTP-TR-3, Nov. 1, 1969.

L. W. Loechel, Martin Marietta Corporation, Denver, Colo., *The Effect of Testing Variables on the Transition Temperature in Steel*, MCR-69-189, Nov. 20, 1969.

W. O. Shabbits, W. H. Pryle, and E. T. Wessel, Westinghouse Electric Corporation, PWR Systems Division, Pittsburgh, Pa., *Heavy-Section Fracture Toughness Properties of A533 Grade B Class 1 Steel Plate and Submerged Arc Weldment*, WCAP-7414, December 1969.

C. E. Childress, Union Carbide Corp. Nuclear Div., Oak Ridge Natl. Lab., Oak Ridge, Tenn., *Fabrication History of the Third and Fourth ASTM A-533 Steel Plates of the Heavy Section Steel Technology Program*, ORNL-4313-2, February 1970.

P. B. Crosley and E. J. Ripling, Materials Research Laboratory, Inc., Glenwood, Ill., *Crack Arrest Fracture Toughness of A533 Grade B Class 1 Pressure Vessel Steel*, HSSTP-TR-8, March 1970.

F. J. Loss, Naval Research Laboratory, Washington, D.C., *Dynamic Tear Test Investigations of the Fracture Toughness of Thick-Section Steel*, NRL-7056, May 14, 1970.

T. R. Mager, Westinghouse Electric Corporation, PWR Systems Div., Pittsburgh, Pa., *Post-Irradiation Testing of 2T Compact Tension Specimens*, WCAP-7561, August 1970.

F. J. Witt and R. G. Berggren, Union Carbide Corp. Nuclear Div., Oak Ridge Natl. Lab., Oak Ridge, Tenn., *Size Effects and Energy Disposition in Impact Specimen Testing of ASTM A533 Grade B Steel*, ORNL/TM-3030, August 1970.

D. A. Canonico, Union Carbide Corp. Nuclear Div., Oak Ridge Natl. Lab., Oak Ridge, Tenn., *Transition Temperature Considerations for Thick-Wall Nuclear Pressure Vessels*, ORNL/TM-3114, October 1970.

T. R. Mager, Westinghouse Electric Corporation, PWR Systems Div., Pittsburgh, Pa., *Fracture Toughness Characterization Study of A533, Grade B, Class 1 Steel*, WCAP-7578, October 1970.

W. O. Shabbits, Westinghouse Electric Corp., PWR Systems Div., Pittsburgh, Pa., *Dynamic Fracture Toughness Properties of Heavy Section A533 Grade B Class 1 Steel Plate*, WCAP-7623, December 1970.

C. E. Childress, Union Carbide Corp. Nuclear Div., Oak Ridge Natl. Lab., Oak Ridge, Tenn., *Fabrication Procedures and Acceptance Data for ASTM A-533 Welds and a 10-in.-Thick ASTM A-543 Plate of the Heavy Section Steel Technology Program*, ORNL-TM-4313-3, January 1971.

D. A. Canonico and R. G. Berggren, Union Carbide Corp. Nuclear Div., Oak Ridge Natl. Lab., Oak Ridge, Tenn., *Tensile and Impact Properties of Thick-Section Plate and Weldments*, ORNL/TM-3211, January 1971.

C. W. Hunter and J. A. Williams, Hanford Eng. Dev. Lab., Richland, Wash., *Fracture and Tensile Behavior of Neutron-Irradiated A533-B Pressure Vessel Steel*, HEDL-TME-71-76, February 6, 1971.

C. E. Childress, Union Carbide Corp. Nuclear Div., Oak Ridge Natl. Lab., Oak Ridge, Tenn., *Manual for ASTM A533 Grade B Class 1 Steel (HSST Plate 03) Provided to the International Atomic Energy Agency*, ORNL/TM-3193, March 1971.

P. N. Randall, TRW Systems Group, Redondo Beach, Calif., *Gross Strain Crack Tolerance of A533-B Steel*, HSSTP-TR-14, May 1, 1971.

C. L. Segaser, Union Carbide Corp. Nuclear Div., Oak Ridge Natl. Lab., Oak Ridge, Tenn., *Feasibility Study, Irradiation of Heavy-Section Steel Specimens in the South Test Facility of the Oak Ridge Research Reactor*, ORNL/TM-3234, May 1971.

H. T. Corten and R. H. Sailors, University of Illinois, Urbana, Ill., *Relationship Between Material Fracture Toughness Using Fracture Mechanics and Transition Temperature Tests*, T&AM Report 346, August 1, 1971.

L. A. James and J. A. Williams, Hanford Eng. Dev. Lab., Richland, Wash., *Heavy Section Steel Technology Program Technical Report No. 21, The Effect of Temperature and Neutron Irradiation Upon the Fatigue-Crack Propagation Behavior of ASTM A533 Grade B, Class 1 Steel*, HEDL-TME 72-132, September 1972.

P. B. Crosley and E. J. Ripling, Materials Research Laboratory, Inc., Glenwood, Ill., *Crack Arrest in an Increasing K-Field*, HSSTP-TR-27, January 1973.

W. J. Stelzman and R. G. Berggren, Union Carbide Corp. Nuclear Div., Oak Ridge Natl. Lab., Oak Ridge, Tenn., *Radiation Strengthening and Embrittlement in Heavy-Section Steel Plates and Welds*, ORNL-4871, June 1973.

J. M. Steichen and J. A. Williams, Hanford Eng. Dev. Lab., Richland, Wash., *High Strain Rate Tensile Properties of Irradiated ASTM A533 Grade B Class 1 Pressure Vessel Steel*, HEDL-TME 73-74, July 1973.

J. A. Williams, Hanford Eng. Dev. Lab., Richland, Wash., *The Irradiation and Temperature Dependence of Tensile and Fracture Properties of ASTM A533, Grade B, Class 1 Steel Plate and Weldment*, HEDL-TME 73-75, August 1973.

J. A. Williams, Hanford Eng. Dev. Lab., Richland, Wash., *Some Comments Related to the Effect of Rate on the Fracture Toughness of Irradiated ASTM A553-B Steel Based on Yield Strength Behavior*, HEDL-SA 797, December 1974.

J. A. Williams, Hanford Eng. Dev. Lab., Richland, Wash., *The Irradiated Fracture Toughness of ASTM A533, Grade B, Class 1 Steel Measured with a Four-Inch-Thick Compact Tension Specimen*, HEDL-TME 75-10, January 1975.

J. G. Merkle, G. D. Whitman, and R. H. Bryan, Union Carbide Corp. Nuclear Div., Oak Ridge Natl. Lab., Oak Ridge, Tenn., *An Evaluation of the HSST Program Intermediate Pressure Vessel Tests in Terms of Light-Water-Reactor Pressure Vessel Safety*, ORNL/TM-5090, November 1975.

J. A. Davidson, L. J. Ceschini, R. P. Shogan, and G. V. Rao, Westinghouse Electric Corporation, Pittsburgh, Pa., *The Irradiated Dynamic Fracture Toughness of ASTM A533, Grade B, Class 1 Steel Plate and Submerged Arc Weldment*, WCAP-8775, October 1976.

J. A. Williams, Hanford Eng. Dev. Lab., Richland, Wash., *Tensile Properties of Irradiated and Unirradiated Welds of A533 Steel Plate and A508 Forgings*, NUREG/CR-1158 (ORNL/SUB-79/50917/2), July 1979.

J. A. Williams, Hanford Eng. Dev. Lab., Richland, Wash., *The Ductile Fracture Toughness of Heavy Section Steel Plate*, NUREG/CR-0859, September 1979.

K. W. Carlson and J. A. Williams, Hanford Eng. Dev. Lab., Richland, Wash., *The Effect of Crack Length and Side Grooves on the Ductile Fracture Toughness Properties of ASTM A533 Steel*, NUREG/CR-1171 (ORNL/SUB-79/50917/3), October 1979.

G. A. Clarke, Westinghouse Electric Corp., Pittsburgh, Pa., *An Evaluation of the Unloading Compliance Procedure for J-Integral Testing in the Hot Cell, Final Report*, NUREG/CR-1070 (ORNL/Sub-7394/1), October 1979.

P. B. Crosley and E. J. Ripling, Materials Research Laboratory, Inc., Glenwood, Ill., *Development of a Standard Test for Measuring K_{Ia} with a Modified Compact Specimen*, NUREG/CR-2294 (ORNL/SUB-81/7755/1), August 1981.

H. A. Domian, Babcock and Wilcox Company, Alliance, Ohio, *Vessel V-8 Repair and Preparation of Low Upper-Shelf Weldment*, NUREG/CR-2676 (ORNL/Sub/81-85813/1), June 1982.

R. D. Cheverton, S. K. Iskander, and D. G. Ball, Union Carbide Corp. Nuclear Div., Oak Ridge Natl. Lab., Oak Ridge, Tenn., *PWR Pressure Vessel Integrity During Overcooling Accidents: A Parametric Analysis*, NUREG/CR-2895 (ORNL/TM-7931), February 1983.

J. G. Merkle, Union Carbide Corp. Nuclear Div., Oak Ridge Natl. Lab., Oak Ridge, Tenn., *An Examination of the Size Effects and Data Scatter Observed in Small Specimen Cleavage Fracture Toughness Testing*, NUREG/CR-3672 (ORNL/TM-9088), April 1984.

W. R. Corwin, Martin Marietta Energy Systems, Inc., Oak Ridge Natl. Lab., Oak Ridge, Tenn., *Assessment of Radiation Effects Relating to Reactor Pressure Vessel Cladding*, NUREG/CR-3671 (ORNL-6047), July 1984.

W. R. Corwin, R. G. Berggren, and R. K. Nanstad, Martin Marietta Energy Systems, Inc., Oak Ridge Natl. Lab., Oak Ridge, Tenn., *Charpy Toughness and Tensile Properties of a Neutron Irradiated Stainless Steel Submerged-Arc Weld Cladding Overlay*, NUREG/CR-3927 (ORNL/TM-9709), September 1984.

J. J. McGowan, Martin Marietta Energy Systems, Inc., Oak Ridge Natl. Lab., Oak Ridge, Tenn., *Tensile Properties of Irradiated Nuclear Grade Pressure Vessel Plate and Welds for the Fourth HSST Irradiation Series*, NUREG/CR-3978 (ORNL/TM-9516), January 1985.

J. J. McGowan, Martin Marietta Energy Systems, Inc., Oak Ridge Natl. Lab., Oak Ridge, Tenn., *Tensile Properties of Irradiated Nuclear Grade Pressure Vessel Welds for the Third HSST Irradiation Series*, NUREG/CR-4086 (ORNL/TM-9477), March 1985.

W. R. Corwin, G. C. Robinson, R. K. Nanstad, J. G. Merkle, R. G. Berggren, G. M. Goodwin, R. L. Swain, and T. D. Owings, Martin Marietta Energy Systems, Inc., Oak Ridge Natl. Lab., Oak Ridge, Tenn., *Effects of Stainless Steel Weld Overlay Cladding on the Structural Integrity of Flawed Steel Plates in Bending, Series 1*, NUREG/CR-4015 (ORNL/TM-9390), April 1985.

W. J. Stelzman, R. G. Berggren, and T. N. Jones, Martin Marietta Energy Systems, Inc., Oak Ridge Natl. Lab., Oak Ridge, Tenn., *ORNL Characterization of Heavy-Section Steel Technology Program Plates 01, 02, and 03*, NUREG/CR-4092 (ORNL/TM-9491), April 1985.

G. D. Whitman, Martin Marietta Energy Systems, Inc., Oak Ridge Natl. Lab., Oak Ridge, Tenn., *Historical Summary of the Heavy-Section Steel Technology Program and Some Related Activities in Light-Water Reactor Pressure Vessel Safety Research*, NUREG/CR-4489 (ORNL-6259), March 1986.

R. H. Bryan, B. R. Bass, S. E. Bolt, J. W. Bryson, J. G. Merkle, R. K. Nanstad, and G. C. Robinson, Martin Marietta Energy Systems, Inc., Oak Ridge Natl. Lab., Oak Ridge, Tenn., *Test of 6-in.-Thick Pressure Vessels. Series 3: Intermediate Test Vessel V-8A — Tearing Behavior of Low Upper-Shelf Material*, NUREG-CR-4760 (ORNL-6187), May 1987.

D. B. Barker, R. Chona, W. L. Fourney, and G. R. Irwin, University of Maryland, College Park, Md., *A Report on the Round Robin Program Conducted to Evaluate the Proposed ASTM Standard Test Method for Determining the Plane Strain Crack Arrest Fracture Toughness, K_{Ia}, of Ferritic Materials*, NUREG/CR-4966 (ORNL/Sub/79-7778/4), January 1988.

L. F. Miller, C. A. Baldwin, F. W. Stallman, and F. B. K. Kam, Martin Marietta Energy Systems, Inc., Oak Ridge Natl. Lab., Oak Ridge, Tenn., *Neutron Exposure Parameters for the Metallurgical Test Specimens in the Fifth Heavy-Section Steel Technology Irradiation Series Capsules*, NUREG/CR-5019 (ORNL/TM-10582), March 1988.

J. J. McGowan, R. K. Nanstad, and K. R. Thoms, Martin Marietta Energy Systems, Inc., Oak Ridge Natl. Lab., Oak Ridge, Tenn., *Characterization of Irradiated Current-Practice Welds and A533 Grade B Class 1 Plate for Nuclear Pressure Vessel Service*, NUREG/CR-4880 (ORNL-6484/V1 and V2), July 1988.

R. D. Cheverton, W. E. Pennell, G. C. Robinson, and R. K. Nanstad, Martin Marietta Energy Systems, Inc., Oak Ridge Natl. Lab., Oak Ridge, Tenn., *Impact of Radiation Embrittlement on Integrity of Pressure Vessel Supports for Two PWR Plants*, NUREG/CR-5320 (ORNL/TM-10966), February 1989.

J. G. Merkle, Martin Marietta Energy Systems, Inc., Oak Ridge Natl. Lab., Oak Ridge, Tenn., *An Overview of the Low-Upper-Shelf Toughness Safety Margin Issue*, NUREG/CR-5552 (ORNL/TM-11314), August 1990.

R. D. Cheverton, T. L. Dickson, J. G. Merkle, and R. K. Nanstad, Martin Marietta Energy Systems, Inc., Oak Ridge Natl. Lab., Oak Ridge, Tenn., *Review of Reactor Pressure Vessel Evaluation Report for Yankee Rowe Nuclear Power Station (YAEC No. 1735)*, NUREG/CR-5799 (ORNL/TM-11982), March 1992.

UNIRRADIATED MATERIAL PROPERTIES OF MIDLAND WELD WF-70*

D. E. McCabe, R. K. Nanstad,
S. K. Iskander, and R. L. Swain

1. Introduction

The objective of the Heavy-Section Steel Irradiation (HSSI) Program Tenth Irradiation Series is to characterize the properties before and after irradiation of Babcock and Wilcox (B&W) WF-70 weld metal. The designation WF-70 stands for a specific heat of weld wire used with a specific lot of Linde 80 flux, and this particular weld has been used in about seven currently operating power generating reactors.[1] The test material became available to Oak Ridge National Laboratory because of a decision made by Consumers Power Company of Midland, Michigan, to not operate an almost completed nuclear power plant. The vessel of the Midland Reactor Unit 1 became available for research studies, and a consortium of utilities, vendors, and the U.S. Nuclear Regulatory Commission (NRC) recognized this as an opportunity to expand and possibly improve the data base on WF-70. The part of the HSSI Program focusing on WF-70 was developed to understand its properties before and after irradiation. In particular, WF-70 is a high-copper weld metal, nominally 0.4 wt % Cu, and is noted as being a low upper-shelf (LUS) material. WF-70 develops less than 68-J (50-ft-lb) energy at drop-weight (DWT) nil-ductility temperature (NDT) + 33°C (NDT + 60°F), which requires that reference nil-ductility temperature, RT_{NDT}, be determined from the Charpy curve.[2] The upper-shelf energy (USE) is nominally 89 J (65 ft-lb). *Title 10, Code of Federal Regulations, Part 50*, Appendix G,[3] requires that unirradiated beltline materials must have a 102-J (75-ft-lb) USE and no less than 68-J (50-ft-lb) USE during the operating lifetime. Materials that do not have the Code-required 102 J (75 ft-lb) are considered low USE and have a higher probability of slipping below 68 J (50 ft-lb). For such cases, a fitness-for-service analysis is required for continued operation. Currently, the fracture mechanics properties required for the analysis are obtained through correlations developed with other production lots of materials that may or may not be accurate for a plant-specific analysis.

*Research was sponsored by the Office of Nuclear Regulatory Research, Division of Engineering, U.S. Nuclear Regulatory Commission, under Interagency Agreement DOE 1886-8109-8L with the U.S. Department of Energy under Contract DE-AC05-84OR21400 with Martin Marietta Energy Systems, Inc.

2. Materials

Figure 1 shows the sampling plan for the Midland beltline weld (seam 1) and nozzle course weld (seam 3). Sections 1-9 to 1-15 of the beltline and 3-1 and 3-4 of the nozzle course weld were obtained for this program. Both welds are double-V submerged-arc (WF-70) welds (SAWs) made with heat No. 72105 weld wire and lot 8669 Linde-80 flux. However, the nozzle course weld had B&W WF-67 on the inside half on the double-V, which was not of interest to this test program. The beltline weld had a few short segments of repair weld that were also avoided in the sampling plan of fracture mechanics specimen. Both welds had been postweld heat treated (PWHT) at 607°C (1125°F) for 24 h. The pieces of the beltline (see Figure 1), were about 1.1 m long (45 in.), and vessel thickness at that location was about 216 mm (8.5 in.). A macrograph of the weld cross section is shown in Figure 2. The two nozzle pieces were about 1 m (41 in.) long, and vessel thickness at that position was about 317 mm (12.5 in.). This cross section is shown in Figure 3. Again, only the WF-70 material was included in the current characterization plan.

ORNL-DWG 92-11823A

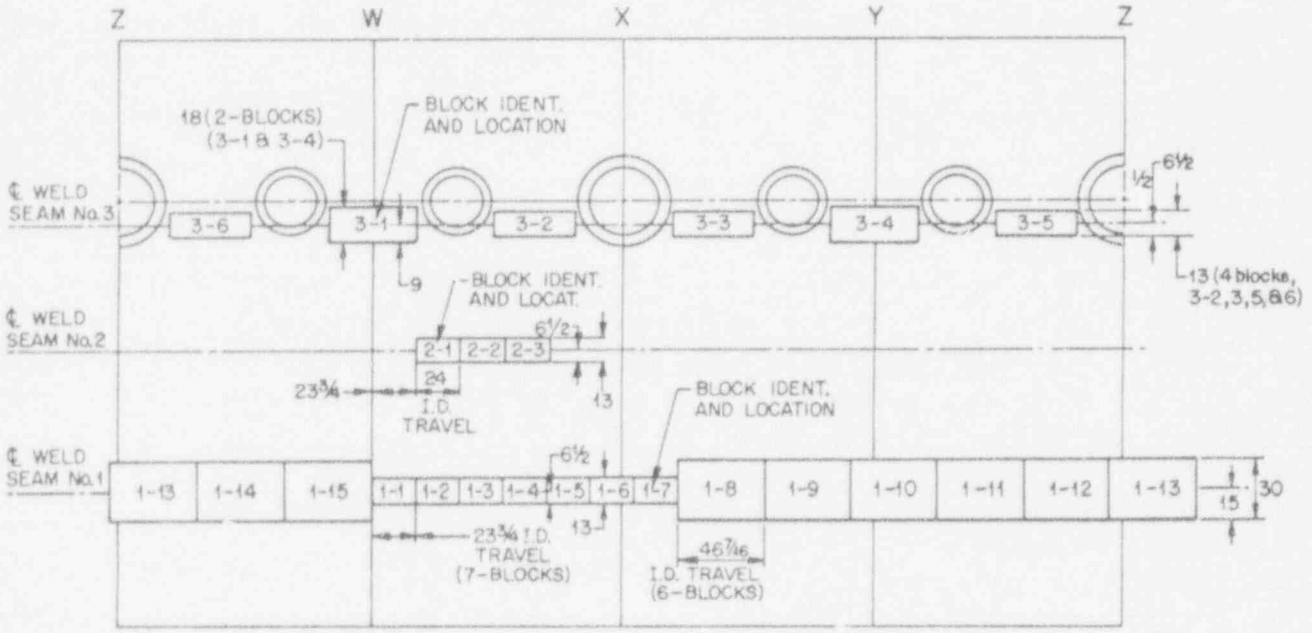

Figure 1. Sampling layout for Midland beltline sections 1-8 through 1-15 and nozzle course sections 3-1 through 3-5.

YP8664B

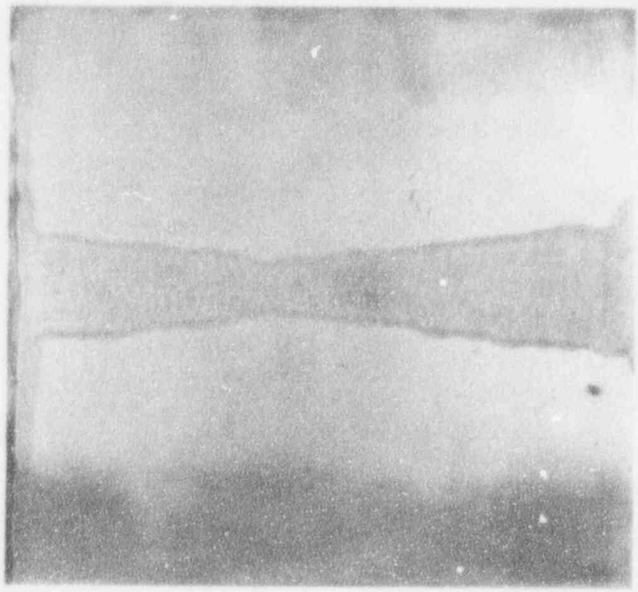

Figure 2. Macrograph of Midland beltline weld section 1-13.

YP12922

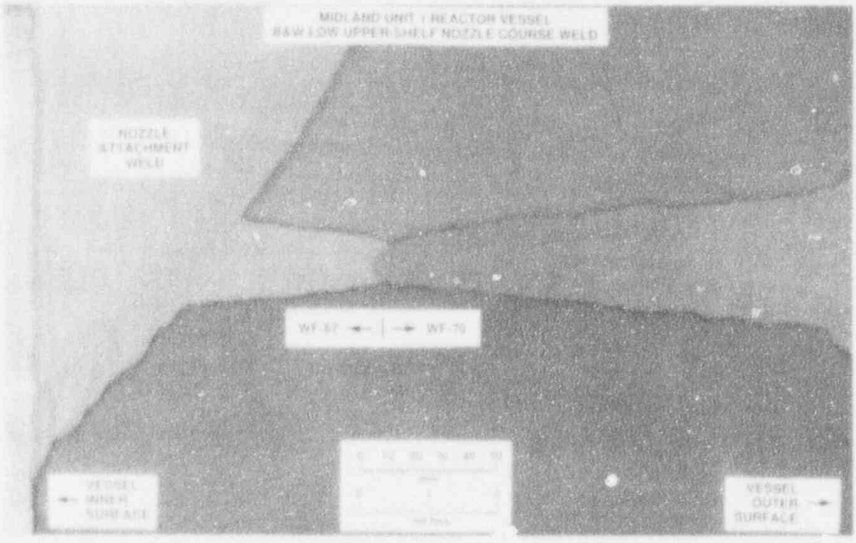

Figure 3. Macrograph of Midland nozzle course weld section 3-1 showing weld WF-67 on the inner half and WF-70 on the outer half. A nozzle attachment weld appears in this section.

3. Test Plan

The material property characterization plan had three major milestones, the first of which was to conduct a comprehensive evaluation of chemical composition and toughness in the form of Charpy V-notch (CVN) surveys around the vessel girth and through the thickness. DWT NDT tests were also included.[4] This material characterization work has been previously reported.[5] The principal findings will be summarized here for convenience when comparing to the fracture mechanics results. The second milestone involves the development of fracture mechanics-related material toughness properties that includes a study of specimen size effects on J_R curve as well as the identification of transition temperature in the form of K_{Jc} values. A K_{Jc} value is defined as the elastic-plastic fracture toughness at the onset of cleavage fracture. The third major milestone is the development of postirradiation properties, and these results will be reported later.

3.1 Scoping Work

The beltline weld was sampled at four equally spaced positions around the vessel girth and at five through-thickness locations (1/4t, 1/2t, 5/8t, 3/4t, and 7/8t) for chemistry and CVN toughness. The NDT was determined at the same four girth positions, but only at the 1/4t and 3/4t through-thickness locations.[5]

Table 1 summarizes the overall averages and extremes of variation for the five chemical elements considered to affect irradiation sensitivity. All were essentially the same in the two welds except for the copper content. The typical through-thickness variation is shown in Table 2 for the beltline weld and in Table 3 for the nozzle weld. Such copper variations do not normally have a significant effect on the unirradiated properties.[6] However, the expected difference in transition temperature shift due to irradiation damage (ΔTT) is well known.[7] Other elements were far more uniform than copper content. Table 3 shows that there is a considerable difference in copper content between WF-67 and WF-70 of the nozzle weld metals. Also, the copper content of the WF-70 nozzle material was uniformly higher than that of the beltline WF-70 weld.

Reference temperature, RT_{NDT}, for pressure vessel steels is most commonly indexed to the DWT NDT temperature. As previously mentioned, both welds were sampled for DWT NDT at 1/4t and 3/4t through-thickness positions, and these results are given in Table 4. Reproducibility was excellent at -50°C (-58°F) ± 10°C (±18°F). However, because WF-70 is an LUS material, reference temperature is controlled instead by the Charpy V energy curve at the 68-J temperature less 33°C (60°F).

CVN transition curves were also made at 90° intervals around the girth of the beltline weld and at 180° intervals around the nozzle girth. All but one of the beltline pieces were sampled at five locations through the thickness, giving a total of 19 Charpy curves. The nozzle weld was sampled at three through-thickness positions in the WF-70 [illegible], giving six CVN transition curves. Test temperatures for 41- and 68-J (30- and 50-ft-lb) energy levels and USE are presented in Tables 5 and 6. As expected, neither weld metal developed the required 68 J (50 ft-lb) at -17°C (-1.4°F) [NDT + 60°F], and the USE was about 89 J (65 ft-lb), so the LUS weld metal classification for WF-70 was verified. The procedure to determine RT_{NDT} is to establish a lower bound curve fit to the CVN energy data scatter in the transition range and then select the 68-J temperature on this lower bound and subtract 33°C (60°F). The RT_{NDT} temperatures determined in this way are listed in the right-hand columns of Tables 5 and 6. Extreme values in RT_{NDT} for beltline weld differ by 57°C (103°F) and by 26°C (47°F) for nozzle weld material.

An interesting observation was that, although each individual Charpy curve gave an impression of excellent material uniformity (see typical examples in Figure 4) when data from all 19 positions were combined (see Figure 5), the reason for the large scatter of RT_{NDT} temperatures in Table 5 can be understood.

Tensile property determinations were made at temperatures ranging from -100 to 288°C

Table 1. Summary of major radiation-sensitive elements for Midland Unit 1 reactor vessel welds

Section number	n*	Element, wt % ± 1σ				
		Cu[b]	Ni	P	Mn	Si
Beltline weld						
1-9	8	0.26 ± 0.441 (0.22-0.34)	0.566 ± 0.031	0.016 ± 0.0013	1.629 ± 0.050	0.605 ± 0.031
1-11	8	0.258 ± 0.027 (0.23-0.31)	0.57 ± 0.007	0.016 ± 0.0014	1.615 ± 0.015	0.62 ± 0.029
1-13	5	0.248 ± 0.039 (0.21-0.32)	0.604 ± 0.016	0.018 ± 0.002	1.55 ± 0.067	0.62 ± 0.041
1-15	7	0.254 ± 0.026 (0.22-0.29)	0.567 ± 0.009	0.018 ± 0.0013	1.614 ± 0.014	0.644 ± 0.016
Average	28	0.256 ± 0.034 (0.21-0.34)	0.574 ± 0.023	0.017 ± 0.0019	1.607 ± 0.049	0.622 ± 0.033
Nozzle course weld						
3-1	4	0.398 ± 0.034 (0.37-0.46)	0.576 ± 0.021	0.015 ± 0.001	1.59 ± 0.045	0.548 ± 0.051
3-4	5	0.392 ± 0.016 (0.37-0.42)	0.567 ± 0.008	0.015 ± 0.002	1.61 ± 0.018	0.55 ± 0.043
Average	9	0.396 ± 0.028 (0.37-0.46)	0.572 ± 0.017	0.015 ± 0.002	1.59 ± 0.037	0.55 ± 0.048
Total average	37	0.290 ± 0.068 (0.21-0.46)	0.574 ± 0.022	0.016 ± 0.002	1.604 ± 0.046	0.605 ± 0.048

*Number of measurements.
[b]Range of copper shown in parentheses.

Table 2. Chemcial composition of Midland reactor beltline section 1-11

Location	Chemical composition (wt %)																					
	C	Mn	P	S	Si	Cr	Ni	Mo	Cu	V	Nb	Ti	Co	Al	B	W	Cb	As	Sn	Zr	N	O
1/4t	0.083	1.610	0.013	0.006	0.59	0.10	0.57	0.41	0.23	0.006	-	<0.01	0.04	0.04	0.002	0.04	<0.05	0.06	-	0.02	0.018	0.065
	0.078	1.650	0.018	0.005	0.59	0.10	0.57	0.41	0.23	0.005												
1/2t	0.088	1.600	0.017	0.006	0.60	0.11	0.58	0.42	0.24	0.005	-	<0.01	0.04	0.04	0.002	0.03	<0.05	0.08	-	0.02	0.014	0.068
	0.084	1.620	0.018	0.006	0.59	0.10	0.58	0.42	0.25	0.005												
5/8t	0.079	1.610	0.017	0.006	0.63	0.10	0.56	0.41	0.26	0.005	-	<0.01	0.04	0.06	0.002	0.02	<0.05	0.09	-	0.02	0.018	0.068
	0.080	1.620	0.016	0.006	0.65	0.09	0.57	0.41	0.25	0.005												
3/4t	0.083	1.610	0.015	0.007	0.66	0.10	0.57	0.41	0.29	0.004	-	<0.01	0.04	0.04	0.002	0.02	<0.05	0.08	-	0.02	0.019	0.093
	0.083	1.600	0.016	0.007	0.65	0.10	0.56	0.41	0.31	0.006												

Source: Combustion Engineering for C through V, MOS Inspection for Ti through O.

Table 3. Chemical composition of Midland reactor nozzle course section 3-1

Location	Chemical composition (wt %)																					
	C	Mn	P	S	Si	Cr	Ni	Mo	Cu	V	Nb	Ti	Co	Al	B	W	Cb	As	Sn	Zr	N	O
WF-67																						
0.07t	0.087	1.60	0.018	0.009	0.68	0.10	0.56	0.38	0.29	0.006	-	<0.001	0.014	0.016	<0.001	<0.01	0.003	0.006	0.004	<0.001	0.015	0.060
0.2t	0.071	1.53	0.017	0.017	0.55	0.09	0.58	0.37	0.20	0.005	-	<0.001	0.009	0.007	<0.001	<0.01	0.003	0.006	0.008	<0.001	0.012	0.063
0.4t	0.081	1.47	0.016	0.016	0.54	0.11	0.59	0.39	0.15	0.008	-	<0.001	0.010	0.008	<0.001	<0.01	0.003	0.006	0.007	<0.001	0.010	0.064
0.5t	0.110	1.50	0.014	0.008	0.50	0.14	0.61	0.42	0.37	0.012	-	<0.001	0.016	0.021	<0.001	<0.01	0.003	0.006	0.005	<0.001	0.011	0.064
WF-70																						
0.54t	0.100	1.60	0.014	0.008	0.50	0.14	0.59	0.41	0.46	0.010	-	<0.001	0.016	0.019	<0.001	<0.01	0.003	0.006	0.005	<0.001	0.011	0.067
0.7t	0.092	1.61	0.014	0.006	0.55	0.11	0.56	0.39	0.37	0.008	-	<0.001	0.015	0.020	<0.001	<0.01	0.003	0.006	0.004	<0.001	0.012	0.064
0.8t	0.078	1.63	0.015	0.007	0.55	0.11	0.56	0.39	0.38	0.006	-	<0.001	0.015	0.018	<0.001	<0.01	0.003	0.006	0.003	<0.001	0.015	0.074
0.95t	0.060	1.59	0.017	0.007	0.64	0.10	0.56	0.38	0.41	0.006	-	<0.001	0.015	0.015	<0.001	<0.01	0.003	0.007	0.004	<0.001	0.015	0.074

Source: Combustion Engineering.

Table 4. Drop-weight test results for Midland welds

Girth location	NDT temperature [°C(°F)]					
	1-9	1-11	1-13	1-15	3-1*	3-4*
1/4t	-60 (-76)	-60 (-76)	-60 (-76)	-45 (-49)	-45 (-49)	-55 (-67)
3/4t	-50 (-58)	-50 (-58)	-45 (-49)	-55 (-67)	-40 (-40)	-50 (-58)
*Nozzle welds 3-1 and 3-4 at 7/8t positions instead of 1/4t.						

Table 5. Summary of Charpy impact results for Midland Unit 1 reactor vessel beltline weld sections

Through-thickness position	Charpy V-notch tests												RT_{MF},[a] °C (°F), at weld section				RT_{NDT},[b] °C (°F), at weld section			
	41-J temperature, °C (°F), at weld section				68-J temperature, °C (°F), at weld section				Upper shelf energy, J (ft-lb), at weld section											
	1-13	1-9	1-11	1-15	1-13	1-9	1-11	1-15	1-13	1-9	1-11	1-15	1-13	1-9	1-11	1-15	1-13	1-9	1-11	1-15
1/4t	-11 (12)	-6 (21)	-13 (8)	4 (39)	21 (69)	37 (98)	25 (76)	50 (122)	101 (74)	77 (57)	91 (67)	82 (60)	-9 (15)	3 (37)	-9 (16)	16 (61)	-13 (9)	14 (57)	-9 (16)	16 (61)
1/2t	-16 (3)	-11 (13)	-4 (25)	-9 (15)	29 (84)	25 (77)	23 (74)	17 (63)	104 (77)	83 (61)	91 (67)	88 (65)	-5 (24)	-8 (17)	-10 (14)	-16 (3)	2 (36)	-8 (17)	-10 (14)	-15 (5)
5/8t	-22 (-7)	-18 (0)	-10 (13)	3 (37)	9 (48)	18 (64)	17 (63)	49 (121)	108 (80)	88 (65)	90 (66)	85 (62)	-25 (-12)	-16 (3)	-16 (3)	15 (60)	-20 (-3)	-16 (3)	-16 (3)	8 (47)
3/4t	-2 (27)	3 (38)	14 (57)	-6 (21)	37 (98)	53 (128)	58 (136)	28 (82)	90 (66)	81 (60)	84 (62)	89 (66)	3 (37)	20 (68)	24 (76)	-6 (21)	6 (43)	20 (68)	37 (99)	-6 (22)
7/8t		-3 (26)	-13 (8)	-8 (18)		46 (116)	30 (86)	22 (72)		78 (57)	79 (58)	83 (61)		13 (55)	-4 (25)	-12 (11)		13 (56)	18 (65)	-3 (26)
[a]Determined from T_{50} - 60°F (T_{68} - 33°C) using average curve fit, where T_{50} is the temperature corresponding to 50 ft-lb.																				
[b]Determined from T_{50} - 60°F (T_{68} - 33°C) using minimum curve fit, where T_{50} is the temperature corresponding to 50 ft-lb.																				

Table 6. Summary of Charpy impact results for Midland Unit 1 reactor vessel nozzle course weld sections

Through-thickness position	Charpy V-notch tests						RT_{M},* °C (°F), at weld section		RT_{NDT},[b] °C (°F), at weld section	
	41-J temperature, °C (°F), at weld section		68-J temperature, °C (°F), at weld section		Upper-shelf energy, J (ft-lb), at weld section					
	3-1	3-4	3-1	3-4	3-1	3-4	3-1	3-4	3-1	3-4
1/2t	5 (42)	−11 (13)	47 (117)	51 (125)	86 (63)	88 (65)	14 (57)	18 (65)	14 (57)	18 (65)
3/4t	2 (35)	−1 (30)	49 (120)	45 (112)	89 (65)	85 (63)	16 (61)	11 (52)	16 (61)	11 (52)
7/8t	-10 (15)	5 (42)	26 (78)	47 (116)	90 (66)	89 (66)	−8 (18)	14 (57)	−8 (18)	14 (57)

*Determined from T_{50} − 60°F (T_{68} − 33°C) using average curve fit.

[b]Determined from T_{50} − 60°F (T_{68} − 33°C) using minimum curve fit.

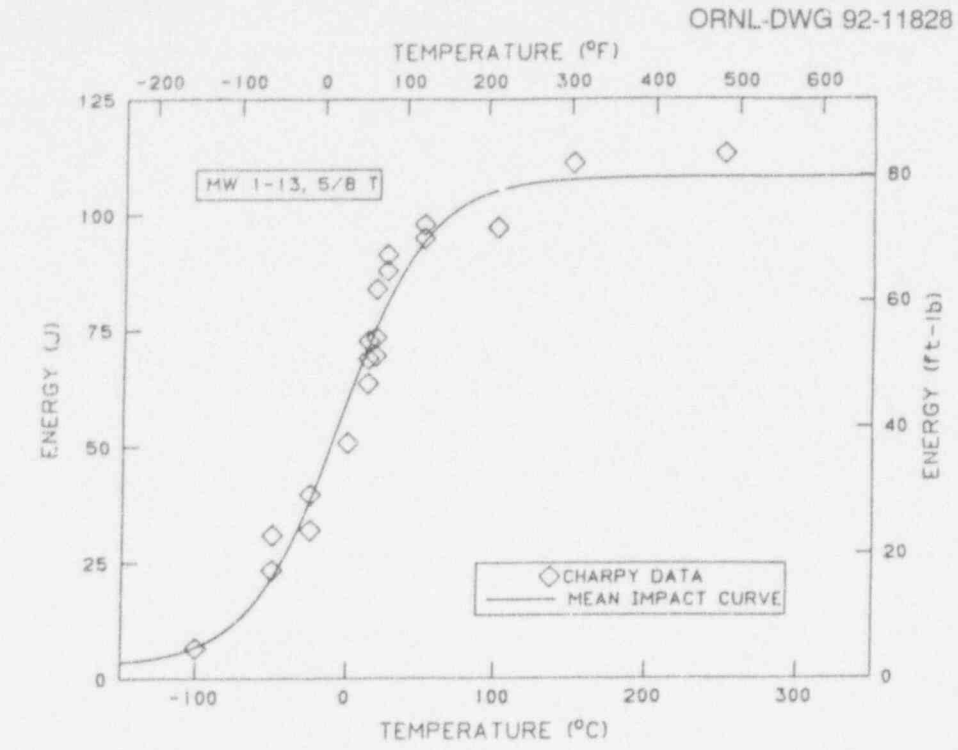

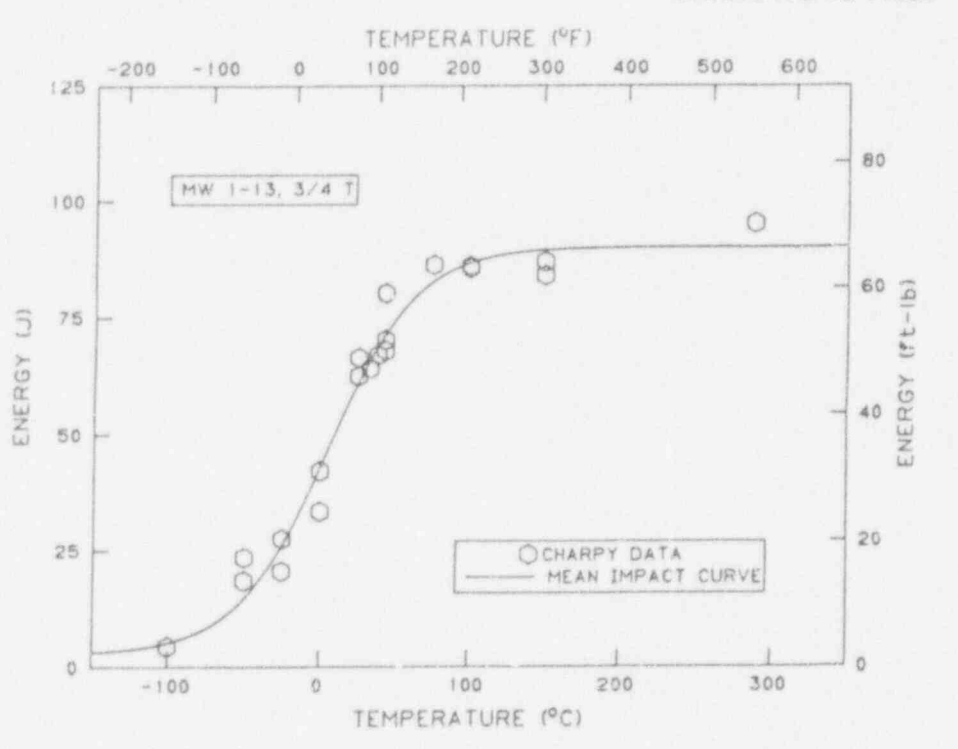

Figure 4. Example of Charpy V-notch energy curves from two through-thickness locations. When observed individually, they suggest uniformity of impact toughness.

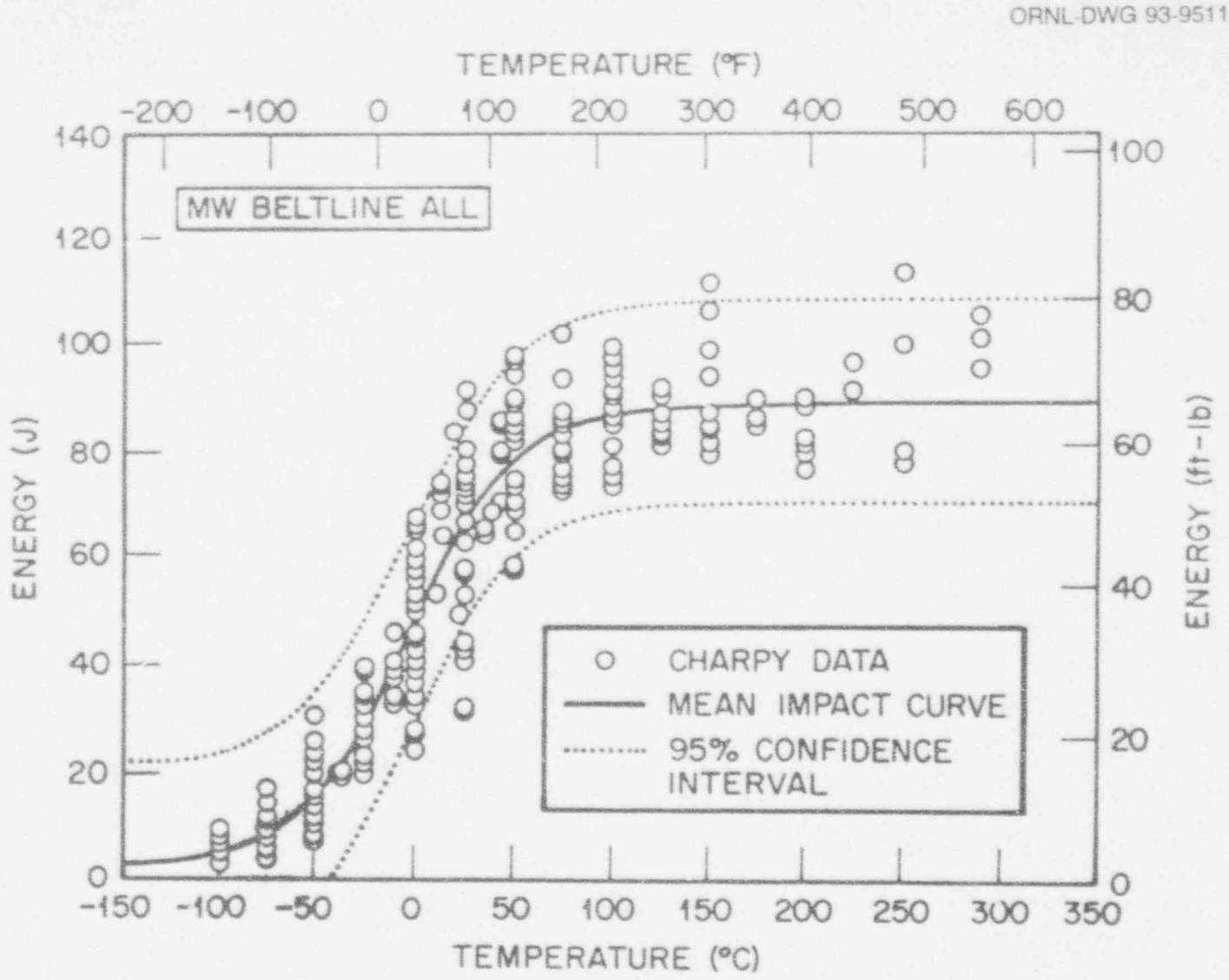

Figure 5. Combined Charpy V-notch data taken around the girth and through-thickness positions of the beltline weld.

(-150 to 550°F). The trend of reduced strength with increased test temperature is clearly evident (see Table 7). However, it appears that the material strength of the nozzle weld is significantly higher than that of the beltline weld. This appeared to have developed despite the fact that both were given essentially the same PWHT. Increased strength is usually accompanied by reduced fracture toughness, but this was not detected in the CVN USEs nor in the NDT or RT_{NDT} transition temperatures. To compare with the measured tensile values, an automated ball indentation (ABI) test was performed on some blocks made of the two weld metals.[9] These blocks were appropriately prepared for the ABI test by surface grinding parallel surfaces. These results were consistent with the properties reported in Table 7 at room temperature.

Principally, on the basis of copper content, a decision was made to define nozzle WF-70 weld metal and beltline WF-70 weld metal as two different materials. The specimen sampling plan, therefore, was designed to evaluate properties of these two materials independently before and after irradiation.

3.2 Fracture Mechanics Properties

The second phase of the test program consisted of fracture mechanics-related toughness development for the unirradiated condition. These data were then used to evaluate (1) a new fracture mechanics-based transition temperature characterization methodology, (2) the Eason et al. multivariable model[6] to estimate J-R curves, and (3) a method to develop the K_{Ja} transition curve using instrumented CVN load-time test records.

3.2.1 Transition Temperature Characterization, K_{Jc}

Beltline WF-70 weld metal was tested in the form of compact specimens in sizes ranging from 1/2T to 4T and at test temperatures ranging from -100 to 0°C (-148 to 32°F); see Table 8. One part of the matrix outlines the beltline test condition variations, and the other the nozzle course test variations, both reporting the median K_{Jc} values from multiple tests at each level. The fewer test conditions applied to the nozzle welds are the result of the limited amount of nozzle material available. Individual data for both matrices are tabulated in Appendix A. For the data reported in Appendix A, some specimens tested at 0°C (32°F) did not fail by cleavage fracture, and those are designated J_{NC} with no reported value. Specimen codes are reported to document the position for each data point within the weld.

3.2.2 Test Procedure

The test practice involved cooling of the specimens to test temperature using vaporized liquid nitrogen. Each specimen was given sufficient soak time at test temperature to ensure thermal stability prior to running of the test, typically 5 min or more. Again, most tests terminated in K_{Jc}- type cleavage fracture. However, some of the specimens tested in the mid-transition temperature range did not fail by cleavage but instead developed slow-stable crack growth. Periodic partial unloading compliance was employed routinely so that crack growth could be measured and J-R curves could be developed in such cases.

Fracture toughness at the onset of cleavage fracture was calculated in terms of J-integral (J_c) [ref. 10], and then all values were converted to their equivalent value in units of stress-intensity factor, K_{Jc}, using the following:

$$K_{Jc} = \sqrt{J_c E}\ , \qquad (1)$$

where E is the plane stress elastic modulus.

At the beginning of the testing, a small experiment in side-groove effects was performed to evaluate the effect on K_{Jc} toughness. The comparison developed is shown in Table 9. Because there is increased constraint with side grooving, one would expect to find either no change or reduced K_{Jc} for specimens that are side grooved. Since the results indicated only a mild reversed effect that could not be rationalized on the physical basis of constraint, it was concluded that there was no evidence of a significant constraint effect on K_{Jc}, and as a consequence, the balance of the testing was performed without

Table 7. Tensile properties of Midland WF-70 weld metal

Temperature		Strength			
		Yield		Ultimate tensile	
°C	°F	MPa	ksi	MPa	ksi
Nozzle					
-100	-148	648	94.0	820	118.9
-75	-103	620	89.9	765	111.0
-50	-58	579	84.0	717	104.0
23	73	545	79.0	655	95.0
160	320	483	70.1	586	85.0
288	550	483	70.1	586	89.0
Beltline					
-100	-148	548	79.5	758	110.0
-75	-103	483	70.1	710	103.0
-50	-58	465	67.4	682	98.9
23	73	407	59.0	586	85.0
288	550	427	61.9	558	80.9

Table 8. Median K_c values [MPa$\sqrt{m}$(ksi$\sqrt{in.}$)] for WF-70 weld metal from multiple tests

Size	Test temperature °C (°F)									
	0 (32)		−25 (−13)		−50 (−58)		−75 (−103)		−100 (−148)	
	MPa$\sqrt{m}$	ksi$\sqrt{in.}$	MPa$\sqrt{m}$	ksi$\sqrt{in.}$	MPa$\sqrt{m}$	ksi$\sqrt{in.}$	MPa$\sqrt{m}$	ksi$\sqrt{in.}$	MPa$\sqrt{m}$	ksi$\sqrt{in.}$
Beltline										
1/2T			203.5	185.0	133.4	121.3				
1T	265	240.9	159.9	145.4	97.8	88.9	67.5	61.4	51.3	46.6
2T	234	212.7	162.7	147.9	106.4	96.7				
4T			109.1	99.2						
Nozzle										
1/2T					91.6	83.3				
1T	191.3	173.9	109.5	99.5	71.3	64.8			46.7	42.5

Table 9. Comparison of K_{jc} for 1T compact specimens with and without side grooves

Test temperature		Beltline				Nozzle			
		With side grooves		Without side grooves		With side grooves		Without side grooves	
°C	°F	MPa√m	ksi√m	MPa√m	ksi√m	MPa√m	ksi√m	MPa√m	ksi√m
0	32	197	179	140	127	220	200	145	132
		274	249	256	233	229	208	168	153
		317	288	296	269			300	273
				a	*a*				
				a	*a*				
Average values:		263	239	321	210	224	204	204	186
−25	−13	119	108	120	109	87	79	84	76
		133	121	139	126	147	134	96	87
		193	176	139	126			97	88
		267	243	143	130			114	104
				151	137			120	109
								121	110
Average values:		178	162	138	126	117	106	105	96

*J-R curve.

side grooving. It is possible that the apparent higher toughness values of the side-grooved specimens could be caused by computational problems associated with the manner in which the effective specimen thickness (B_N) is commonly used in the calculation of J_c.

The data from all the beltline weld specimens of all sizes that failed in cleavage are plotted in Figure 6. Data for the nozzle weld metal are shown in Figure 7. Almost none of these K_{Jc} values satisfy the validity requirements for plane strain K_{Ic} (ref. 11). Hence, these data would not be considered acceptable according to early concepts for evaluation of transition temperature fracture toughness. Lower bound fracture toughness has, for many years, been believed to be achievable only through valid K_{Ic} data. However, recent developments in the technology of ductile-brittle behavior have produced methods that predict specimen size effects and methods by which the transition range behavior can be defined by a different concept of universal curve.[12] This information is currently being documented in the form of an American Society for Testing and Materials (ASTM) standard practice.[10]

ORNL-DWG 94-6596

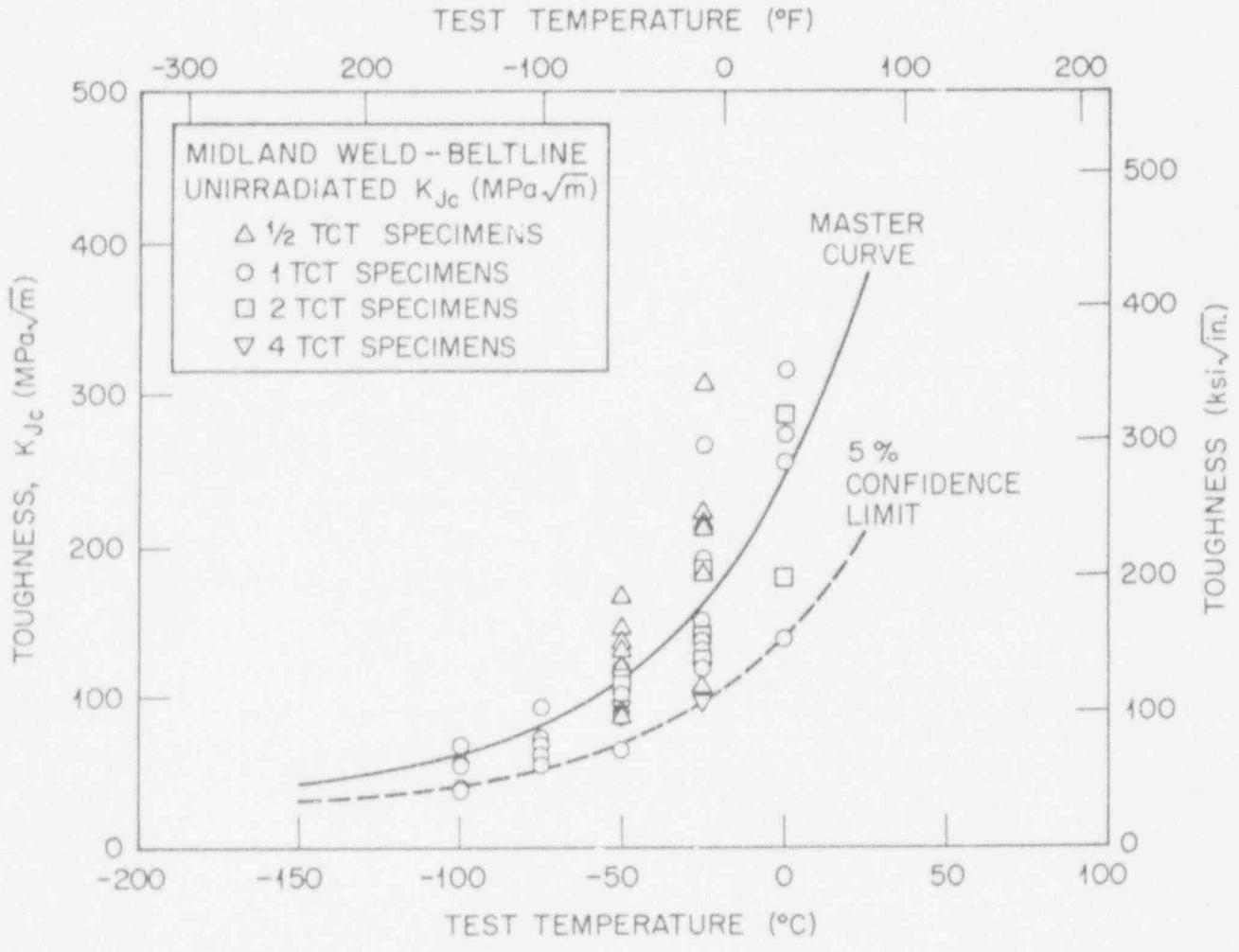

Figure 6. Transition temperature data for the Midland WF-70 beltline weld for four compact specimen sizes and a master curve on 1T specimen size.

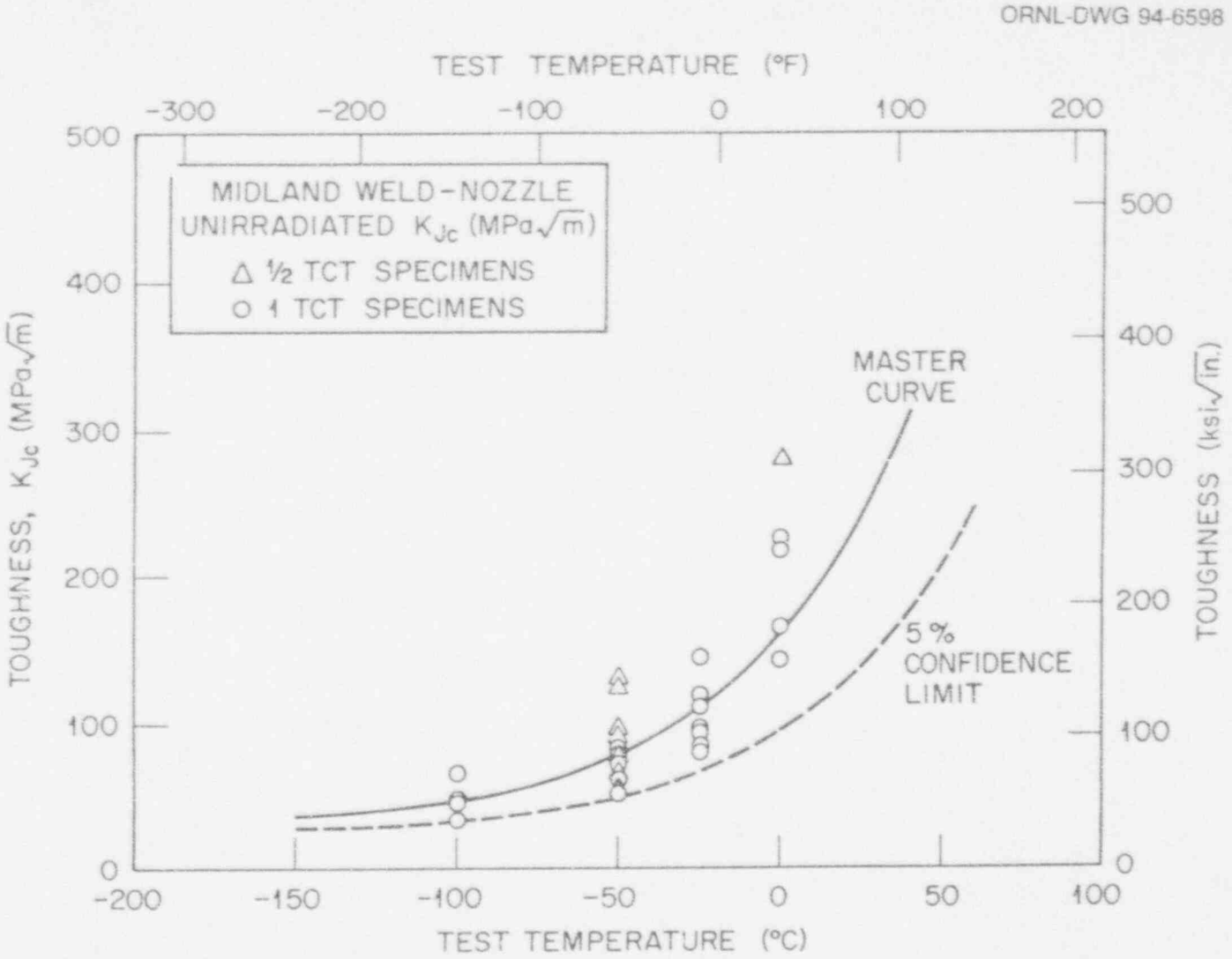

Figure 7. Transition temperature data for the Midland nozzle course weld WF-70 for two compact specimen sizes and a master curve on 1T specimen size.

4. Description of the Proposed Test Practice on Transition Range Definition

The proposed test practice currently under development is designed to obtain useful fracture mechanics information from small specimens that are of a size suitable for insertion into surveillance capsules. One objective is to model transition toughness data scatter with the three-parameter Weibull data distribution model[13] and to employ a weakest-link statistical theory[14] to adjust fracture toughness for specimen size effects. Then, the median trend of fracture toughness, adjusted to a single specimen size, is postulated to fit a universal trend curve, termed a "master curve." Standard deviation of data scatter is a function of the Weibull fitting parameters, and, thus, confidence bounds about the median fracture toughness trend can be calculated. A "reference temperature," T_o, is then determined to position the master curve on the temperature coordinate, and affiliated confidence bound curves are then determined as a function of median toughness. Additionally, a margin adjustment can be applied to the lower confidence bound curve to cover the uncertainty in reference temperature if only a small number of specimens are used to establish the reference temperature.

Data scatter on K_{Jc} values can be fitted using the following three-parameter Weibull function:

$$P_f = 1 - \exp - \left[\frac{K_{Jc} - K_{min}}{K_o - K_{min}} \right]^b , \qquad (2)$$

where:

P_f = the probability that a chosen specimen will develop a specified K_{Jc} toughness,
b = the Weibull slope (parameter 1),
K_{min} = the lowest possible fracture toughness (parameter 2),
K_o = the scale parameter (parameter 3).

Wallin has shown that pressure vessel steels tend to develop a consistent data scatter profile such that two of the above three parameters tend to be constant.[15] That is, when K_{min} is set at 20 MPa√m (18 ksi√in.), the Weibull slope tends to be constant at 4. Then, only the scale parameter, K_o, needs to be determined from the experimental data. Six or more replicate K_{Jc} tests are required to establish the scale parameter with sufficient accuracy.

Given that two of the three Weibull parameters are fixed, as just described, adjustment for specimen size is easily made using the following:[11]

$$K_{Jc(y)} = (K_{Jc(x)} - 20) \left(\frac{B_x}{B_y} \right)^{1/4} + 20 , \qquad (3)$$

where K_{Jc} is the toughness, expressed in units of MPa√m, for specimens of size "x." $K_{Jc(y)}$ is the predicted toughness for specimens of size "y."

Equation (3) can be used to adjust K_{Jc} for size on single datum or to adjust a Weibull scale parameter, K_o, or the median K_{Jc} of a data set.

The median K_{Jc} on 1T size specimens is defined by the following master curve equation:[16]

$$K_{Jc(med)} = 30 + 70 \exp[0.019(T - T_o)] , \qquad (4)$$

Again, the units are expressed in MPa√m. The above equation contains one variable, test temperature, T, and one adjustable parameter, reference temperature, T_o. Standard deviation on K_{Jc} data is defined by:

$$\sigma = 0.28 K_{Jc(med)} [1 - 20/K_{Jc(med)}] , \qquad (5)$$

Assignment of the standard normal deviate obtained from statistical tables can be used to establish confidence bounds. The standard normal deviate at 5% cumulative probability is 1.64. Using this with Eq. (5) results in the following equation:

$$K_{Jc(0.05)} = 25.4 + 37.9 \exp[0.019(T - T_o)] , \qquad (6)$$

Reference temperature, T_o, is the test temperature where the median K_{Jc} for 1T size specimens is expected to be 100 MPa√m. If one wishes to test only six replicate specimens, the temperature selection for optimum accuracy (on establishment of T_o) is near to temperature, T_o. The following crude correlation between the 28-J (20 ft-lb) Charpy energy temperature, T_{28J}, and T_o has been offered as an aid to select a test temperature (in this case for 1T size test specimens):

$$T_o = T_{28J} - 18^\circ C. \qquad (7)$$

The constant on the right side of Eq. (7) can be adjusted for other specimen sizes. As an example, for 1/2T compact specimens, the constant is -28°C (-18.4°F).

Finally, if the lower bound confidence curve of Eq. (6) is to be used to address safety issues, a margin can be added to account for the uncertainty in reference temperature, T_o. The standard deviation on this uncertainty is estimated using the following:[17]

$$\sigma_{T_o} = 18/\sqrt{N}\ , \qquad (8)$$

where N is the number of K_{Jc} datum used to establish T_o.

Equation (8) is most accurate when the K_{Jc} data development is near 100 MPa√m. The standard normal deviate on T_o should be obtained for two-tail standard normal deviates, and a reasonable confidence level assignment is 85%.

4.1 Master Curve Establishment from Midland K_{Jc} Data

Estimates of temperatures corresponding to the 28-J CVN energy level for beltline and nozzle welds were obtained from data such as that shown in Figure 5. Both weld metals indicated -23°C (-9.4°F), and using Eq. (7) adjusted for 1/2T specimen size, a test temperature of -50°C (-58°F) was indicated to obtain 100-MPa√m (91 ksi√in.) median K_{Jc}. As indicated in Tables 8, A1, and A2, 1/2T compact specimens were tested at -50°C (-58°F), giving median K_{Jc} of 91.6 MPa√m (83.3 ksi√in.) for the nozzle weld and 133 MPa√m (121 ksi√in.) for the beltline weld. These values were converted to 1T equivalents of 80.2 and 115.3 MPa√m (72.9 and 104.8 ksi√in.), respectively. Then, the equivalent values were used to establish reference temperatures, T_o, giving -60°C (-76°F) for the beltline weld and -33°C (-27°F) for the nozzle course weld, a 27°C (49°F) difference in transition temperature. This toughness difference was not detected from the DWT NDT tests nor the CVN evaluations.

Figures 6 and 7 show the master curves derived from the 1/2T compact specimen data as well as the 5% cumulative probability curves. The data points shown are not specimen size adjusted. Despite this, the 5% confidence bound tends to enclose most of the unadjusted data.

An example margin adjustment to the 5% confidence limit based on the six replicate specimens and 85% confidence margin adjustment is shown in Figure 8. Here, a 10°C (18°F) margin has been calculated and added to the T_o in Eq. (6).

The postirradiated specimens will be similarly evaluated to establish the transition temperature shift.

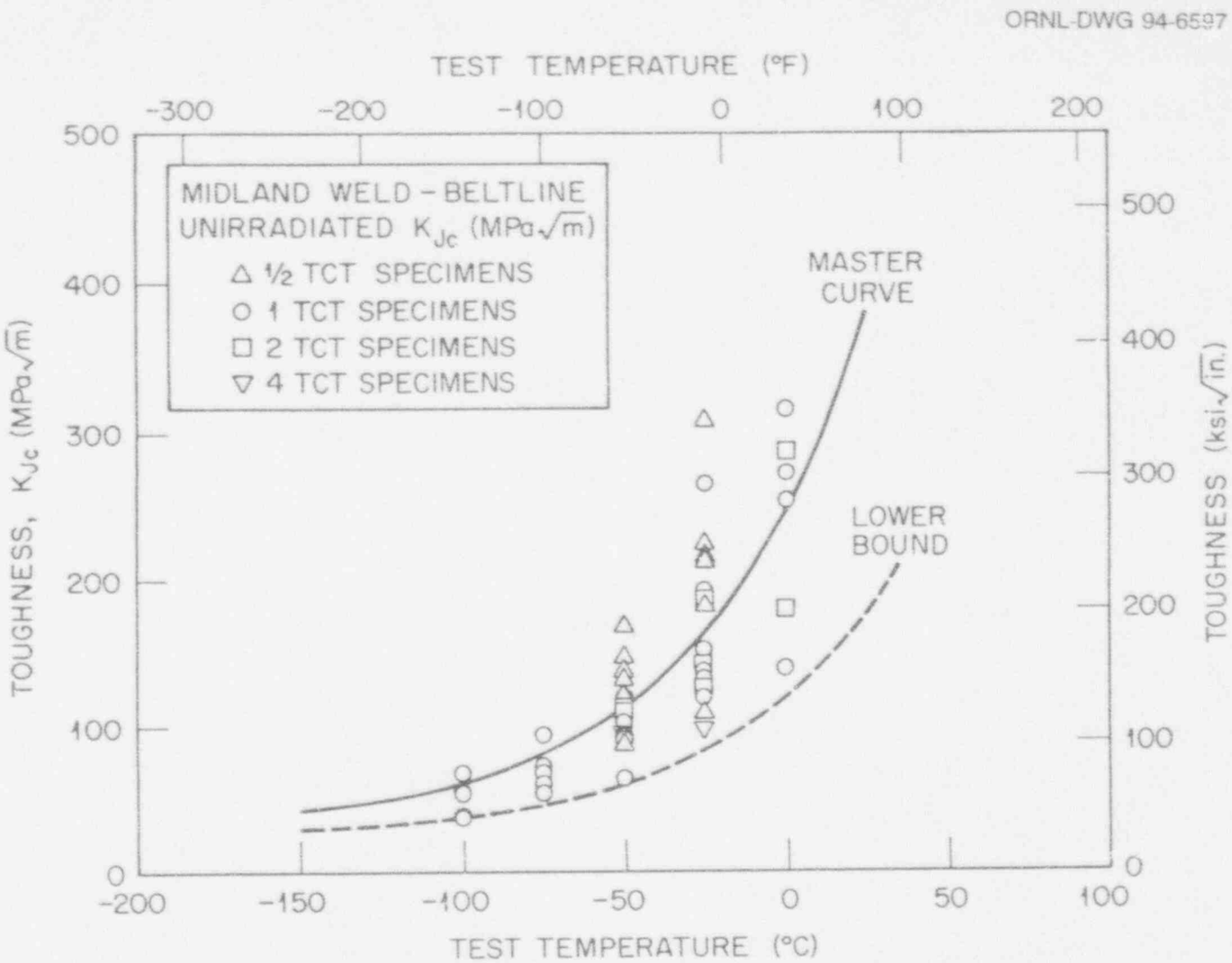

Figure 8. Master curve and 5% confidence limit curve (dashed) adjusted 10°C (18°F) for uncertainty in reference temperature, T_o.

5. Evaluation of J-R Curves

Because WF-70 weld metal is an LUS energy material, J-R curve characterization is needed to demonstrate by analysis that a reactor vessel can be safely operated with this material. Unfortunately, there are many cases where reactor surveillance capsules do not have fracture mechanics-type specimens that are suitable for J-R curve development. Blunt, notched Charpy V specimens are far more common. For such cases, it is now possible to estimate J-R curve using correlations developed from multivariable modeling of data bank information. A model has been developed by Eason et al.[9] that uses a correlation based principally on upper-shelf CVN energy as well as accounting for other experimental variables that influence J-R curves. Variables such as specimen size, chemistry, test temperature, and irradiation exposure are accounted for in the models. This study presented an opportunity to independently compare the correlation model for Linde 80 weld metals to new experimentally generated data.

Table 10 shows the levels of specimen sizes and test temperatures at which J-R curves were developed in this experiment. The experimentally derived J-R curves are shown in Appendix B. All but the last two entries have toughness expressed in terms of deformation theory J. The last two curves used modified J. In most cases, duplicate tests were performed, and the data were combined for a least-squares curve fit. The equation (curve) fitted is of the same form as that used by Eason in the multivariable modeling of data bank information:

$$J_R = A(\Delta a_p)^B \exp\left[C/(\Delta a_p)^{1/2}\right], \qquad (9)$$

where:

A,B,C = curve-fitting constants,
Δa_p = physical slow-stable crack growth.

Table B1 tabulates the least-squares-derived constants of Eq. (9). These values can then be used to generate J-R curve plots. Instructions for calculating these same constants for the Eason et al. multivariable model are given in ref. 9. For the latter, upper-shelf CVN energy and other test condition parameters are used to calculate the constants applicable to Linde 80 welds, and these are presented in Table B2 (ref. 19).

Experimental and calculated constants can be compared, but it is clear that the experimental regression fit constants can be only an approximation to those derived on the basis of data from multiple tests and multiple material sources.

5.1 Specimen Size Effect on J-R Curve

Specimen size effect (experimental) was evaluated on beltline weld metal at 550°F (288°C), and the result is shown in Figure 9. A considerable spread is observed, almost all of which is attributable to the 2T specimens. The 1T and 4T specimens agree reasonably well, and the 1/2T specimens tend to show moderately lower toughness, as might have been expected. Clearly the lack of a consistent trend from 1/2T to 4T is attributable to the 2T specimens that behaved like a different material. Unfortunately, an examination of test records and evaluation of physical evidence have turned up no explainable reason for the inconsistency. Both 2T specimens came from the same through-thickness position at 3/4t, and both were from the same cutout (section 1-10) of the weld (see Figure 1). Other 2T specimens were made from this segment of the weld, and these were put into an irradiation capsule. The above observation will be kept under consideration when evaluating the postirradiation results. Size effects were not determined on nozzle weld metal because there were only 1/2T and 1T specimens.

Table 10. J-R curve test matrix

Specimen size	Number of specimens at various temperatures[a]		
	21°C (70°F)	150°C (302°F)	288°C (550°F)
Beltline			
1/2T	2	2	2
1T	2	2	2
2T	-	-	2
4T	-	-	2
Nozzle			
1/2T	-	-	2
1T	4[b]	2	2

[a]All specimens 20% side grooved unless noted otherwise.

[b]Two specimens not side grooved.

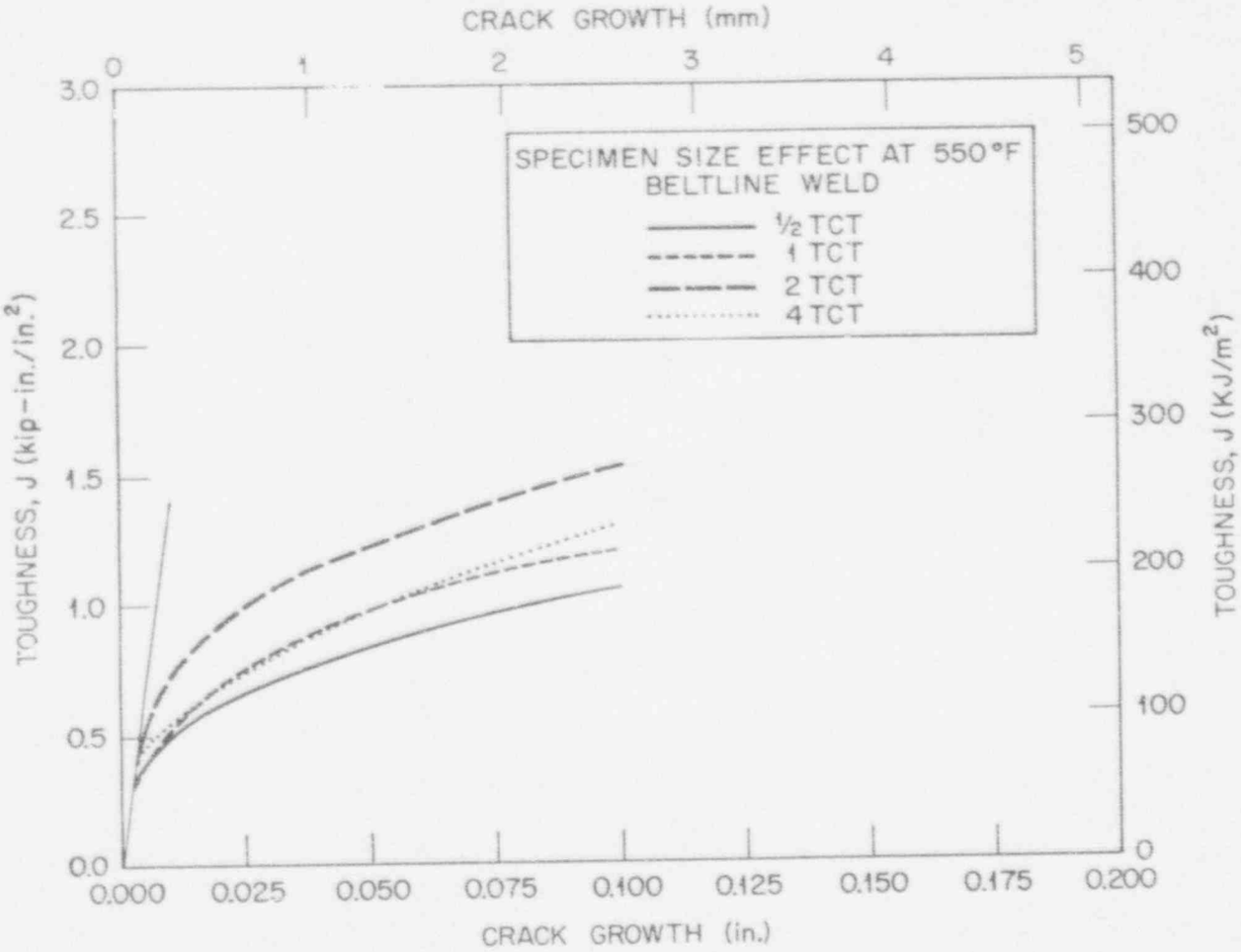

Figure 9. J-R curves of the Midland beltline weld metal with various specimen sizes at 288° C (550° F).

5.2 Evaluation of the Multivariable Model

Figures 10*(a)* through *(d)* compare WF-70 experimental J-R curves to predicted J-R curves using the 89-J (65-ft-lb) USE in the Linde 80 multivariable model. These predicted curves compare to the experimental curves quite well except, of course, for the 2T size specimens, again seeming to bring into question the experimental J-R curve result.

5.3 Effect of Test Temperature

Figures 11*(a)* and *(b)* compare experimental J-R curves over three test temperatures, one figure for 1/2T compact specimens and the other for 1T compact specimens. It is clear that slow-stable crack growth resistance diminishes with increased test temperature. There is some difference in trend between the two figures, but it is likely that this is merely a phenomenon of material property variability.

Table 11 lists J_c values determined from these J-R curves over the same temperature range plus other J_c values generated in mid-transition at 0°C (32°F).

5.4 Modified J versus Deformation Theory J

An unresolved technical issue is the proper way to calculate J-integral when the crack growth conditions of the specimens violate the validity requirements for deformation theory J. The limitations on deformation theory J for massive rigid-body plastic deformation and the tolerance for excessive slow-stable crack growth are commonly ignored, even by those that are well aware of the fundamental problems. The ASTM standard E 1152 on J-R curves allows up to 10% of the initial remaining ligament in bend-type specimens. This growth is almost certain to show some small amount of specimen size dependence. To mitigate this weakness, modified J was developed as a J-like parameter that has the property of crack growth rate independence. The desirability of a growth rate independent property from a J-like parameter had been initially pointed out by Rice et al.[18] Modified J, developed by Ernst et al.,[19] has in fact satisfied the property characteristic suggested by Rice.

Figures 12*(a)*-*(c)* compare modified J and deformation theory J fracture toughness computations. Note that the separation between the two criteria is small when Δa is small relative to initial ligament size [see Figures 12*(a)* and *(b)*]. Figure 12*(c)* shows how modified J-R curves for 1/2T and 1T specimens compare more favorably. Specimen size effects are eliminated by modified J up to the point of massive rigid-body deformation, where divergence will again develop. These J-R curves do not approach that particular limit thereby illustrating that modified J can be used to develop geometry-independent J-R curves. However, an appropriate limitation on specimen deformation, as yet undefined, needs to be established.

5.5 Comparison of Beltline versus Nozzle Weld

Experimentally determined J-R curves that compare the toughness of beltline and nozzle welds are shown in Figures 13*(a)*-*(c)*. These comparisons are made on one specimen size (1T) covering three temperature levels. There is repeated indication that the J-R curve toughness of the nozzle course weld is lower than that of the beltline weld. Again, this lower ductile tearing resistance of the nozzle weld was not detected by the upper-shelf CVN energy.

5.6 Specimens with Side Grooves versus Specimens Without Side Grooves

J-R curve specimens are almost always side grooved to control crack shape, as advised in the ASTM J-R curve test practice.[10] However, side-groove depth (and even the complete absence of side grooves) is not a controlled requirement in the ASTM test standard. Any presumption that J-R curve is not significantly affected by side-groove practice would be wrong, as evidenced by Figure 14*(a)*. The difference in J-R curve slope between 0 and

ORNL-DWG 93-13865

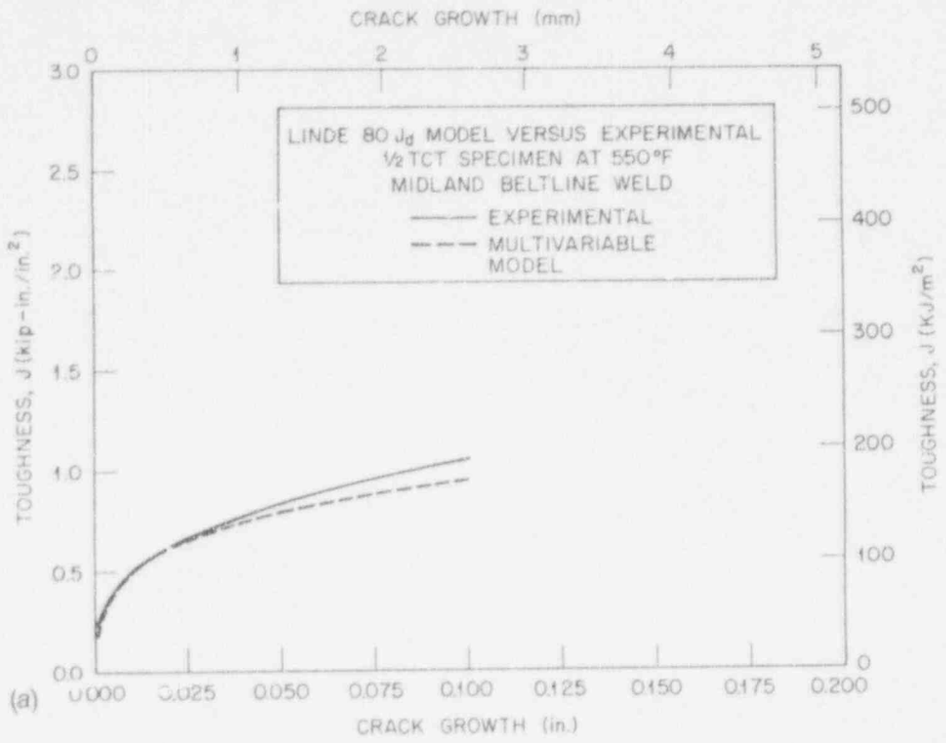

ORNL-DWG 93-13868

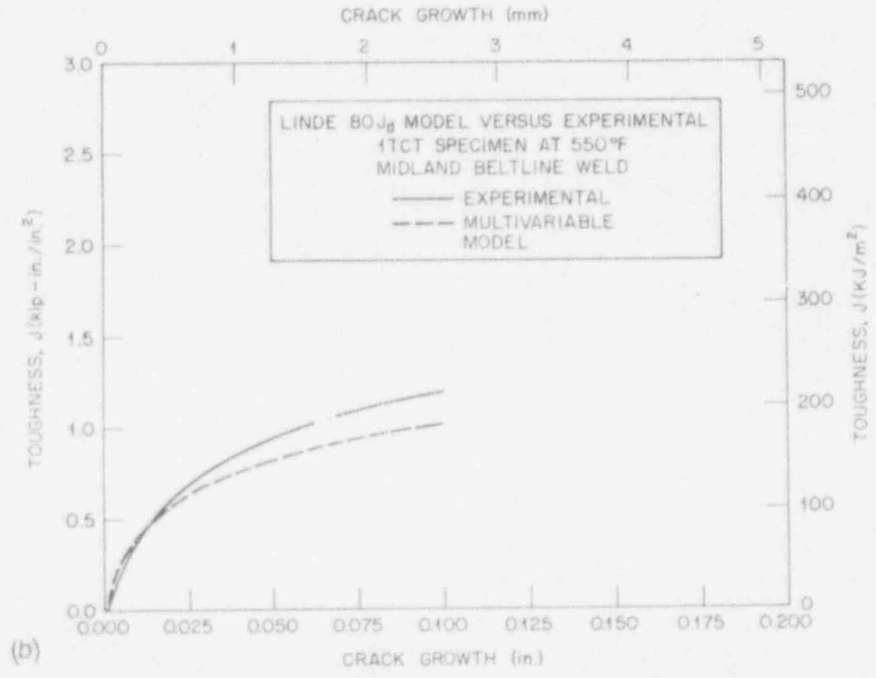

Figure 10. Experimental J-R curve and J-R curve calculated from a Multivariable model for (*a*) 1/2T compact specimen, (*b*) 1T compact specimen, (*c*) 2T compact specimen, and (*d*) 4T compact specimen.

ORNL-DWG 93-13878

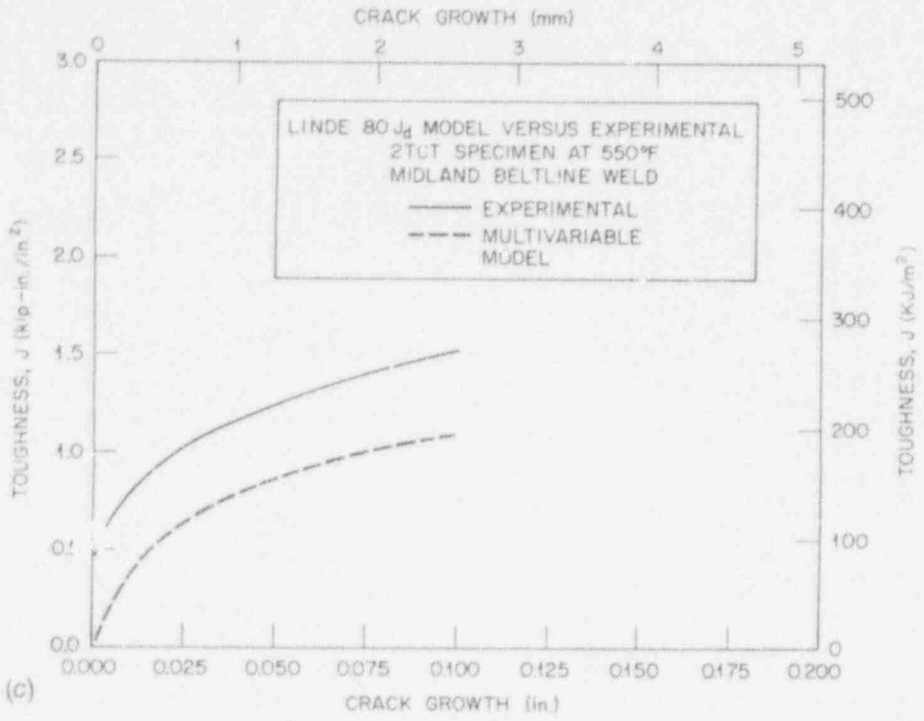

(c)

ORNL-DWG 93-13866

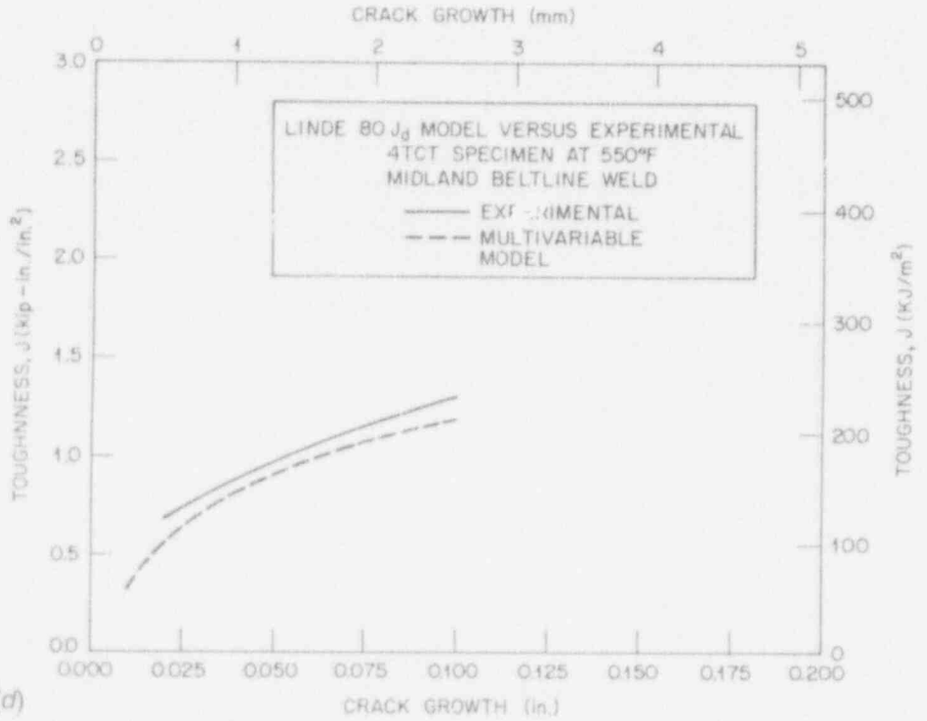

(d)

Figure 10 cont.

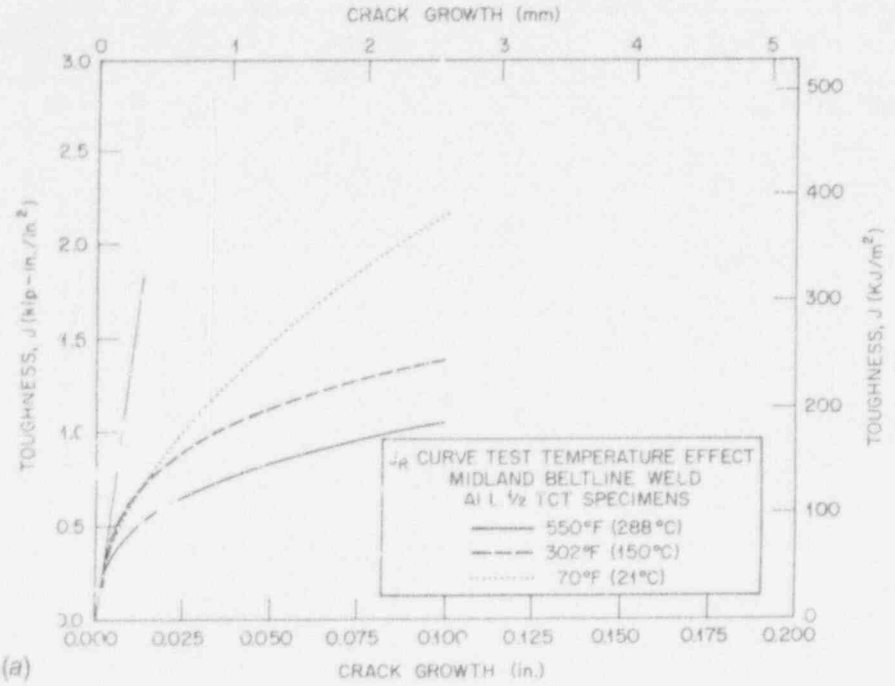

(a)

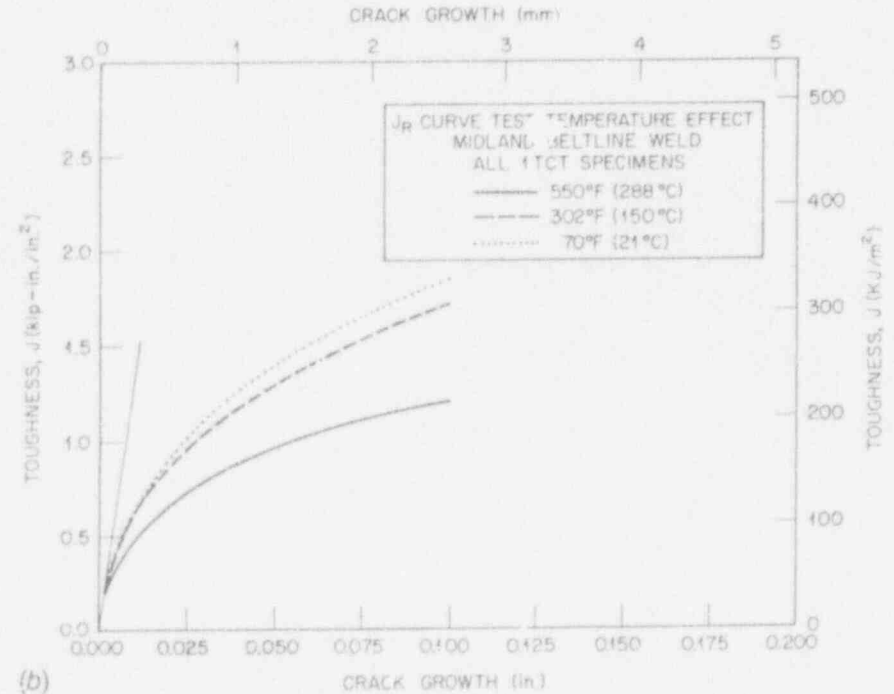

(b)

Figure 11. Effect of test temperature on J-R curve of WF-70 weld metal for (*a*) 1/2T compact specimens and (*b*) 1T compact specimens.

Table 11. Average J_{Ic} values from J-R curves

Specimen size	J_{Ic} values [kJ/m (in.-lb/in.^{2})]			
	0°C (32°F)	21°C (73°F)	150°C (302°F)	288°C (550°C)
Beltline				
1/2T	160 (920)	130 (740)	115 (670)	85 (495)
1T		130 (750)	120 (685)	75 (435)
2T				150 (850)
Nozzle				
1/2T	120 (700)	125 (725)	85 (500)	55 (320)
1T				
2T				

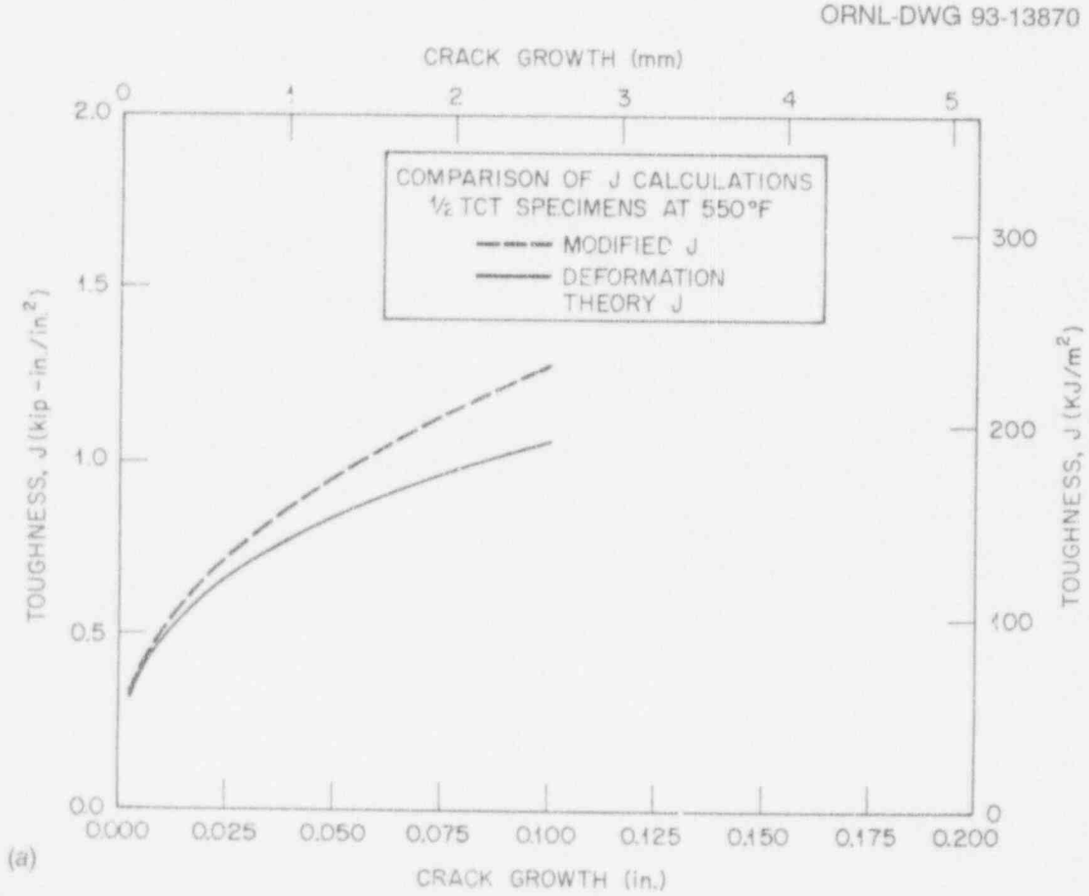

Figure 12. J-R curve comparison on beltline weld metal showing (*a*) specimen size effect on 1/2T compact specimens, (*b*) less size effect for larger 1T compact specimens, and (*c*) comparison on 1/2T compact modified J versus deformation theory J on R-curve for 1T compact specimens.

ORNL-DWG 93-13871

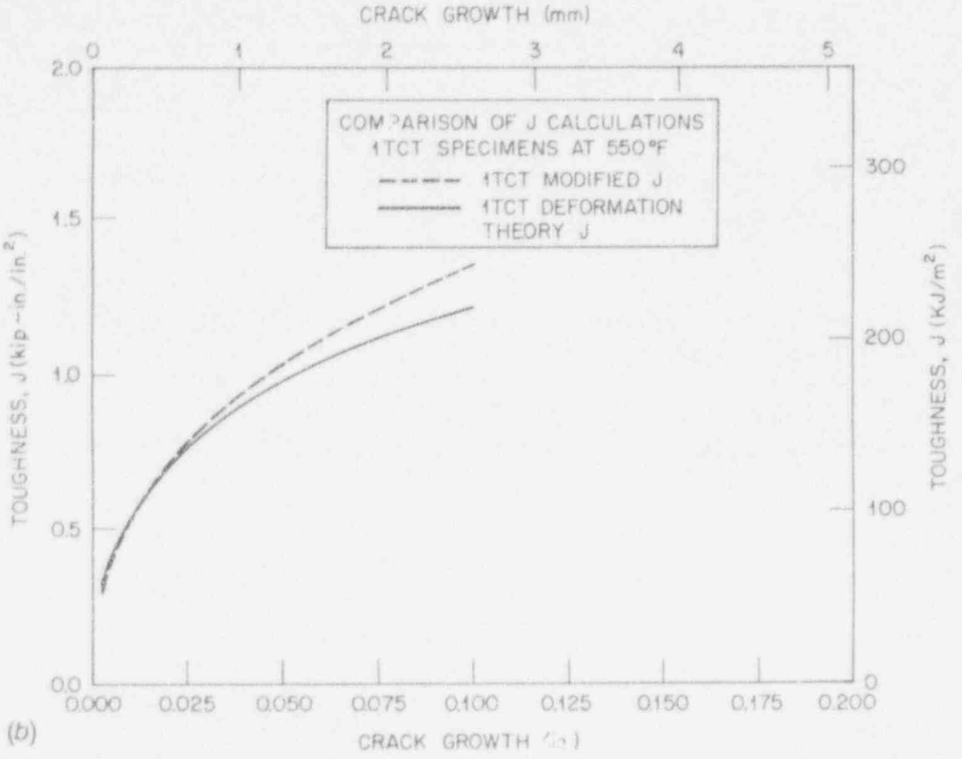

(b)

ORNL-DWG 93-13872

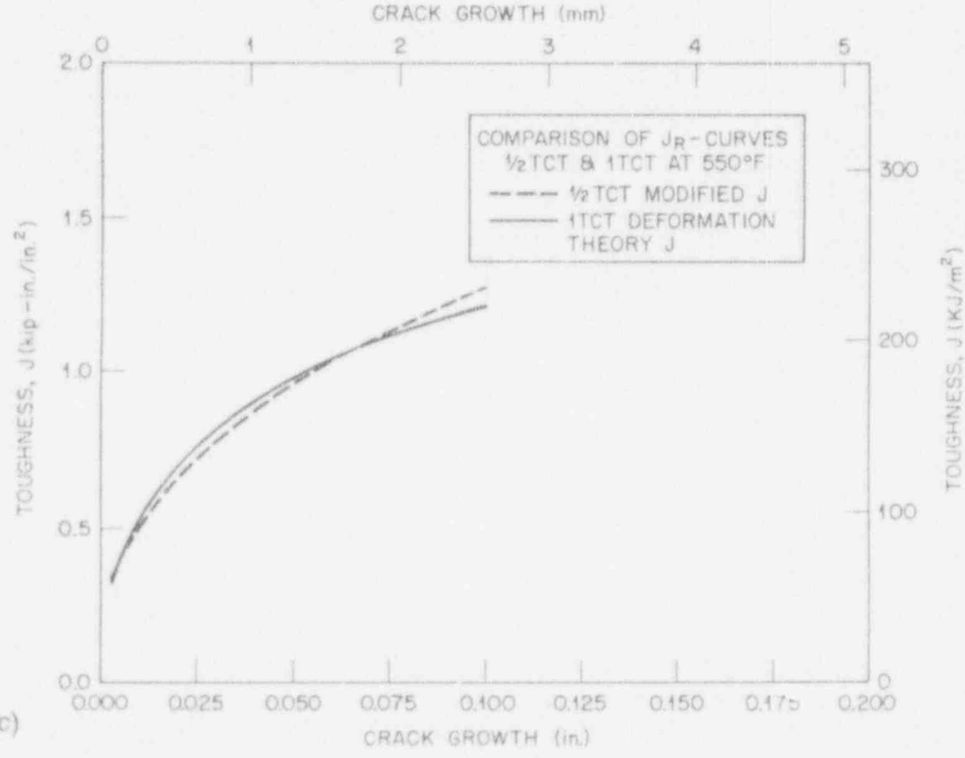

(c)

Figure 12 cont.

ORNL-DWG 93-13873

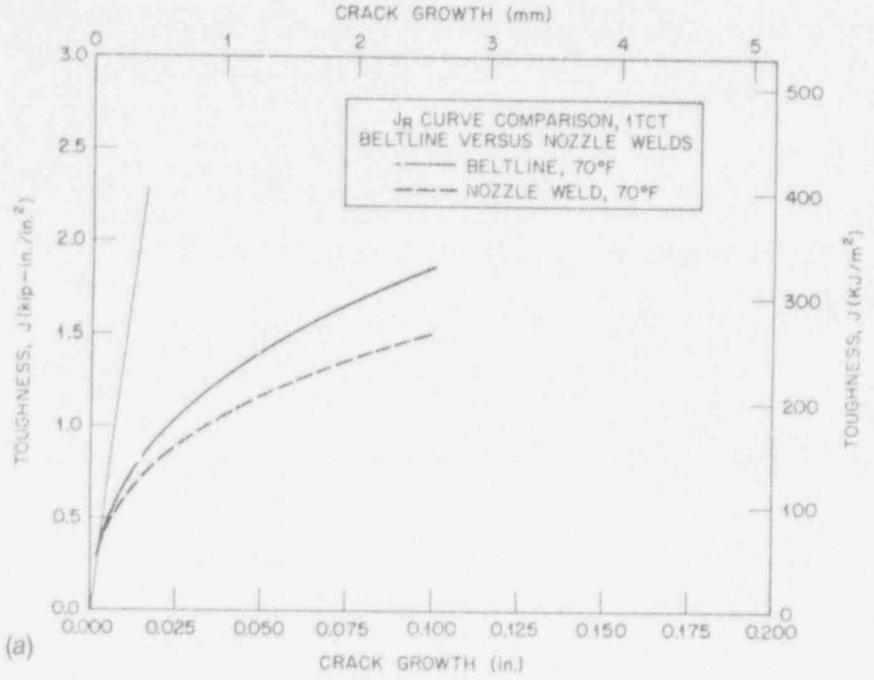

(a)

ORNL-DWG 93-13874

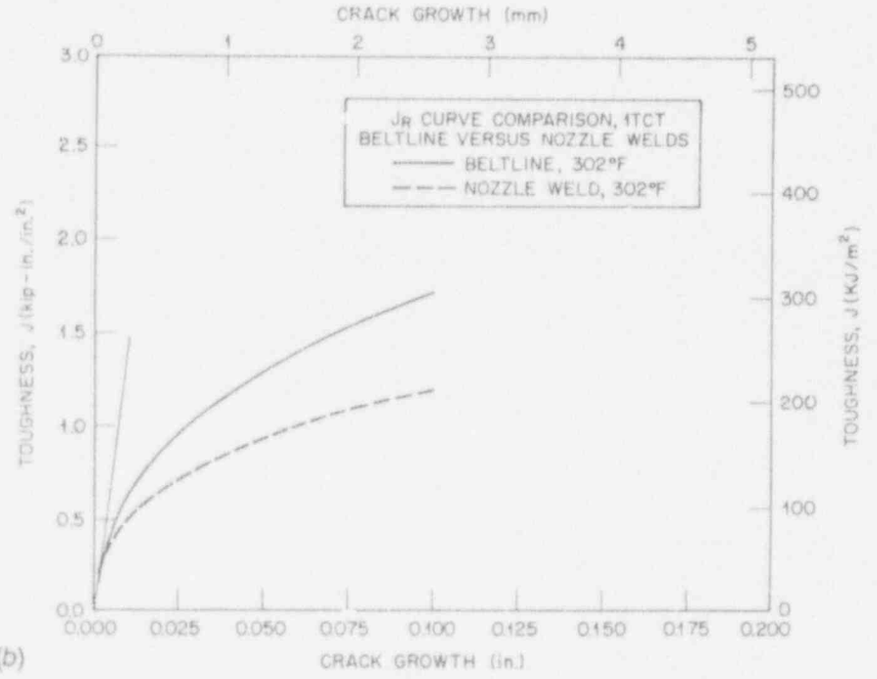

(b)

Figure 13. J-R curves that compare the nozzle versus the beltline weld metal ductile tearing resistance at (*a*) 550° F (288° C), (*b*) 302° F (150° C), and (*c*) 70° F (21° C).

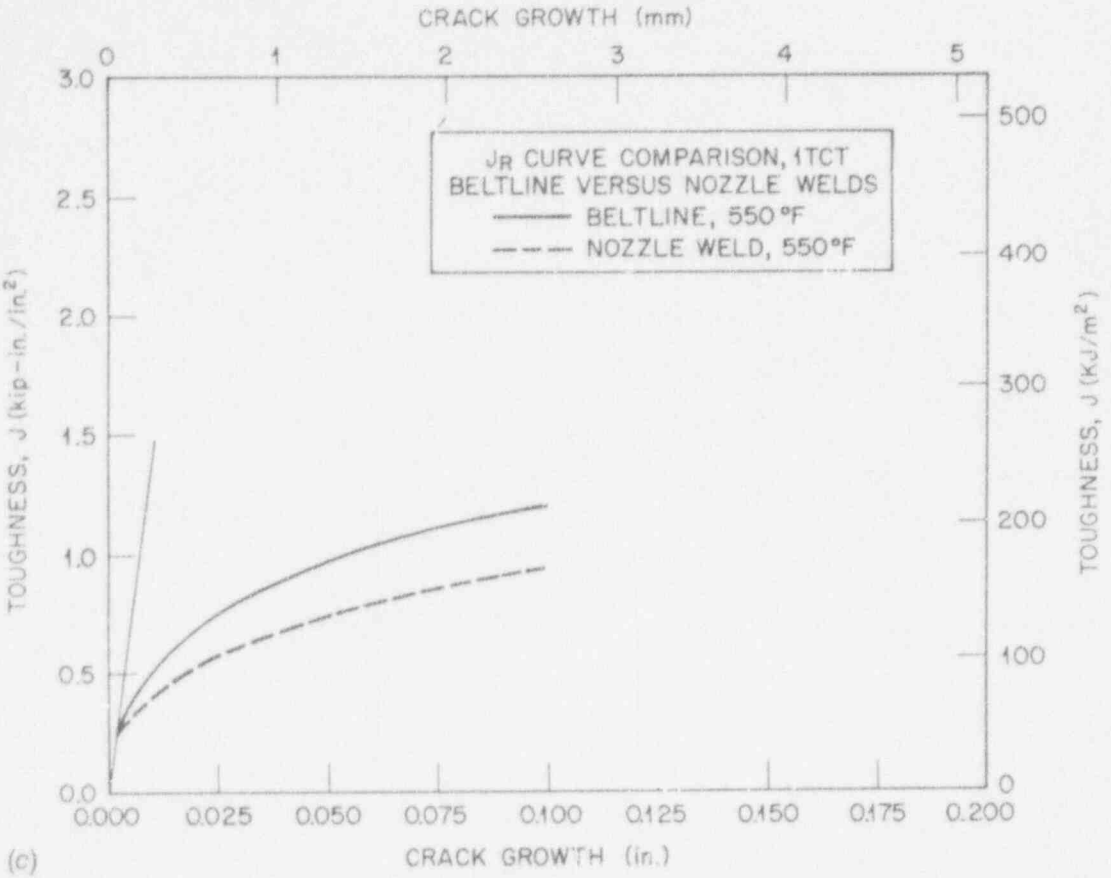

(c)

Figure 13 cont.

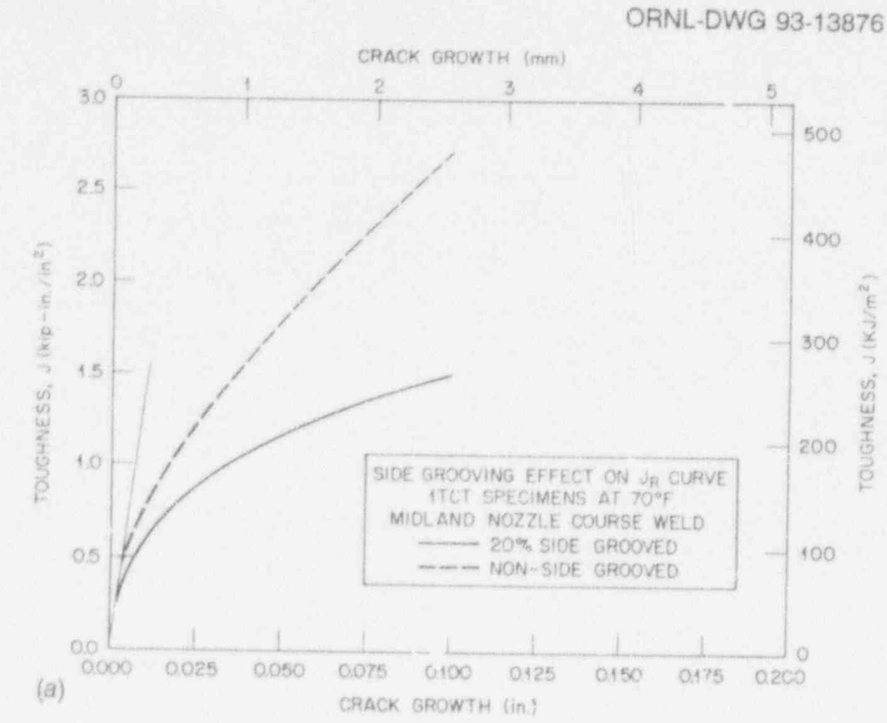

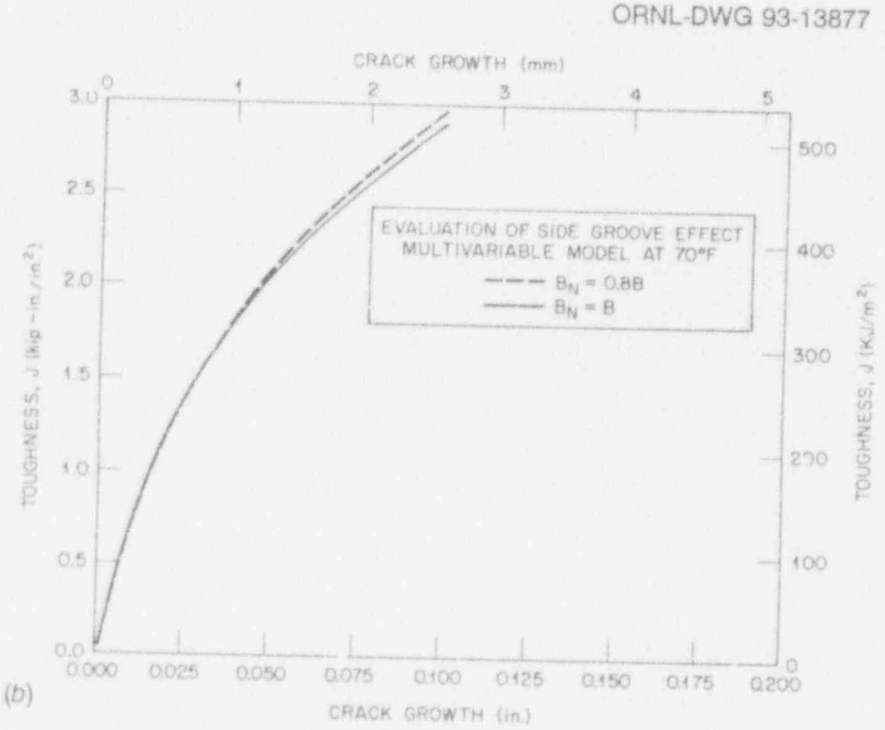

Figure 14. (*a*) J-R curves comparing the effect of side grooving on the nozzle course weld metal. Both are legitimate by ASTM standard E 1152-87. (*b*) Evaluation of the side-groove effect by the multivariable model showing the danger of misuse outside the range of the data fit.

20% side groove used here is about a factor of 2. It should be noted, however, that crack growth was measured by compliance in both cases. There almost always is some inaccuracy of crack size determination on thick specimens without side grooves.[20] In this case, there was an approximate 25% lag of Δa_p behind the 9-point heat tint measurement of final crack size. On the other hand, if each compliance calculated Δa_p is adjusted 25% to compensate for the error, the influence on the dashed line would be relatively minor, and the J-R curve difference remains highly significant. The disturbing aspect of this is that valid J-R curves developed in conformance with an ASTM standard practice can be radically manipulated through side-groove practice. It is also well known that J-R curve slope is a function of side-groove depth without an asymptotic lower bound characteristic, at least up to 50% side groove. Because there is the potential to manipulate apparent material toughness by side-groove practice should be given attention in analyses that relate to safety issues.

The impact of side grooving as viewed by the multivariable model will not indicate significant effect, as is illustrated in the example test case in Figure 14*(b)*. Here, the comparison is made assuming two 1T compact specimens, one without side grooves and one with 20% side groove. The reason for this insensitivity is that the input data used to develop the multivariable models came from side-grooved specimens. The data mix was dominated by specimens within a rather narrow range of 20 to 25% side groove so that the side-groove depth effect on J-R curve is ingrained within the model. The positive side of this is that the multivariable J-R curve estimations, unlike test data, cannot be manipulated to give nonconservative J-R curves.

6. Crack-Arrest Testing, K_{Ia}

The crack-arrest fracture toughness was determined using a specimen with plantform dimensions of the basic 2T compact specimen (see Figure 15). The specimen thickness is not proportional to the conventional 2T design, however, being 25.4 or 33 mm (1 or 1.3 in.) instead of 50.8 mm (2 in.). The crack tips had a brittle weld bead made with McKay DWT stick electrode.

During testing, it was discovered that the running crack introduced by the brittle weld bead would prematurely pop-in at low loads and then arrest in the heat-affected zone (HAZ) of the weld. With continued wedge loading, cleavage cracks would then initiate from the much tougher HAZ material at high-crack drive and often times with some prior slow-stable crack growth. As a result, crack arrest would occur with small remaining ligaments, and the validity conditions of ASTM test standard E 1221-88 on "Determining Plane-Strain Crack-Arrest Fracture Toughness, K_{Ia}, of Ferritic Steels,"[21] were violated. This occurred in all cases but with one exception. One specimen made to 3T plantform dimensions produced one valid K_{Ia} datum (see Table 12 and Figure 16). Even though the majority of the data is invalid according to the stringent requirements of E 1221-88, there is evidence that the ASTM validity requirements may be overly conservative for pressure vessel steels in general and LUS materials in particular. The validity criteria within E 1221-88 are currently being reviewed by the cognizant committee within the ASTM.

The data, while almost entirely invalid, fit well above the American Society of Mechanical Engineers (ASME) K_{Ia} curve when the bounding values determined for the RT_{NDT} of the Midland weld, -20 to 37°C (-3 to 99°F), are used for its indexing (see Figure 16). It is interesting to note that the lower bound of the crack-arrest data coincides exactly with the ASME K_{Ia} curve when -50°C (-58°F) is used as the RT_{NDT} indexing value. While the value of -50°C is in agreement with the average NDT value, it is significantly lower than the established range of RT_{NDT} values which, for the Midland weld, were controlled by its CVN behavior.

Recently, there has been some interest in a K_{Ia} curve estimation scheme that uses instrumented CVN test records.[22] Such is feasible because it is possible to detect the onset of unstable cleavage crack propagation and subsequent crack arrest from load-time traces. The relevant test records occur within a narrow temperature window, just above the lower-shelf region of the Charpy transition temperature curve.

Example test records from the instrumented Charpy machine are shown in Figures 17*(a)-(c)*. Figure 17*(a)* is from a specimen tested on the lower shelf at -25°C (-13°F). The sharp load drop beyond maximum load to near zero load is indicative of cleavage to nearly complete separation of the specimen. Figure 17*(b)* shows the upper-shelf behavior at 25°C (72°F) where there is crack initiation and stable ductile tearing to specimen separation. Figure 17*(c)* at 0°C (32°F) is characteristic of transition range behavior where there is cleavage crack initiation followed by crack arrest. Here, the specimen displacement rate is a little slower in mid-transition, allowing the striker to catch up with the displacement rate of the specimen at load, P_a. The arrest load obtained from several test records through the transition range can be plotted against test temperature, as shown in Figure 18. A calibration load has been suggested for the development of a correlation between P_a (arrest load) and K_{Ia} curves. Wallin[22] has chosen the load of $P_a = 4$ kN (900 lb) to correlate to K_{Ia} data. Temperature, $(T_o)_{Ia}$, is defined as the temperature where the median of K_{Ia} data scatter is about 100 MPa$\sqrt{m}$. This is predicted from the following equation:

$$(T_o)_{Ia} = T_{F4} - 10°C. \qquad (10)$$

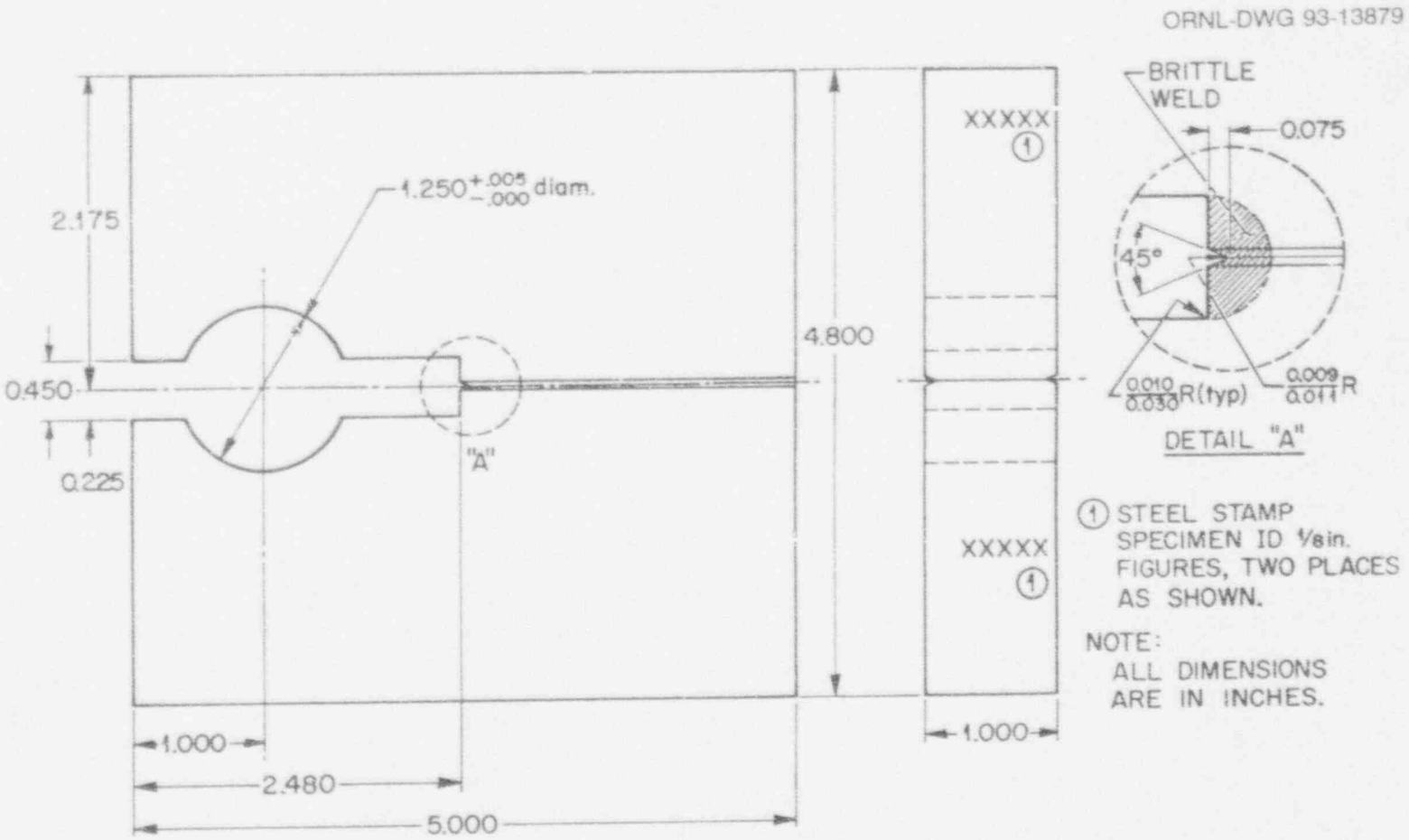

Figure 15. Crack-arrest specimen of 2T planar proportionality.

Table 12. Crack-arrest toughness values, K_a, of submerged-arc weld from the beltline region of the Midland reactor pressure vessel measured using specimens with a nominal width of 104 mm (4 in.), except for specimen MW 15JC, with a nominal width of 150 mm (6 in.)

Specimen	Test temperature		Crack-arrest toughness, K_a		Validity* and comments
	°C	°F	MPa√m	ksi√in.	
MW12A1B	-40	-40	58.5	53.2	a,b
MW12EBB	-40	-40	75.3	68.4	a,b.e
MW12A1	-30	-22	76.3	69.4	a,b,e
MW12D1A	-30	-22	78.7	71.5	a,b,e
MW12HBB	-30	-22	91.8	83.4	a,b,e
MW12EAB	-30	-22	93	84.5	a,b
MW12GAB	-25	-13	92.9	84.4.	a,b
MW15JC	-20	-4	65.3	59.4	*Valid*, 150 mm spec
MW15HAA	-20	-4	101.1	91.9	a,b
MW12FBB	-20	-4	148.4	134.9	a,b,c,e
14DRW34	-10	14	107.5	97.7	a,b,e
MW12HBA	0	32	90	81.8	a,b
MW12HAA	10	50	95.4	86.7	a,b,e

*One or more letters for a specimen indicate that the test results did not meet requirements of the ASTM E 1221-88 validity criteria. a,b = remaining ligament too small; c = specimen too thin; d,e = insufficient crack-jump length.

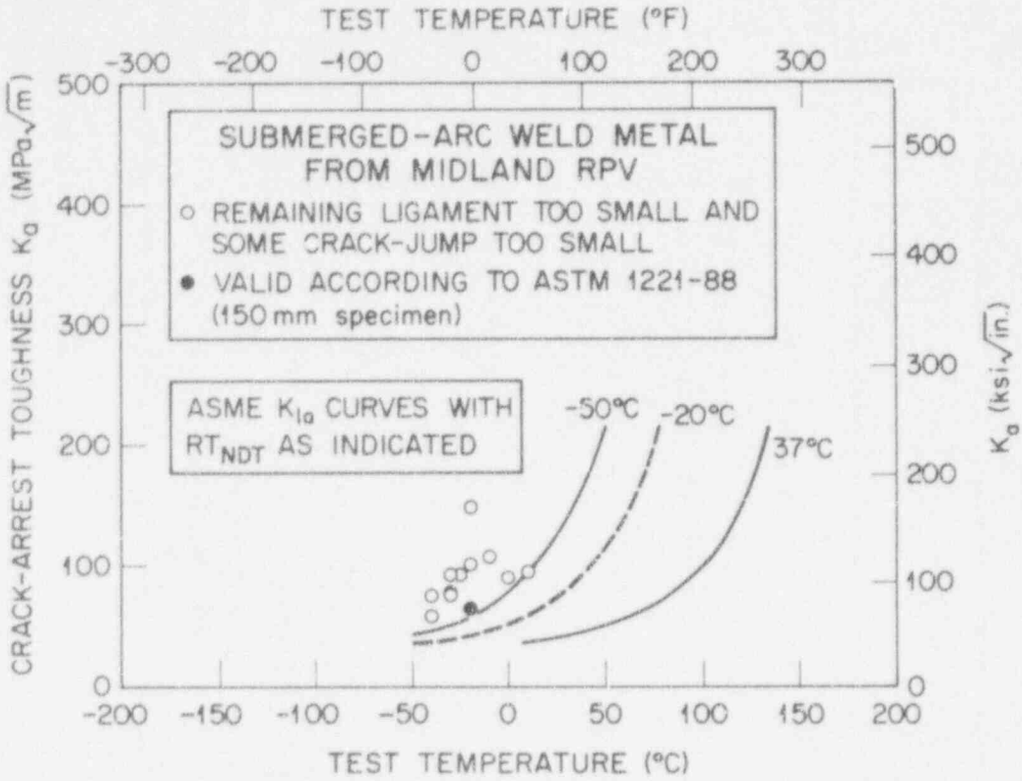

Figure 16. Crack-arrest data for Midland beltline weld metal. The data are compared to the ASME lower bound K_{Ia} Curves established from RT_{NDT} = 37° C (99° F), RT_{NDT} = -20° C (-4° F), and hypothetical RT_{NDT} = -50° C (-58° F).

ORNL-DWG 93-13861

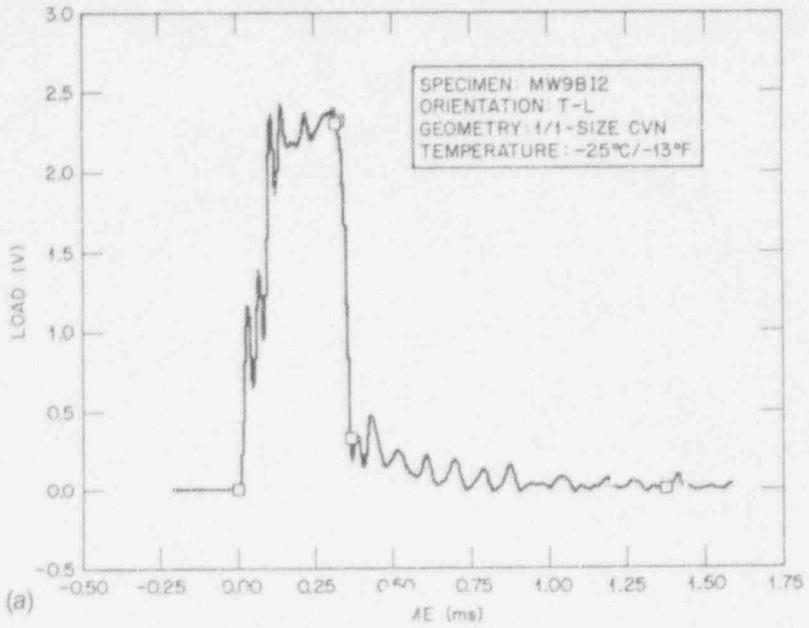

(a)

ORNL-DWG 93-13862

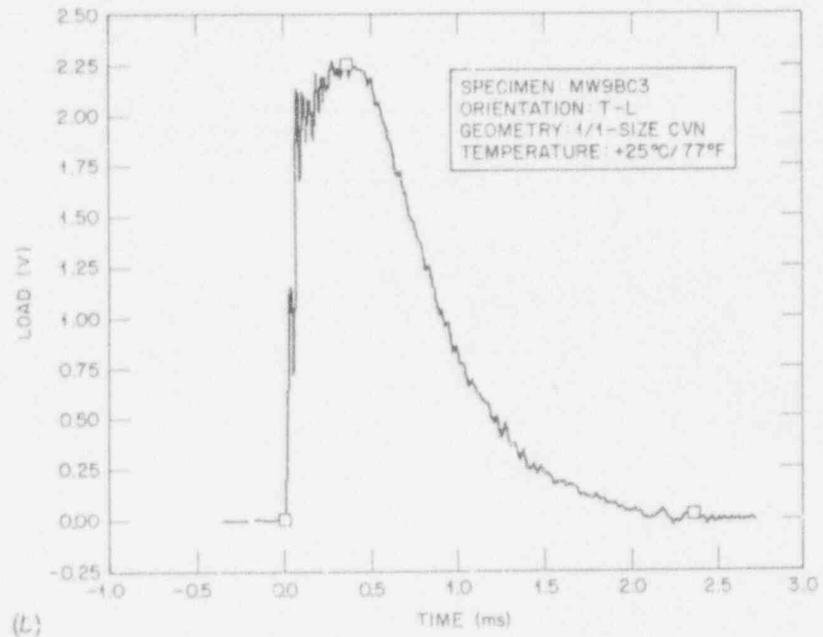

(b)

Figure 17. Load-time traces for a Charpy specimen of the beltline weld metal: (*a*) Tested on the lower shelf (note low crack-arrest load), (*b*) tested on the upper shelf (ductile tearing beyond the maximum load), and (*c*) tested in the transition range (note crack-arrest load, P_a).

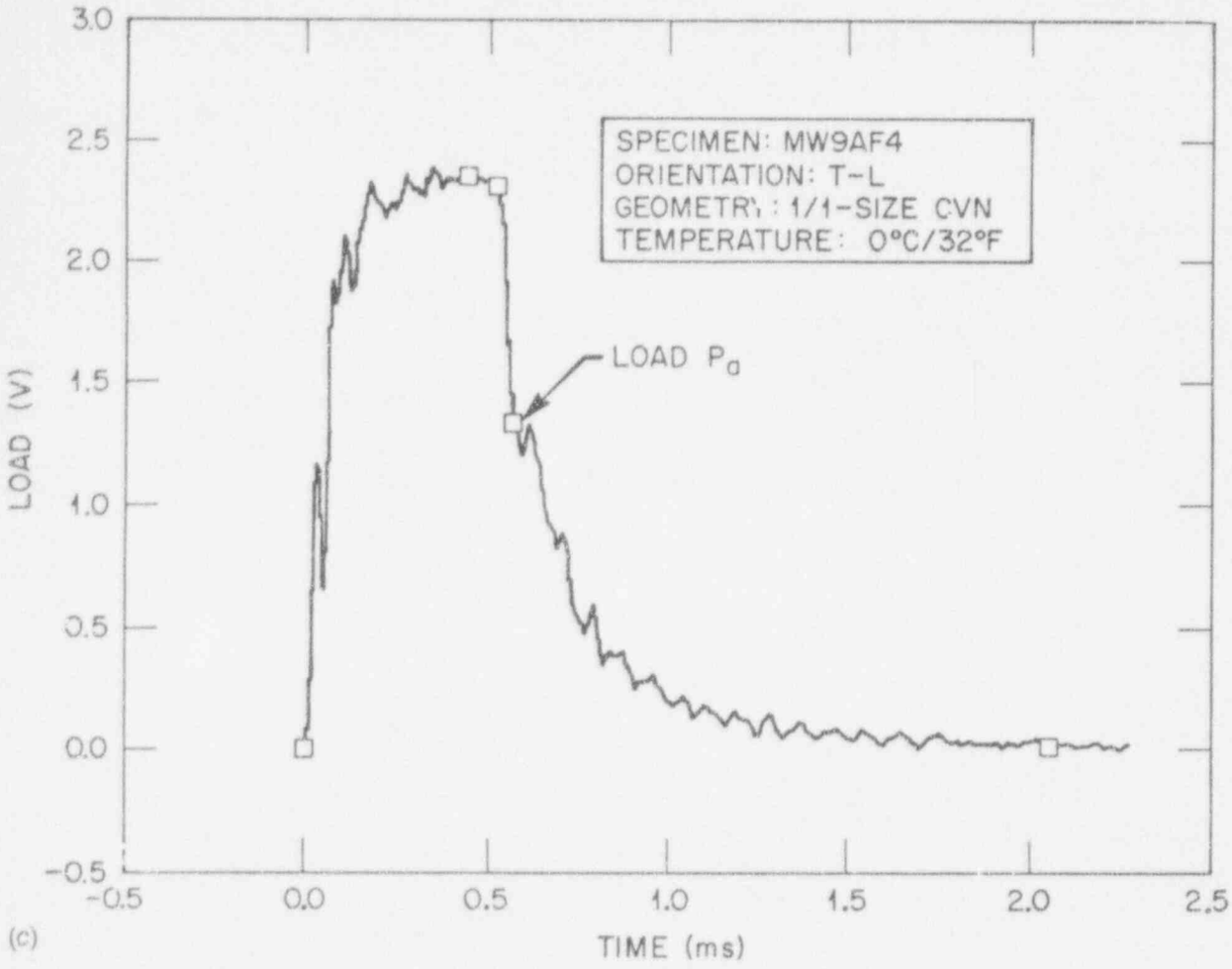

Figure 17 cont.

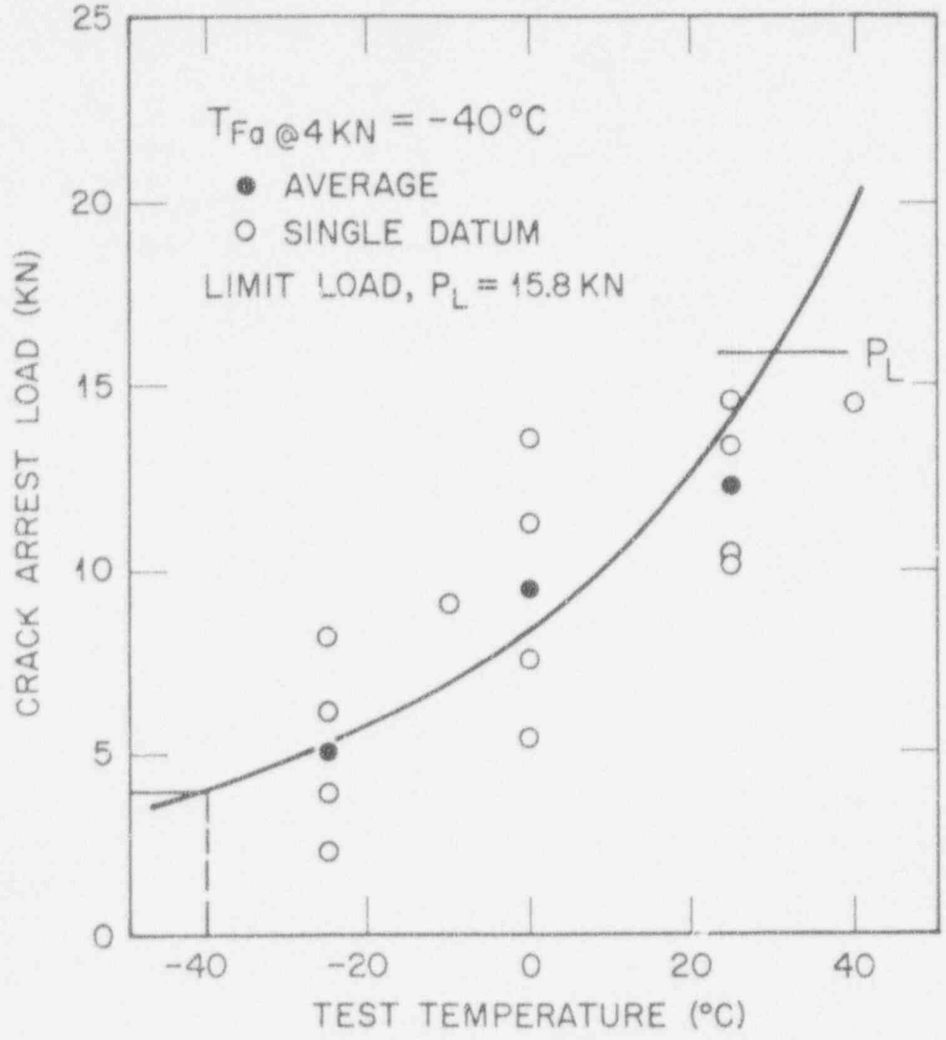

Figure 18. Plot of crack-arrest loads for the beltline weld metal obtained from test records similar to Figure 17(c).

It appears that T_{F4} in Figure 18 is -40°C (-40°F) and so the estimate for $(T_o)_{Ia}$ is -50°C (-58°F). Wallin has maintained that the universal crack-arrest median K_{Ia} curve has the same shape as the previously mentioned master curve. Temperature $[(T_o)_{Ia}]$ is inserted into the following relationship for median K_{Ia}:

$$K_{Ia} = 30 + 70 \exp\{0.019[T - (T_o)_{Ia}]\}. \quad (11)$$

Experimentally determined K_a (invalid data) is fitted with the master curve and 95% confidence curve in Figure 19. In this case, T_o [replacing T_o in Eq. (11)] of about -10°C (14°F) was indicated. Hence, the CVN inferred $(T_o)_{Ia}$ differed by about 40°C (50°F) from the experimental data. It is clear that more evaluation work is needed. A supporting data package of valid K_{Ia} values would be of more help in the evaluation.

ORNL-DWG 94-6595

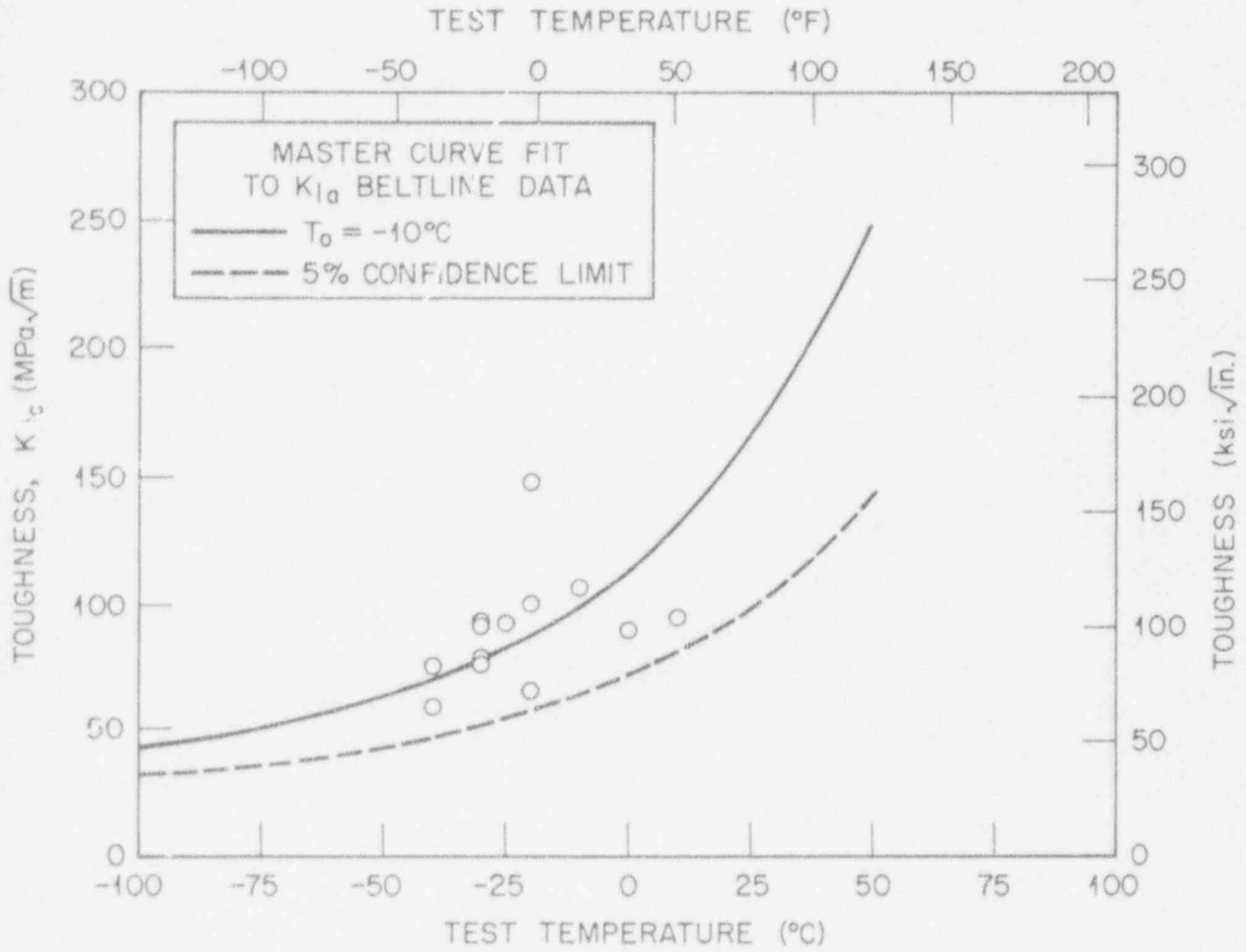

Figure 19. K_{Ia} experimental data from crack arrest in specimens similar to Figure 15; reference temperature, T_o, is -10°C (14°F).

7. Discussion

The present data development work on the Midland WF-70 weld metal has provided good baseline properties to compare to the irradiation-damaged properties. The nozzle weld metal has been singled out from the beltline weld metal as a different material on the basis of copper content, determined in the initial scoping work. At the same time, Charpy transition curves and DWT NDT tests reported in the same early work indicated no difference in the fracture properties. However, fracture mechanics tests in this report clearly indicated a difference in fracture toughness transition temperature of 27°C (81°F) between nozzle course and beltline welds. Likewise, J-R curves indicated lower ductile tearing resistance in the nozzle course weld, and tensile tests showed the nozzle weld to have higher strength.

Because none of the 19 beltline CVN transition temperature curves or six nozzle course curves had developed at least 103-J (75-ft-lb) USE, these materials were verified to be LUS weld metal. The 19 sampling positions for beltline Charpy curves produced 19 RT_{NDT} temperatures varying from +37°C (+99°F) to -20°C (-4°F). The application of these 19 RT_{NDT} values to position the ASME lower bound K_{Ic} curve covers the area bounded by the dashed lines shown in Figure 20. The fracture toughness data in the form of static K_{Jc} were shown to be almost bounded by an ASME K_{Ic} curve using a reference temperature, RT_{NDT}, of -50°C (-58°F) from the DWT NDT tests. Likewise, the K_a data were bounded using this same reference temperature. However, ASME acceptance standards in Section III (NB-2331) stipulate the use of Charpy curves such as might be applied in the plant-specific analysis which, for Midland, could position the lower bound K_{Ic} curve for design over a relatively wide range of temperatures. Clearly, the assessment of the material embrittlement would be a matter of probability, making the decision to license a plant for continued operation dependent on sampling location and chance ordering of the Charpy specimens.

A ductile-to-brittle transition temperature (DBTT) procedure that uses fracture mechanics test practices is currently under development in a task group activity within ASTM. This method addresses the statistical variability of material toughness as a part of the analysis procedure. Six 1/2T compact specimens of nozzle weld and six 1/2T specimens of beltline weld were used to set up master curves that define the transition toughness and confidence limits on scatter for data obtained from all specimen sizes. This method of material characterization has worked quite well in this case.

J-R curves were developed on beltline and nozzle course weld metals. Both showed loss of ductile tearing resistance with increased test temperature from room temperature to 288°C (550°F). There also was convincing evidence of a difference in J-R curve toughness between beltline and nozzle weld metals. This difference did not show up in the upper-shelf Charpy energy determinations, both indicating about 89-J (65-ft-lb) USE.

The multivariable model of Eason et al. to develop J-R curves from Charpy USE was tested against the experimental J-R curves. The model for Linde 80 welds was used. The comparison of predicted versus experimental J-R curve for beltline weld was quite decent in this case. An unavoidable weakness of the methodology, however, is the use of Charpy USEs that tend to lack the sensitivity needed to detect subtle changes in J-R curve toughness.

Side-grooving of compact specimens was evaluated on a relatively small scale within this experiment. It was determined that the choice between side grooving or not K_{Jc} (transition range) testing is not significant. On the other hand, side grooving is a major variable in J-R curve development. In this experiment, J-R curve slope was shown to be increased by a factor of about two without side grooves. Side-grooving recommendations in ASTM Standard E 1152 ("Standard Test Method for Determining J-R Curves") fail to point out or emphasize the significance of such considerations. Side-groove depth has an important impact on J-R curves.

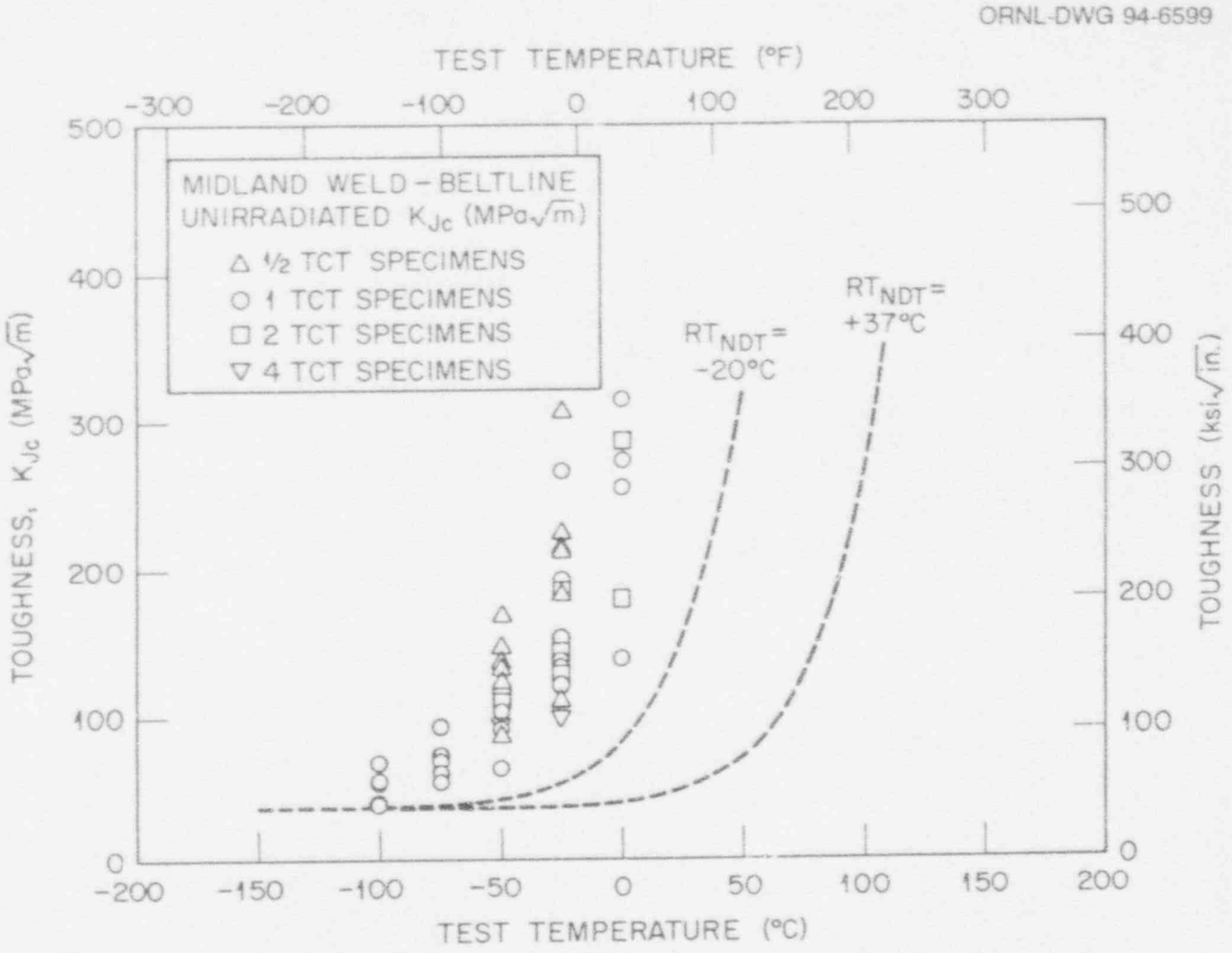

Figure 20. K_{Jc} data from the beltline weld metal tested in four specimen sizes. The data are compared to the ASME lower bound K_{Ic} established from RT_{NDT} = 37° C (98.6° F) and RT_{NDT} = -20° C (-4° F).

Crack-arrest tests were performed on beltline weld metal with a great deal of difficulty. A new brittle weld bead crack starter material (McKay DWT) was used to control crack initiation, but because of easy crack pop-in in the brittle bead, most cleavage cracks initiated from the HAZ of these brittle zone welds. Consequently, initiation K_i was high and ligament size at arrest was nearly always too small for K_{Ia} validity. As a result, the accuracy of the K_{Ia} values reported here can be questioned. The transition temperature shift from static to dynamic appeared to be about 50 K, which seems a bit high. Nonetheless, there is reason to believe that the crack-arrest data may be representative of the material. The one valid result obtained with the larger specimen is seen in Figure 16 to correspond reasonably well with the remainder of the invalid data, even though it lies toward the lower bound of the data set. The fact that the wide range of RT_{NDT} values determined for the Midland weld bound the crack-arrest data with significantly different amounts of margin raises further questions about the applicability of using an RT_{NDT} based on Charpy properties as the correct indexing parameter for the class of LUS welds. Indeed, the overall question of the most appropriate method to adjust predictions of fracture toughness of pressure vessel materials to account for irradiation-induced embrittlement is being examined within the HSSI Program. To complement this work, a technique of inferring K_{Ia} from test records of the instrumented Charpy test was tried. In this case, the static-to-dynamic transition temperature shift was about 10°C (18°F). The ASME K_{Ic}-K_{Ia} curve shift at the 100-MPa$\sqrt{m}$ (91-ksi$\sqrt{in.}$) level is on the order of 36°C (64°F), so it is difficult to draw firm conclusions on the significance of these results.

8. Plans for Irradiated Specimens

HSSI capsules 10.05 and 10.06 contain 1/2T, 1T, and 2T compact specimens and crack-arrest specimens, as well as numerous standard notched and precracked Charpy specimens of beltline and nozzle course material. There are also sixteen 1/2T compact specimens and CVN specimens from the HSSI Fifth Irradiation Series and many other previously well-characterized materials.

The overall plan of attack for irradiation evaluations will be designed to satisfy the following objectives:

1. Establish a master curve for irradiated beltline and nozzle course welds using a few 1/2T compact specimens of each material. Compare the master curve to all the irradiated results.

2. Determine if the master curve of the irradiated materials can be established from slow-bend precracked Charpy specimens.

3. Establish the data scatter of CVN transition range data. Establish the data scatter on RT_{NDT} and ΔTT_{41J} and compare this to the fracture mechanics-based results.

4. Determine postirradiation K_{Ia} lower bound using 15 crack-arrest specimens. This evaluation would also include further exploration of crack-arrest determined by instrumented Charpy impact tests.

5. Evaluate the effect of irradiation on J-R curve for WF-70 weld metal. Also, compare experimental and multivariable copper-fluence model predicted J-R curves.

1

IMAGE EVALUATION TEST TARGET (MT-3)

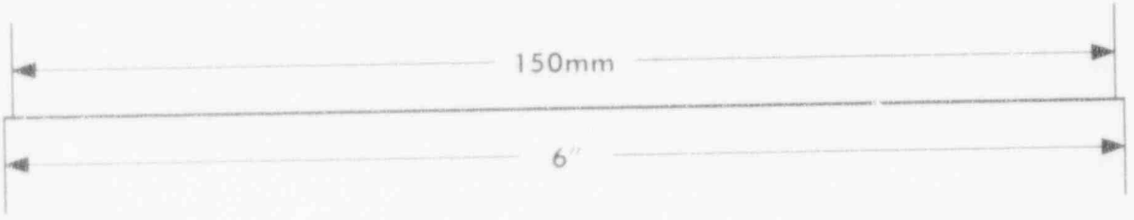

1

IMAGE EVALUATION TEST TARGET (MT-3)

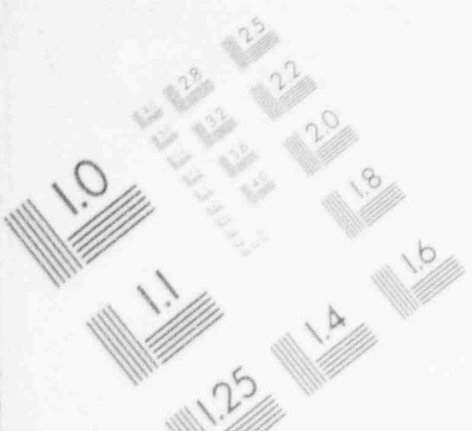

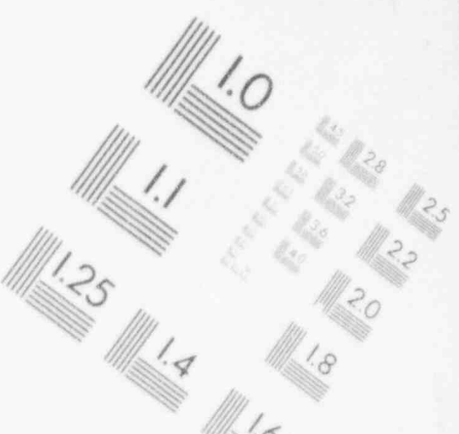

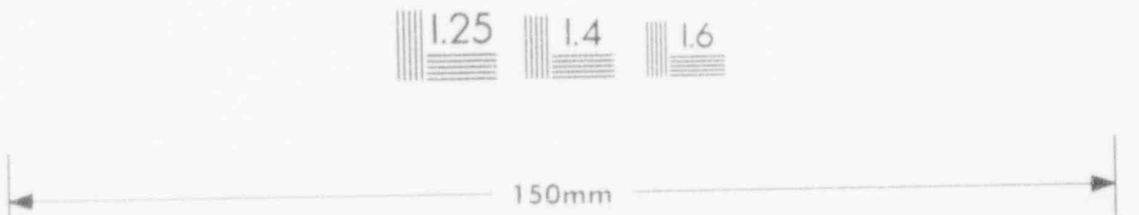

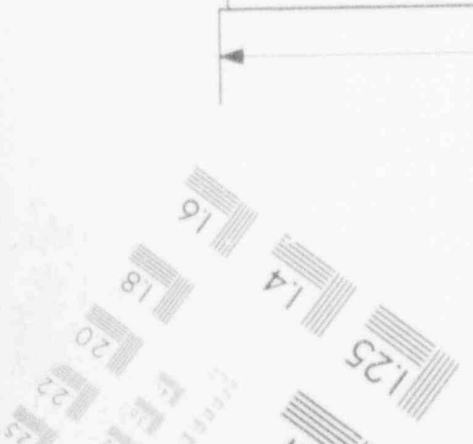

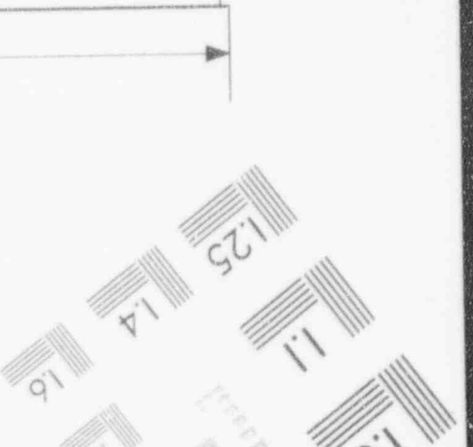

1

IMAGE EVALUATION TEST TARGET (MT-3)

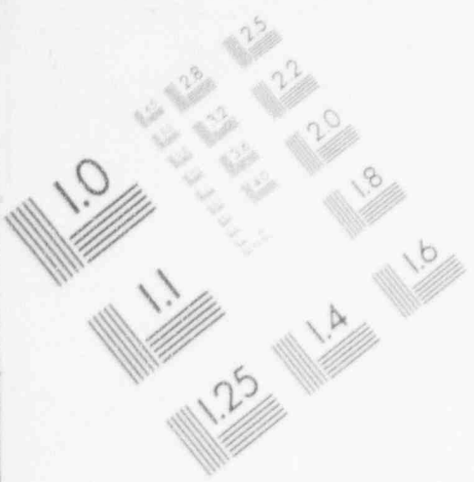

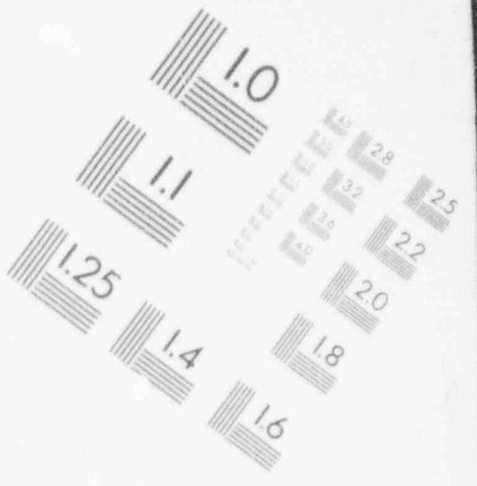

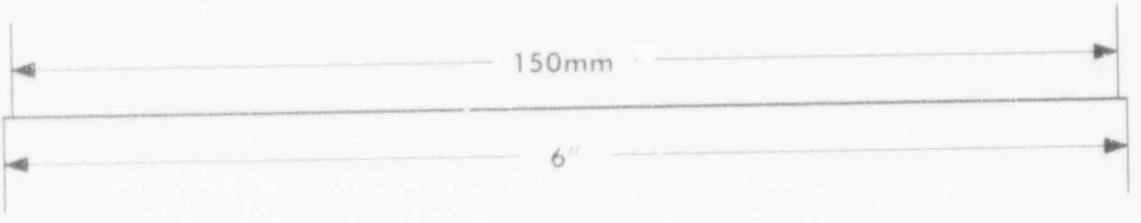

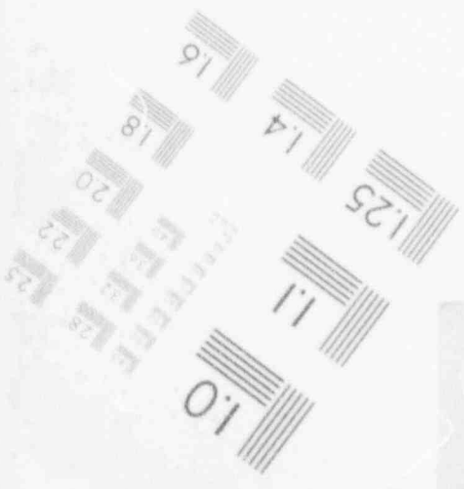

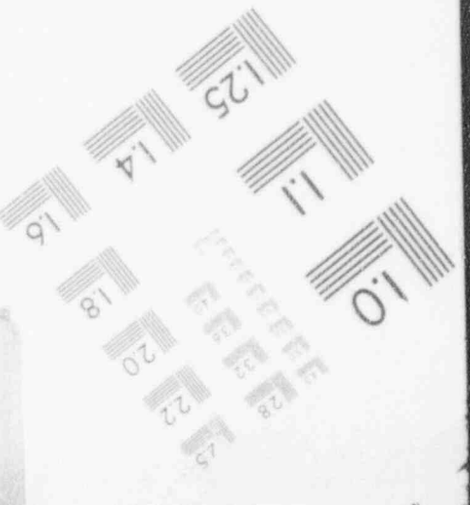

9. References

1. B&W Owners Group, Materials Committee of the Reactor Vessel Integrity Program, WF-70 Evaluation Program, Review Meeting with NRC, B&W Nuclear Service Company, Lynchburg, Va., June 13, 1991.*

2. *ASME Boiler and Pressure Vessel Code. An American National Standard*, Sect. III, NB-2331, American Society of Mechanical Engineers, New York, 1986.†

3. "Title 10," *Code of Federal Regulations*, Part 50, U.S. Government Printing Office, Washington, D.C., January 1987.†

4. *Standard Test Method for Conducting Drop-Weight Test to Determine Nil-Ductility Transition Temperature for Ferritic Steels*, ASTM E 208-91, American Society for Testing and Materials, Philadelphia, 1992.†

5. R. K. Nanstad, D. E. McCabe, F. L. Swain, and M. K. Miller, Martin Marietta Energy Systems, Inc., Oak Ridge Natl. Lab., *Chemical Composition and RT_{NDT} Determinations for Midland Weld WF-70*, USNRC Report NUREG/CR-5913 (ORNL-6740), December 1992.‡

6. R. K. Nanstad, D. E. McCabe, B. H. Menke, S. K. Iskander, and F. M. Haggag, "Effects of Radiation on K_{Ic} Curves for High-Copper Welds," pp. 214-33 in *Effects of Radiation on Materials: 14th International Symposium (Vol. II)*, ed. N. H. Packan, R. E. Stoller, and A. S. Kumar, American Society for Testing and Materials, Philadelphia, 1990.†

7. U. S. Nuclear Regulatory Commission, *Regulatory Guide 1.99*, Revision 2, "Radiation Embrittlement of Reactor Vessel Materials," May 1988.**

8. F. M. Haggag, R. K. Nanstad, and D. N. Braski, "Structural Integrity Evaluation Based on an Innovative Field Indentation Microprobe," pp. 101-7 in *Innovative Approaches to Irradiation Damage and Fracture Analysis*, PVP-Vol. 170, ed. D. L. Marriott,, T. R. Mager, and W. H. Bamford, American Society of Mechanical Engineers, New York, 1989.†

9. E. D. Eason, J. E. Wright, and E. E. Nelson, Modeling and Computing Sevices, Inc., *Multivariable Modeling of Pressure Vessel and Piping J-R Data*, USNRC Report/CR-5729 (MCS 910401), May 1991.‡

10. *Standard Test Method for Determining J-R Curves*, ASTM E 1152-87, American Society for Testing and Materials, Philadelphia, 1992.†

11. *Standard Test Method for Plane-Strain Fracture Toughness of Metallic Materials*, ASTM E 399-90, Vol. 03.01, American Society for Testing and Materials, Philadelphia, 1992.

12. K. Wallin, "A Simple Theoretical Charpy V - K_{Ic} Correlation for Irradiation Embrittlement," pp. 93-100 in *Innovative Approaches to Irradiation Damage and Fracture Analysis*, PVP-Vol. 170, ed. D. L. Marrott, T. R. Mager, and W. H. Bamford, American Society of Mechanical Engineers, New York.‡

*Available from B&W Nuclear Techonologies, P.O. Box 109 Lynchburg, VA 24506-0935

†Available in public technical libraries

‡Available for purchase from National Technical Information Service, Springfield, VA 22161.

**Available from U.S. Government Printing Office, Washington, DC 20402. ATTN: Regulatory Guide Account.

13. J. D. Landes and D. E. McCabe, "Effect of Section Size on Transition Temperature Behavior of Structural Steels," pp. 378-92 in *Fracture Mechanics: Fifteenth Symposium, ASTM STP 883*, ed. R. J. Sanford, American Society for Testing and Materials, Philadelphia, 1984.†

14. T. L. Anderson, D. Stienstra, and R. H. Dodds, "A Theorethical Framework for Addressing Fracture in the Ductile-Brittle Transition Region," pp.186-214 in *Reflections in Fracture Mechanics Research*, ASTM STP 1207, American Society for Testing and Materials, Philadelphia, 1994.†

15. K. Wallin, "The Scatter in K_{Ic} - Results," *Eng. Frac. Mech.* **19**(6), 1085-93 (1994).

16. D. E. McCabe, J. G. Merkle, and R. K. Nanstad, "A Perspective on Transition Temperature and K_{Jc} Data Characterization," pp. 215-32 in *Reflections in Fracture Mechanics Research*, ASTM STP 1207, American Society for Testing and Materials, Philadelphia, 1994.†

17. K. Wallin, "Recommendations for the Application of Fracture Toughness Data for Structural Intergrity Assessments," pp. 465-94 in *Proceedings of the IAEA/CSNI Specialists Meeting on Fracture Mechanics Verification by Large Scale Testing, Oak Ridge, Tenn., Oct. 26-29, 1992.*†

18. J. R. Rice, W. J. Drugan, and T. L. Sham, "Elastic-Plastic Analysis of Growing Cracks," pp. 128-38 in *Fracture Mechanics: Twelfth Conference*, ASTM STP 700, American Society for Testing and Materials, Philadelphia, 1979.†

19. H. A. Ernst and J. D. Landes, "Predictions of Instability Using the Modified J, J_M Resistance Curve Approach," pp. 128-38 in *Elastic-Plastic Fracture Mechanics Technology*, ASTM STP 896, American Society for Testing and Materials, Philadelphia, 1985.†

20. T. Hollstein, J. G. Blauel, and B. Voss, "On the Determination of Elastic-Plastic Fracture Material Parameters: A Comparison of Different Test Methods," pp. 104-16 in *Elastic-Plastic Fracture Test Methods: The Users Experience*, ASTM STP 8856, American Society for Testing and Materials, Philadelphia, 1992.†

21. *Standard Test Method on Determining Plane-Strain Crack-Arrest Fracture Toughness*, K_{Ia}, ASTM E 1221-88, American Society for Testing and Materials, Philadelphia, 1992.†

22. K. Wallin, *Descriptive Potential of Charpy-V Fracture Arrest Parameter with Respect to Crack Arrest K_{Ia}*, VTT-MET B-221, Technical Research Centre of Finland, Espoo, Finland, January 1993.†

†Available in public technical libraries.

Appendix A

Tabulation of Specimen Codes and K_{Jc} Values

Table A1. Test data for four specimen sizes of WF-70 beltline weld metal
(1 Mpa√m = 1.1 ksi√in.)

Test temperature (°C)	Values, K_{Jc} (MPa√m)									
	1/2T		1T				2T		4T	
	Code[a]	K_{Jc}	Code[a]	K_{Jc}	Code[a]	K_{Jc}	Code[a]	K_{Jc}	Code[a]	K_{Jc}
21			11FB	*b*	15GA	*b*				
			11FC[c]	*b*	15GB	*b*				
0			9FA	*b*	9CB[c]	274.0	10G2	180.2		
			11GC[c]	*b*	15FA	255.6	10C2	287.1		
			11GD	*b*	15GD[c]	181.6	D2	*b*		
			11IA	316.7	9IA	140.0				
-25	10EIFB	183.2	9FC[c]	266.9	9FB	143.2	12C1	184.2	14B	119.8
	11MDA	108.5	15FC	138.9	15FD[c]	119.2	10C1	144.4	14A	98.4
	11JEA	214.9	9CC	150.7			15J1	141.0		
	9HFB	220.0	11FA	193.5			10D1	124.7		
	11MCB	212.6	11GA	139.4			10B1	120.0		
	11LEA	307.6	9FD[c]	132.7						
-50	10E2F	167.3	9GA[c]	120.2			10B2	105.2		
	9LFB	146.8	11GB	118.1			10H2	108.4		
	10EIEB	137.7	11FD[c]	103.3			12C2	97.7		
	10EIEA	131.1	15GC[c]	91.9			12D1	115.0		
	10EIFA	119.3	15FB	88.4			15J2	94.0		
	10E2E	91.6	9CD	65.0						
-75			10EIB	93.8						
			10EIA	67.7						
			10EIC	72.2						
			9JD	61.1						
			9ND	55.7						
			11LA	55.0						
-100			11IB	68.4						
			9KA	55.8						
			11KB	54.9						
			9IB	54.6						
			10EID	40.1						
			11KA	38.4						

[a]Example code 11GC: 11 indicates beltline section 1-11, G indicates slice piece G from slice order A through M, and C indicates through-thickness slice position C.
[b]J-R curves (no instability).
[c]Side-grooved specimens.

Table A.2. Test data for two specimen sizes of WF-70 nozzle course weld metal (1 MPa√m = 1.1 ksi√in.)

Test temperature (°C)	Values, K_{Jc} (MPa√m)							
	1/2T				1T			
	Code[a]	K_{Jc}	Code[a]	K_{Jc}	Code[a]	K_{Jc}	Code[a]	K_{Jc}
21					31DB[b] 34FG[b] 31DB[b]	*c* *c* *c*	34IE 31DA 34CB	*c* *c* *c*
0	H34M I34M	*c* 281.8			34IA 34CA 31AC 31FA	144.6 167.3 239.7 220.1	84FA	228.4
-25					31CB 34JE 31KD 34JA	146.8 120.6 113.7 120.9	31ID 31BC 34EB 34AC	97.4 95.9 87.3 84.5
-50	B34M A34M G34M F34M	133.7 125.7 98.1 93.2	J34M E34M D34M	77.9 69.2 58.5[d]	34EA 31CA 34KE	84.5 84.6 63.9	34BC[b] 34LD 31EB[b]	63.8 76.4 54.8
-100					31JE 31IB 31JD	67.9 50.2 49.1	34LC 31JB 31HB	47.1 36.8 35.6

[a]Example code 11GC: 11 indicates beltline section 1-11, G indicates slice piece G from slice order A through M, and C indicates through-thickness slice position C.

[b]Side-grooved specimens.

[c]J-R curves (no instability).

[d]K_{Jc} at crack pop-in.

Appendix B

Regression Constants on J-R Curve Model

and

Experimental J-R Curves

Regression Constants on J-R Curve Model

$$J = A(\Delta a_p)^B \exp[C*(\Delta a_p)^D] ,$$

where J is deformation theory, J(kip-in./in.^{2}), and Δa_p is physical crack growth (in.).

The constants in the multivariable model were developed to calculate J-R curves in the English units, presumably for convenience in the application of the J-R curves to work engineering problems. To avoid the labor of rederiving the various constants of the multivariable model for metric equivalent, English units will be used in these comparisons.

Table B1. J-R experimental fits to data [$J_d = A(\Delta a)^B \exp[C * (\Delta a)^D]$]

Figure	Test conditions					J-R curve-fitting parameters			
	Weld	J	Side groove (%)	Specimen size (T)	Test temperature (°F)	A	B	C	D
B1	Beltline	Deformation theory	20	1/2	550	2.322	0.343	0.00225	-0.5
B2	Beltline	Deformation theory	20	1	550	2.251	0.0387	-0.134	-0.5
B3	Beltline	Deformation theory	20	2	550	3.067	0.310	0.00787	-0.5
B4	Beltline	Deformation theory	20	4	550	3.624	0.494	0.0379	-0.5
B5	Beltline	Deformation theory	20	1/2	300	2.670	0.254	-0.0207	-0.5
B6	Beltline	Deformation theory	20	1	300	4.352	0.366	-0.0258	-0.5
B7	Beltline	Deformation theory	20	1/2	Rm	7.749	0.576	0.0181	-0.5
B8	Beltline	Deformation theory	20	1	Rm	4.375	0.263	-0.0808	-0.5
B9	Nozzle	Deformation theory	20	1/2	550	2.390	0.409	-0.00192	-0.5
B10	Nozzle	Deformation theory	20	1	550	2.202	0.306	-0.0466	-0.5
B11	Nozzle	Deformation theory	20	1	300	2.896	0.379	-0.0022	-0.5
B12	Nozzle	Deformation theory	20	1	Rm	3.566	0.346	-0.0190	-0.5
B13	Nozzle	Deformation theory	No	1	Rm	11.305	0.671	0.0379	-0.5
B14	Beltline	Modified J	20	1/2	550	3.482	0.464	0.02121	-0.5
B15	Beltline	Modified J	20	1	550	3.168	0.305	-0.0501	-0.5

Table B2. J-R curve constants calculated from multivariable model for Linde 80 welds (using deformation theory, beltline and nozzle, 20% side grooved)

Specimen size (T)	Test temperature (°F)	J-R curve-fitting parameters			
		A	B	C	D
1/2	550	1.744	0.231	−0.022	−0.5
1	550	1.928	0.175	−0.072	−0.5
2	550	2.132	0.119	−0.121	−0.5
4	550	2.357	0.063	−0.170	−0.5
1/2	300	3.743	0.319	−0.029	−0.5
1	300	4.138	0.263	−0.079	−0.5
2	300	4.576	0.208	−0.128	−0.5
4	300	5.060	0.152	−0.177	−0.5
1/2	Rm	7.648	0.402	−0.036	−0.5
1	Rm	8.456	0.346	−0.086	−0.5
2	Rm	9.350	0.290	−0.135	−0.5
4	Rm	10.340	0.235	−0.184	−0.5

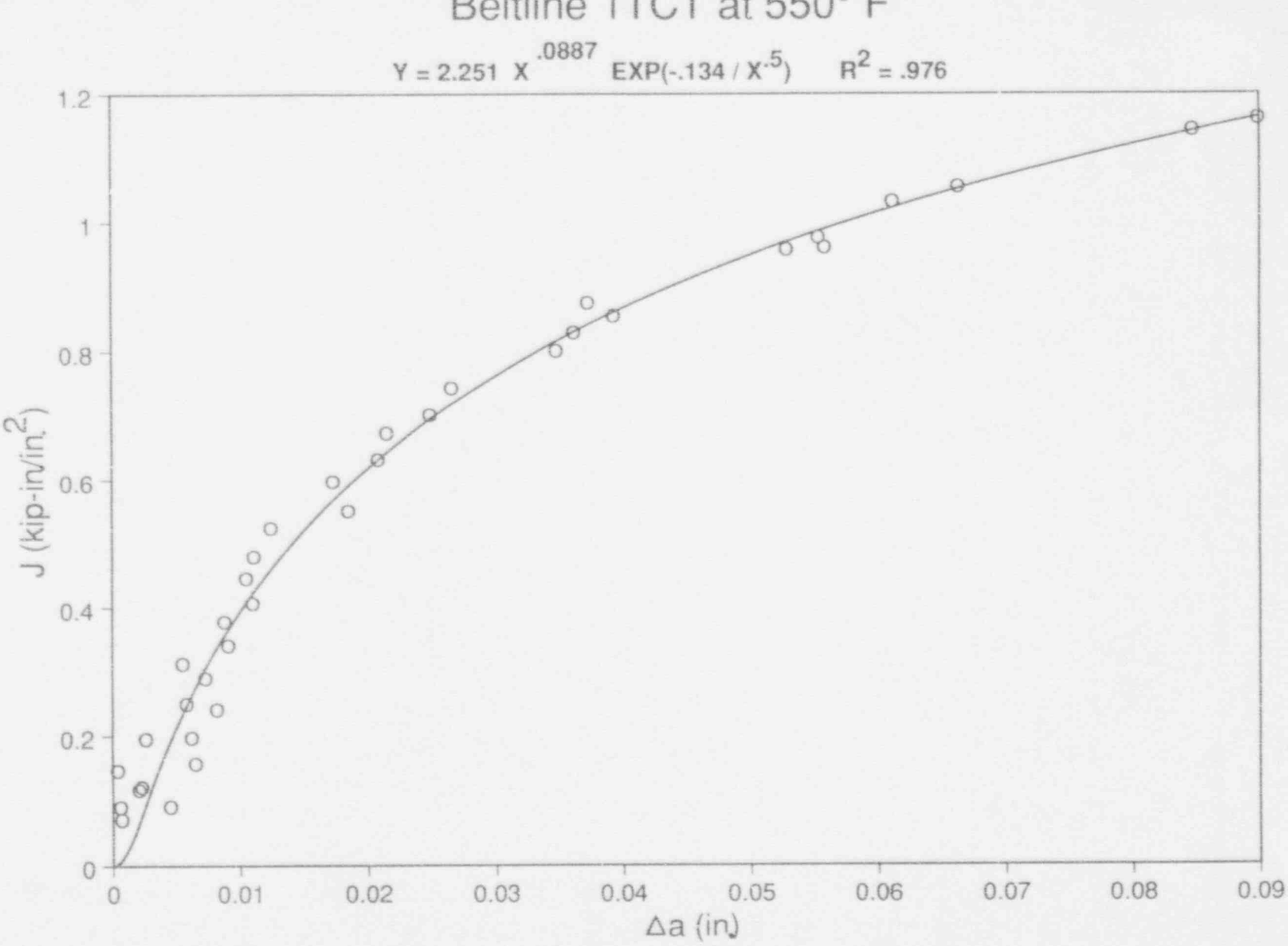
Beltline 1TCT at 550° F
Y = 2.251 X^.0887 EXP(-.134 / X^.5) R^2 = .976
J (kip-in/in^2)
Δa (in)
0
0.2
0.4
0.6
0.8
1
1.2
0.01
0.02
0.03
0.04
0.05
0.06
0.07
0.08
0.09

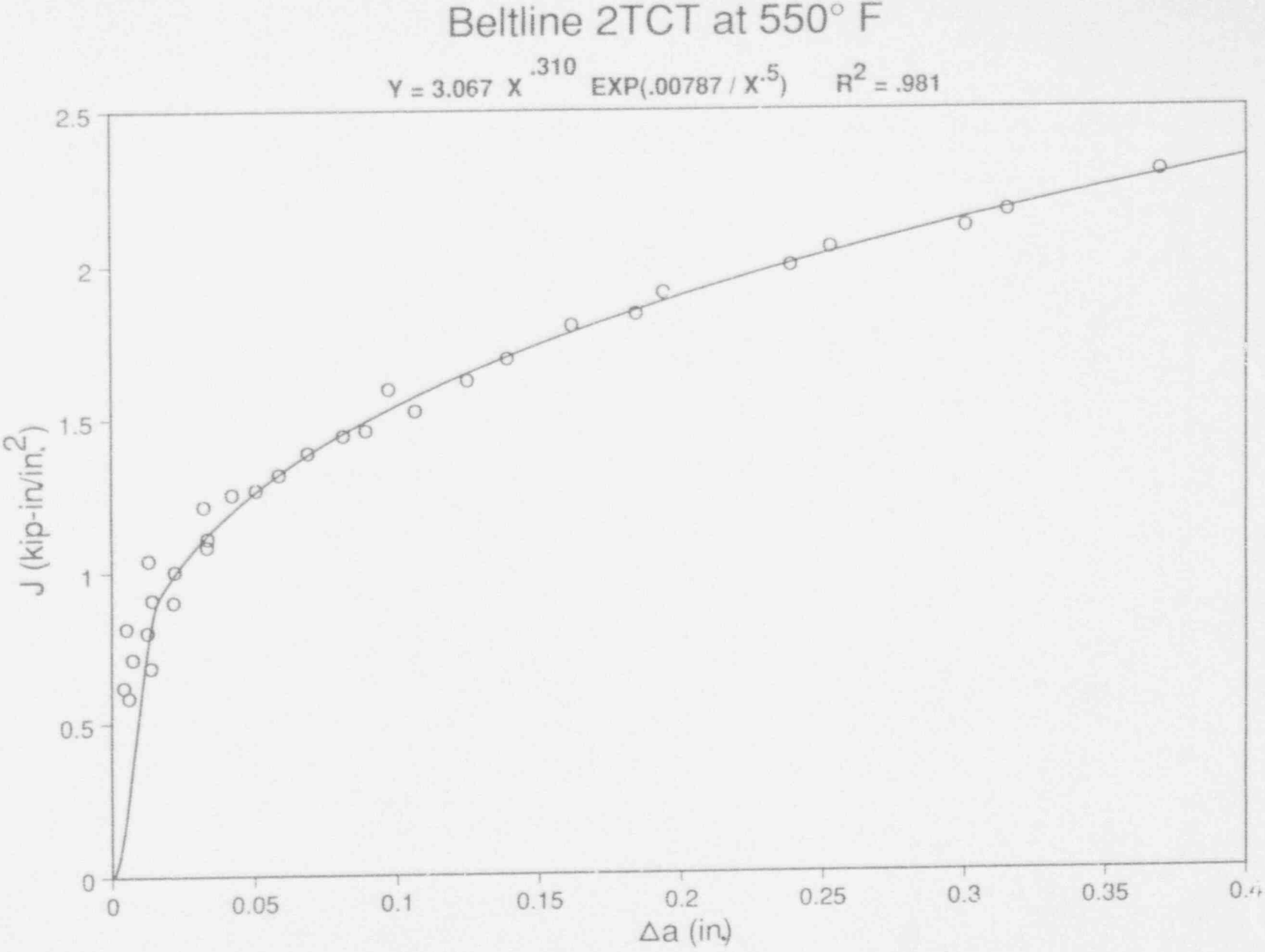
Beltline 2TCT at 550° F
Y = 3.067 X^.310 EXP(.00787 / X^.5) R^2 = .981
J (kip-in/in.^2)
Δa (in.)
0
0.5
1
1.5
2
2.5
0.05
0.1
0.15
0.2
0.25
0.3
0.35

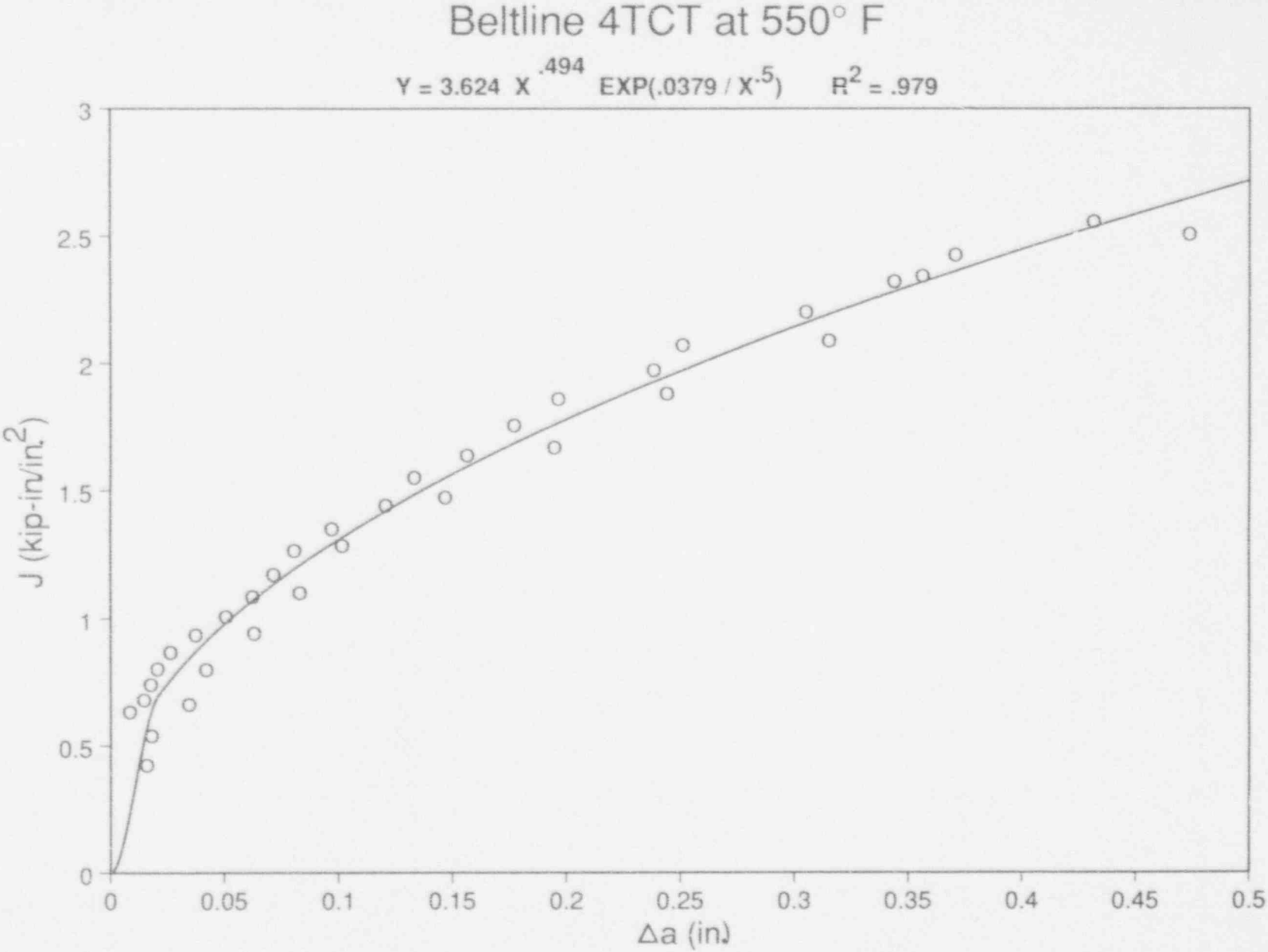
Beltline 4TCT at 550° F
Y = 3.624 X^.494 EXP(.0379 / X^-.5) R^2 = .979
J (kip-in/in^2)
Δa (in.)
0
0.5
1
1.5
2
2.5
3
0.05
0.1
0.15
0.2
0.25
0.3
0.35
0.4
0.45
0.5

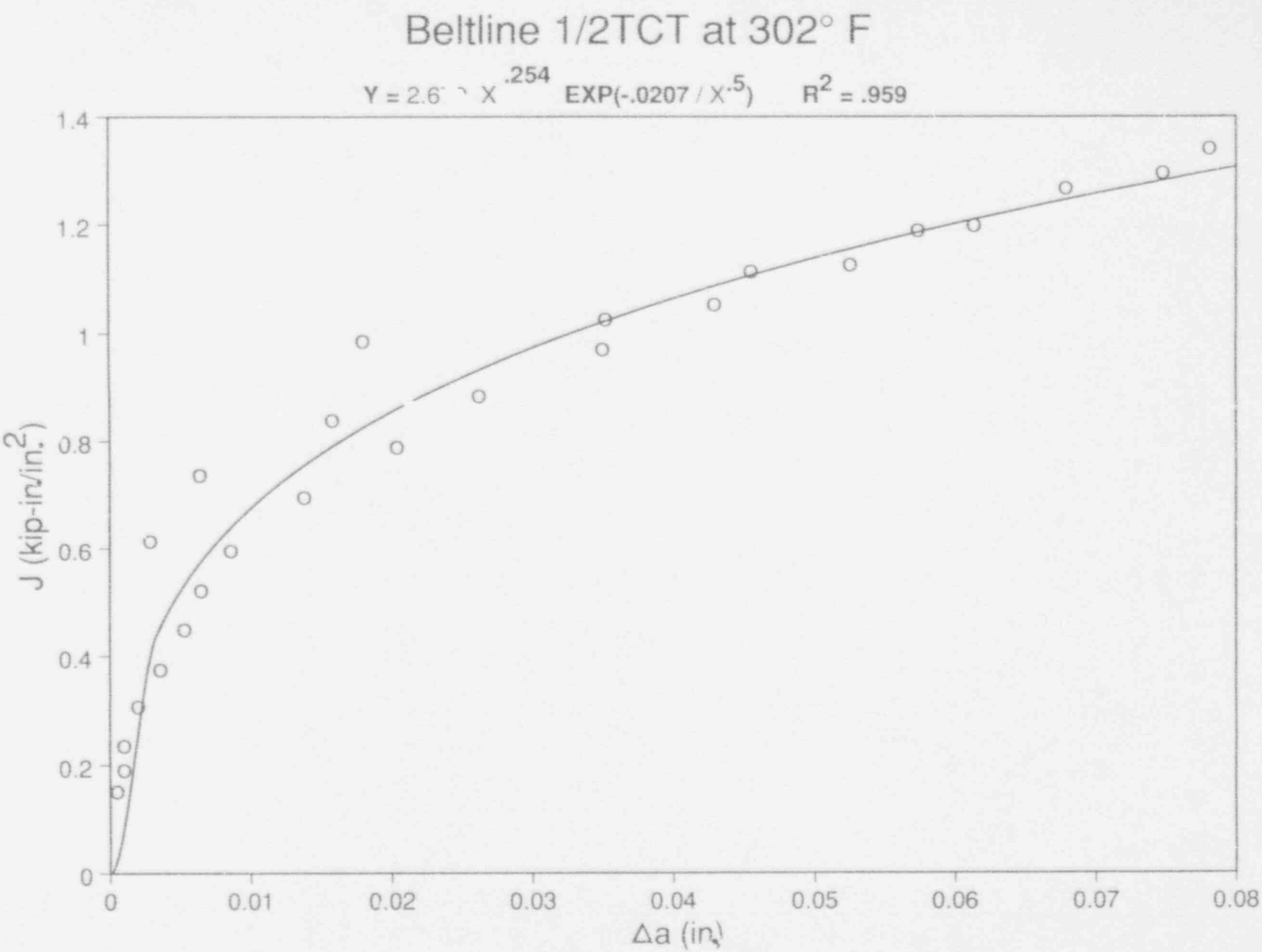
Beltline 1/2TCT at 302° F
Y = 2.6 X^.254 EXP(-.0207 / X^.5) R^2 = .959
J (kip-in/in.^2)
Δa (in)
0
0.2
0.4
0.6
0.8
1
1.2
1.4
0.01
0.02
0.03
0.04
0.05
0.06
0.07
0.08

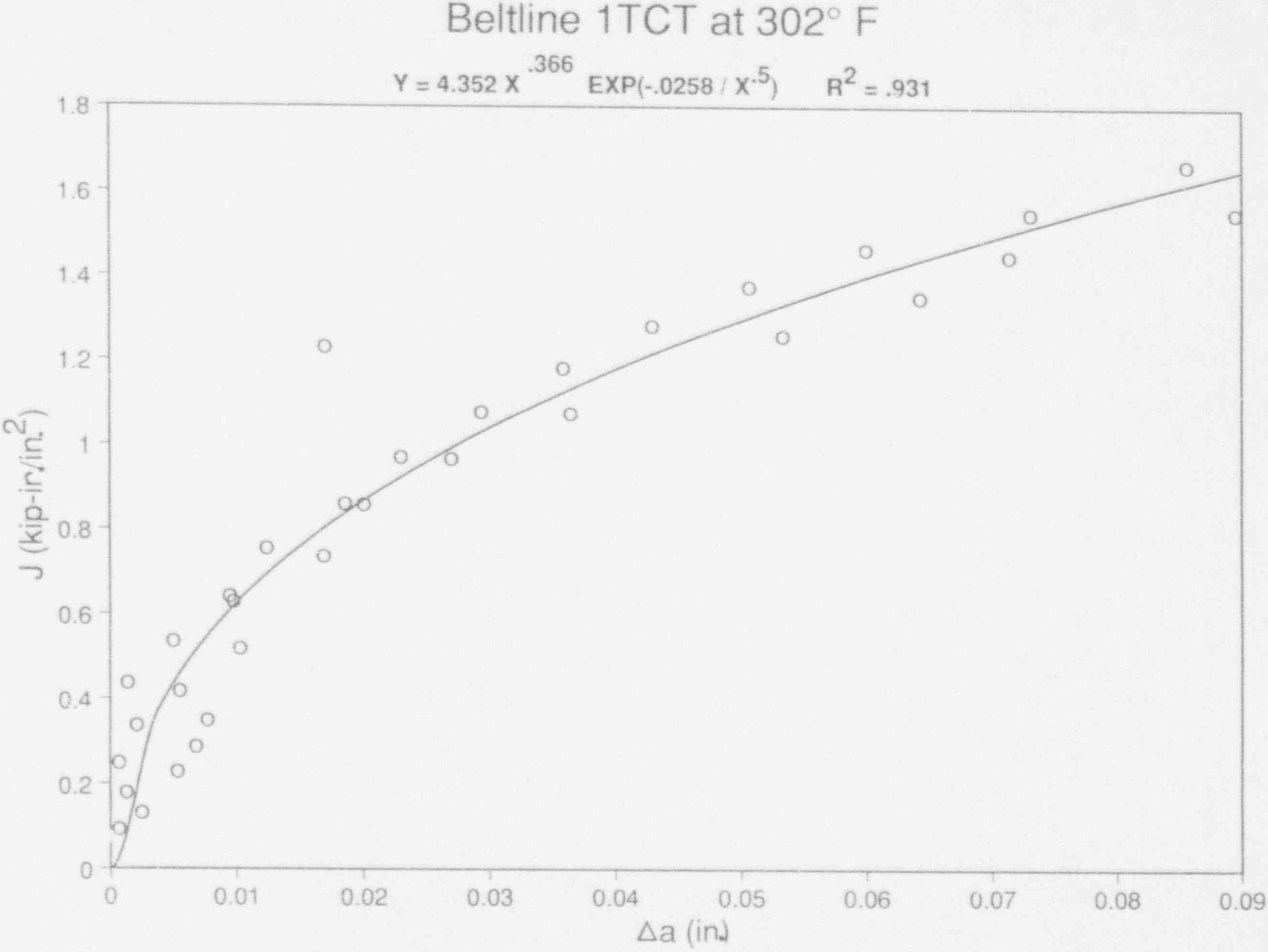
Beltline 1TCT at 302° F
Y = 4.352 X^.366 EXP(-.0258 / X^.5) R^2 = .931
J (kip-in/in^2)
Δa (in)
0
0.2
0.4
0.6
0.8
1
1.2
1.4
1.6
1.8
0.01
0.02
0.03
0.04
0.05
0.06
0.07
0.08
0.09

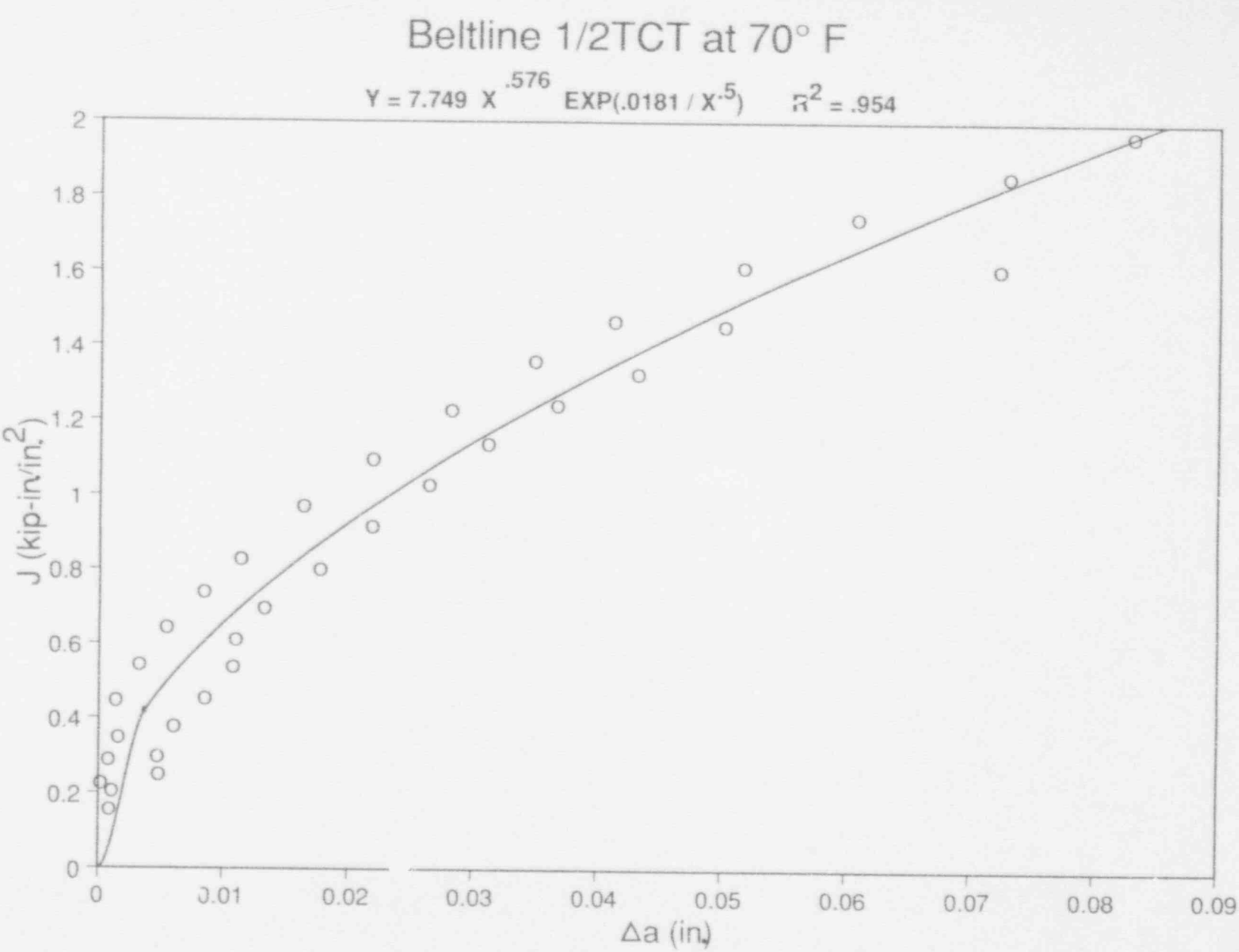
Beltline 1/2TCT at 70° F
Y = 7.749 X^.576 EXP(.0181 / X^-5) R^2 = .954
J (kip-in/in^2)
Δa (in)
0
0.2
0.4
0.6
0.8
1
1.2
1.4
1.6
1.8
2
0.01
0.02
0.03
0.04
0.05
0.06
0.07
0.08
0.09

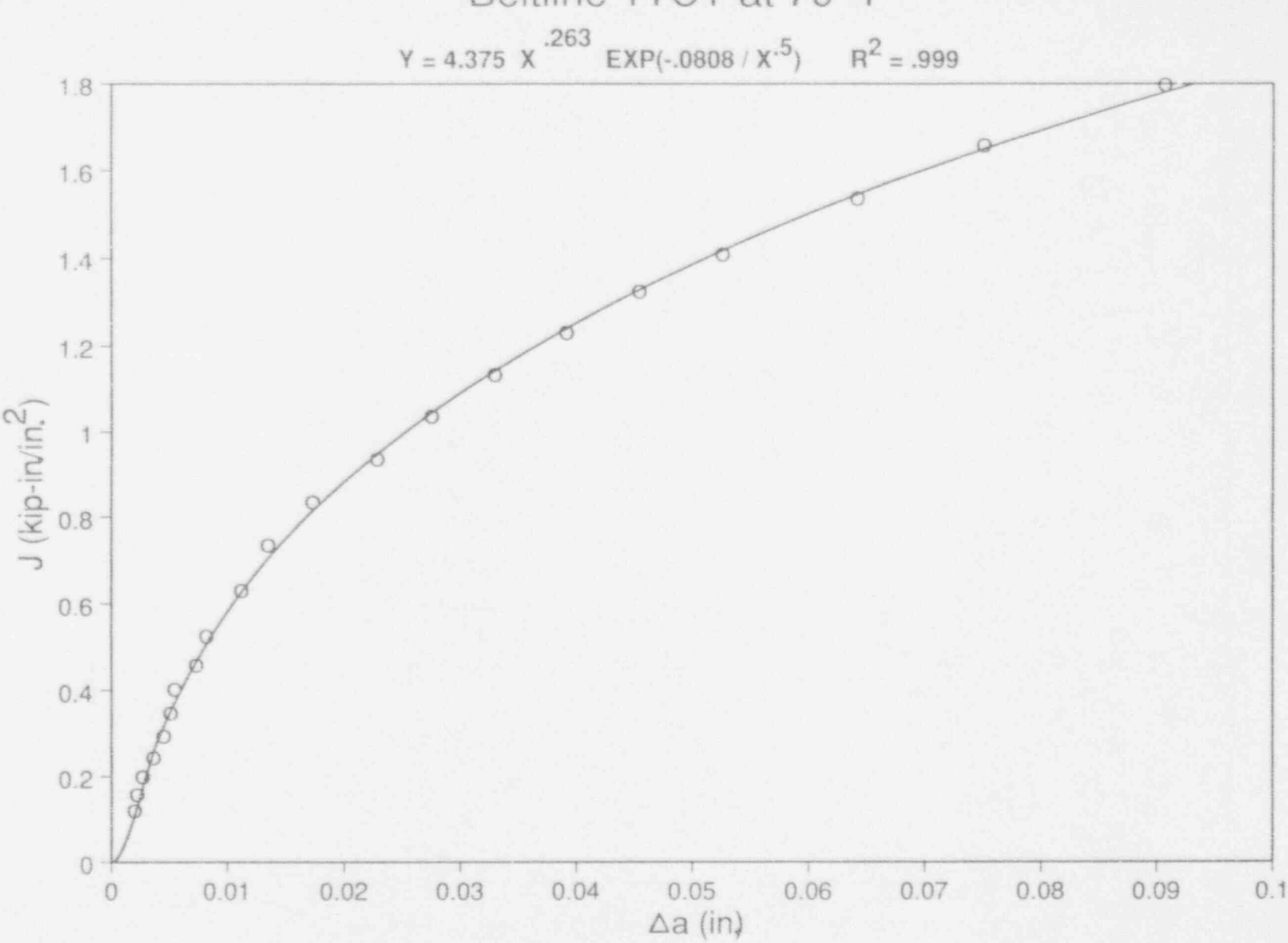
Beltline 1TCT at 70° F
Y = 4.375 X^.263 EXP(-.0808 / X^.5) R^2 = .999
J (kip-in/in.^2)
Δa (in)
0
0.2
0.4
0.6
0.8
1
1.2
1.4
1.6
1.8
0.01
0.02
0.03
0.04
0.05
0.06
0.07
0.08
0.09
0.1

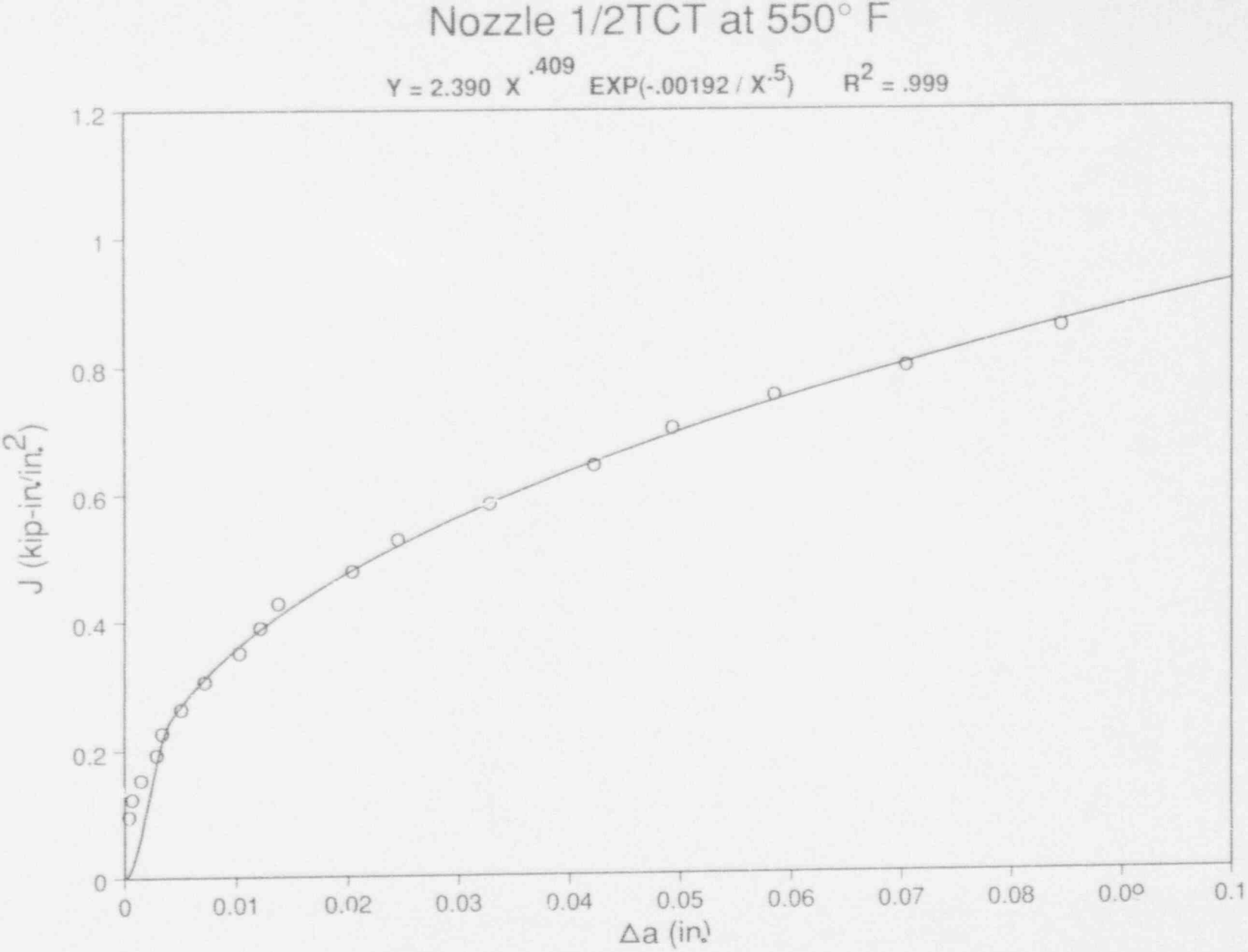
Nozzle 1/2TCT at 550° F
Y = 2.390 X^.409 EXP(-.00192 / X^.5) R^2 = .999
J (kip-in/in^2)
Δa (in)
0
0.2
0.4
0.6
0.8
1
1.2
0.01
0.02
0.03
0.04
0.05
0.06
0.07
0.08
0.0°
0.1

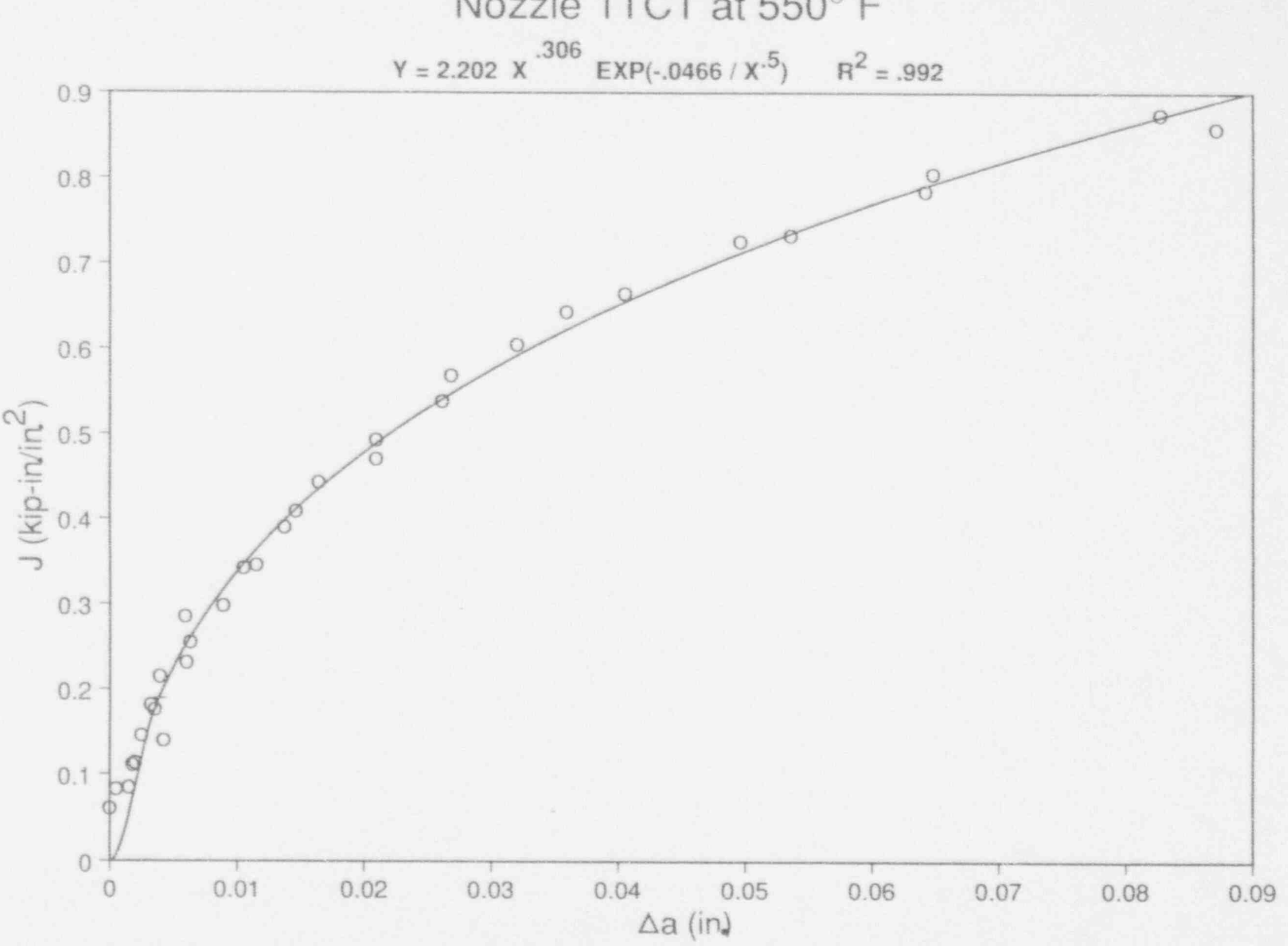
Nozzle 1TCT at 550° F
Y = 2.202 X^.306 EXP(-.0466 / X^.5) R^2 = .992
J (kip-in/in^2)
Δa (in)
0
0.1
0.2
0.3
0.4
0.5
0.6
0.7
0.8
0.9
0.01
0.02
0.03
0.04
0.05
0.06
0.07
0.08
0.09

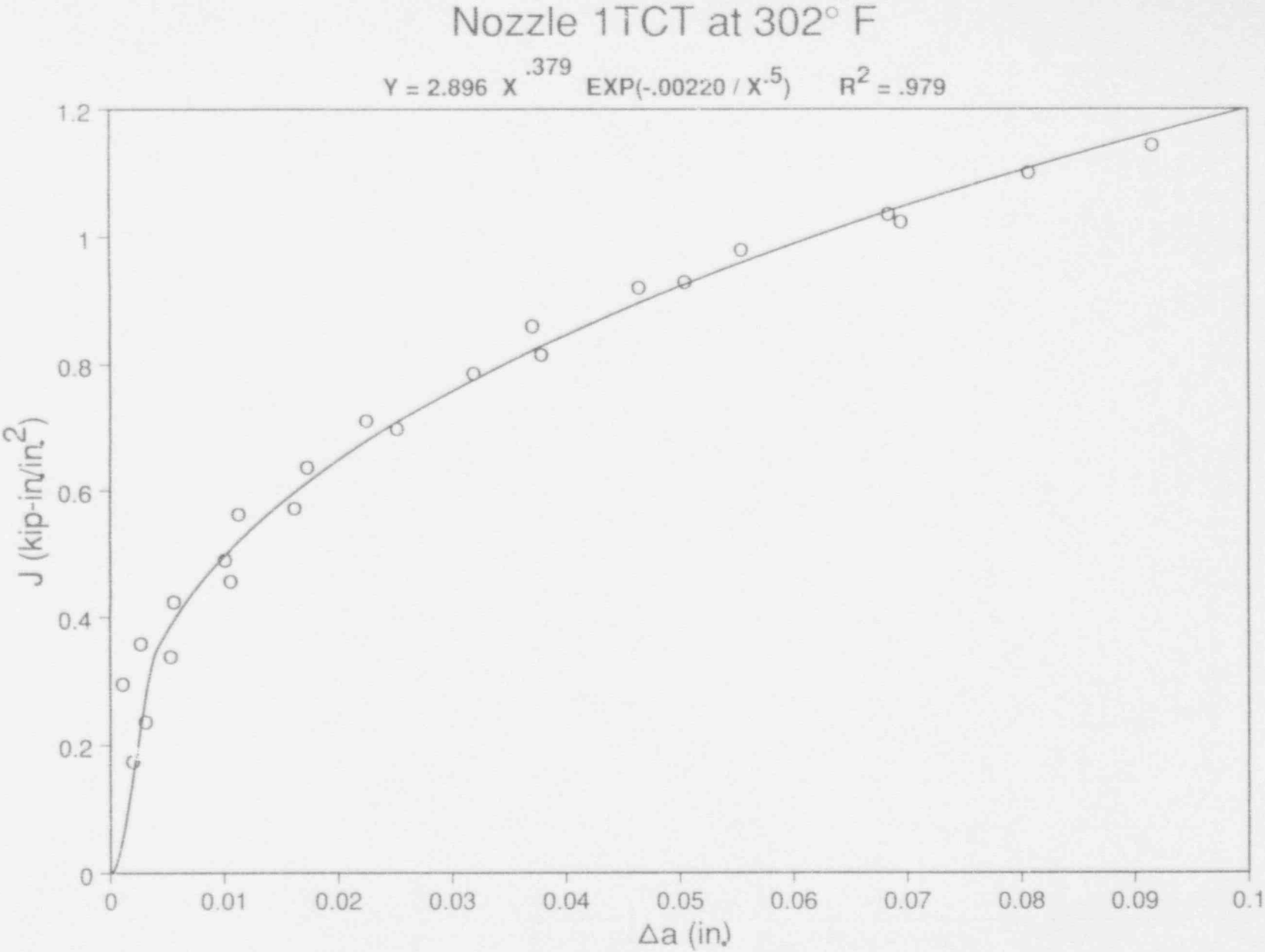
Nozzle 1TCT at 302° F
Y = 2.896 X^.379 EXP(-.00220 / X^.5) R^2 = .979
J (kip-in/in^2)
Δa (in.)
0
0.2
0.4
0.6
0.8
1
1.2
0.01
0.02
0.03
0.04
0.05
0.06
0.07
0.08
0.09
0.1

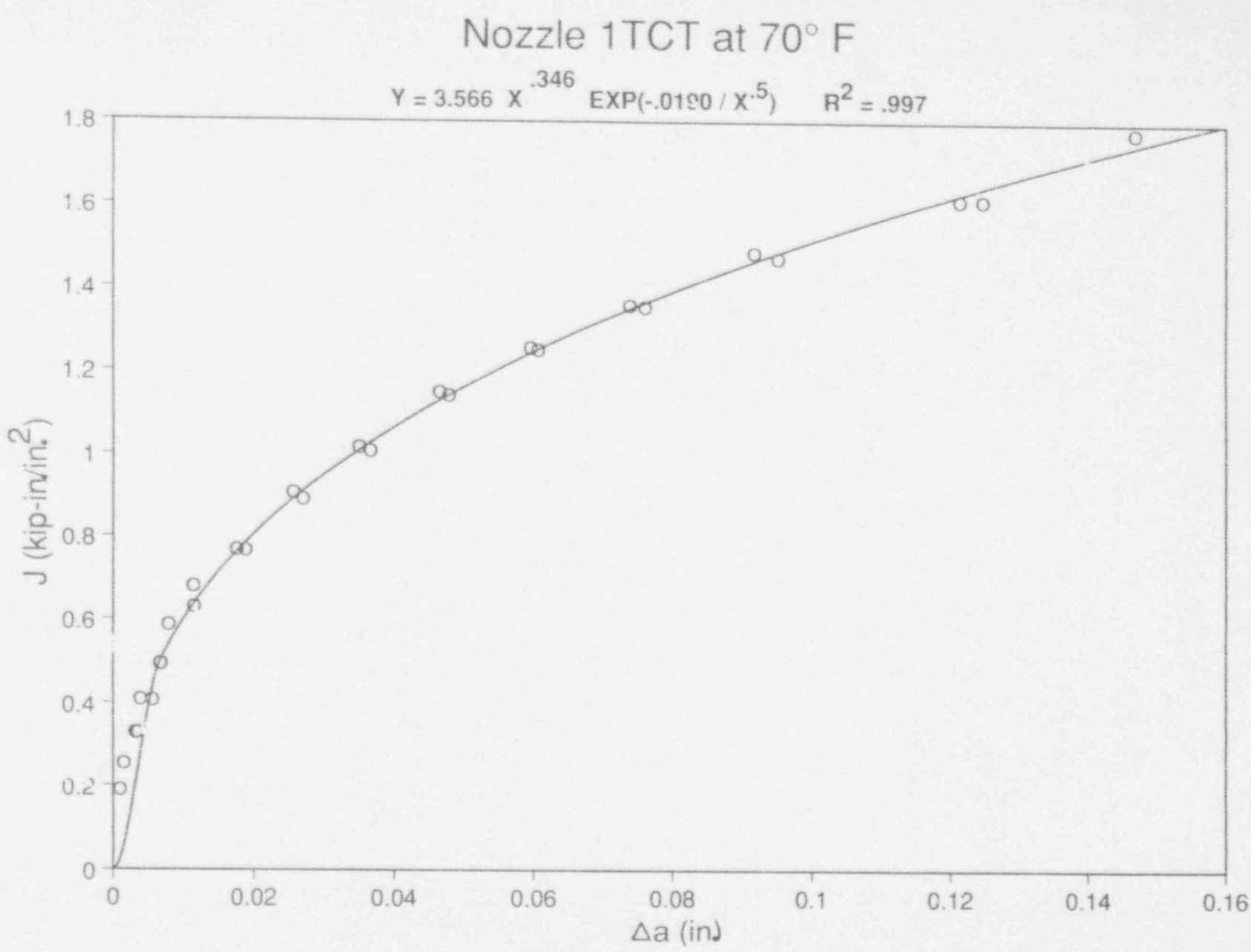
Nozzle 1TCT at 70° F
Y = 3.566 X^.346 EXP(-.0190 / X^.5) R^2 = .997
J (kip-in/in^2)
Δa (in)
0
0.2
0.4
0.6
0.8
1
1.2
1.4
1.6
1.8
0
0.02
0.04
0.06
0.08
0.1
0.12
0.14
0.16

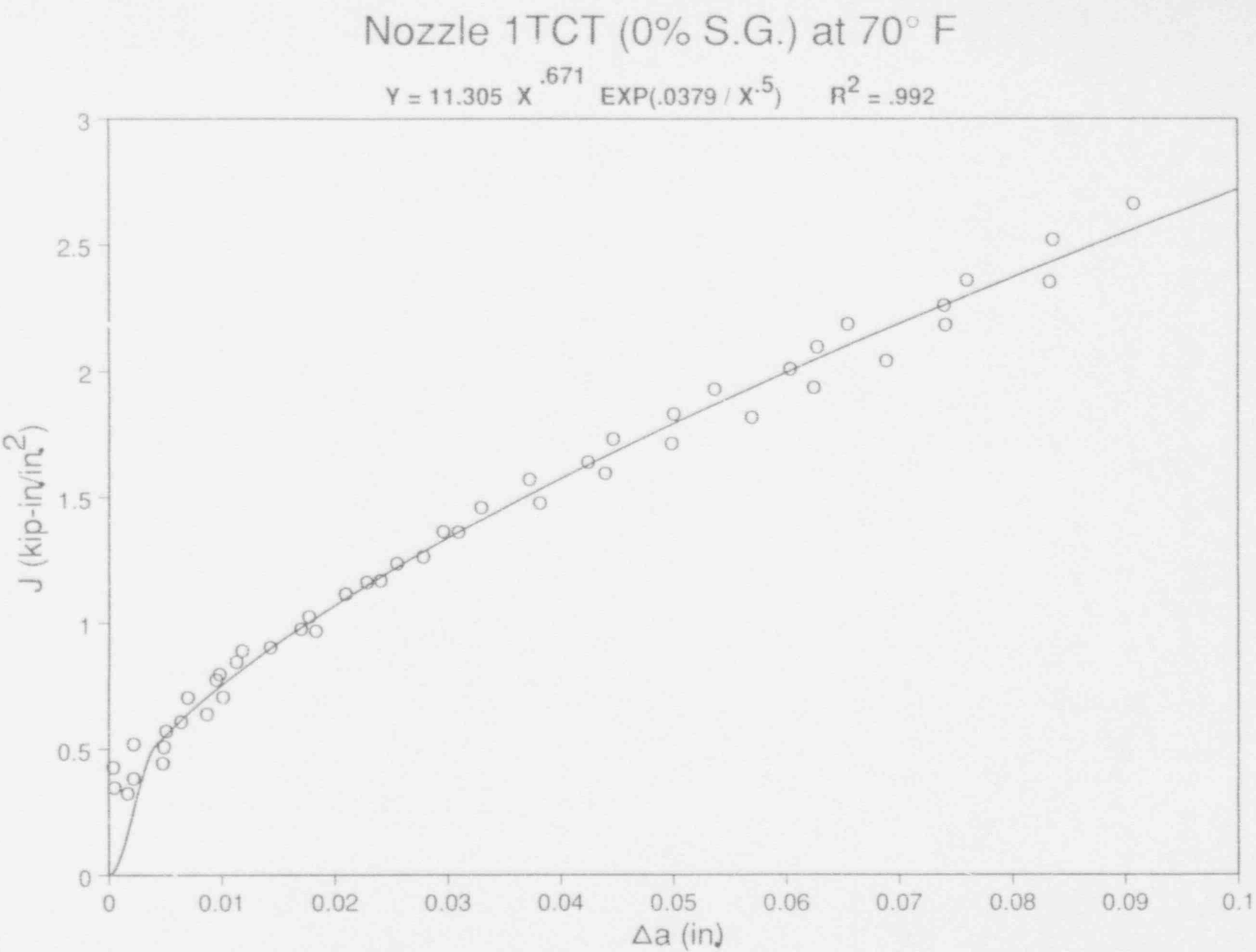
Nozzle 1TCT (0% S.G.) at 70° F
Y = 11.305 X^.671 EXP(.0379 / X^.5) R^2 = .992
J (kip-in/in^2)
Δa (in)
0
0.5
1
1.5
2
2.5
3
0.01
0.02
0.03
0.04
0.05
0.06
0.07
0.08
0.09
0.1

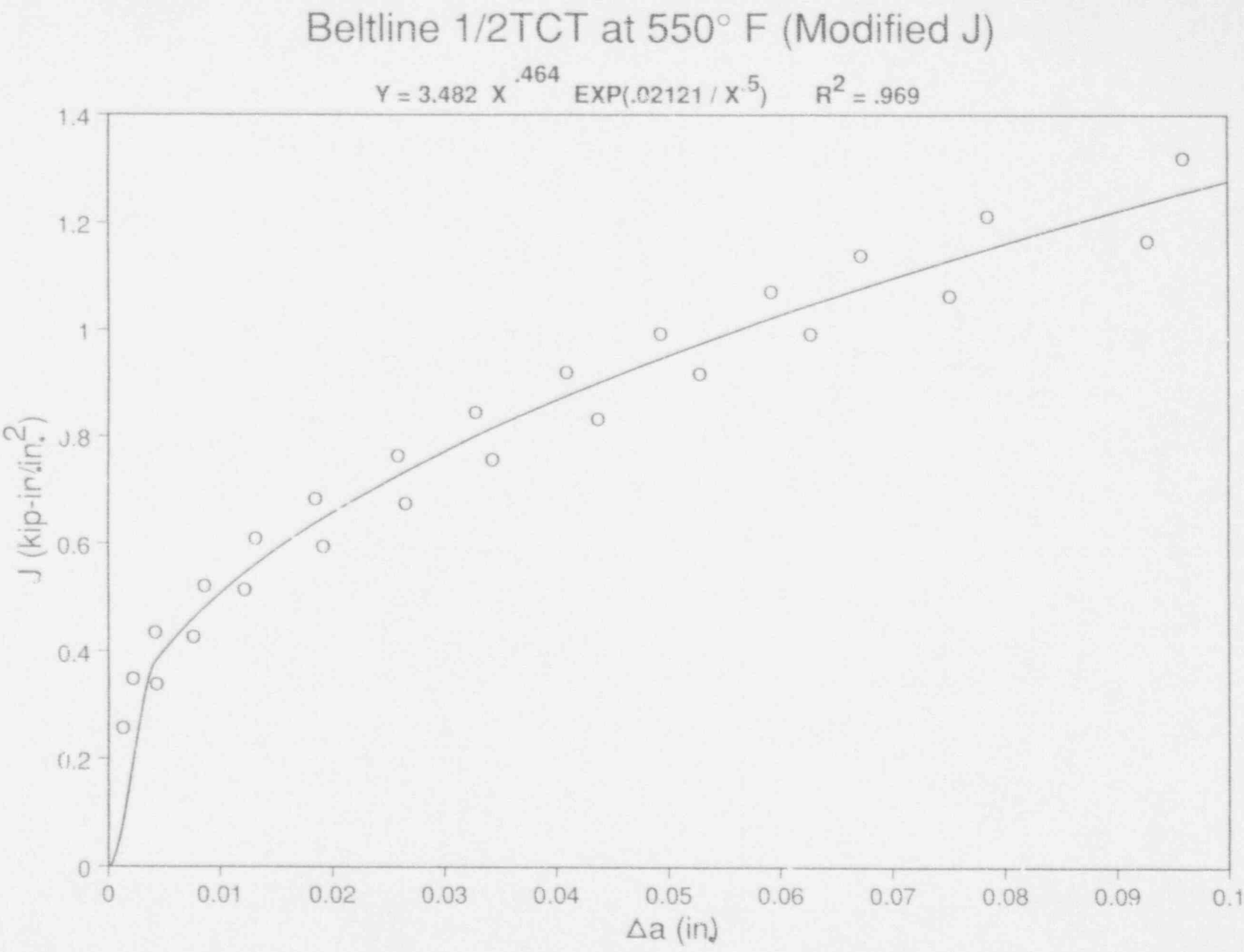
Beltline 1/2TCT at 550° F (Modified J)
Y = 3.482 X^.464 EXP(.02121 / X^.5) R^2 = .969
J (kip-in/in^2)
Δa (in)
0
0.2
0.4
0.6
0.8
1
1.2
1.4
0
0.01
0.02
0.03
0.04
0.05
0.06
0.07
0.08
0.09
0.1

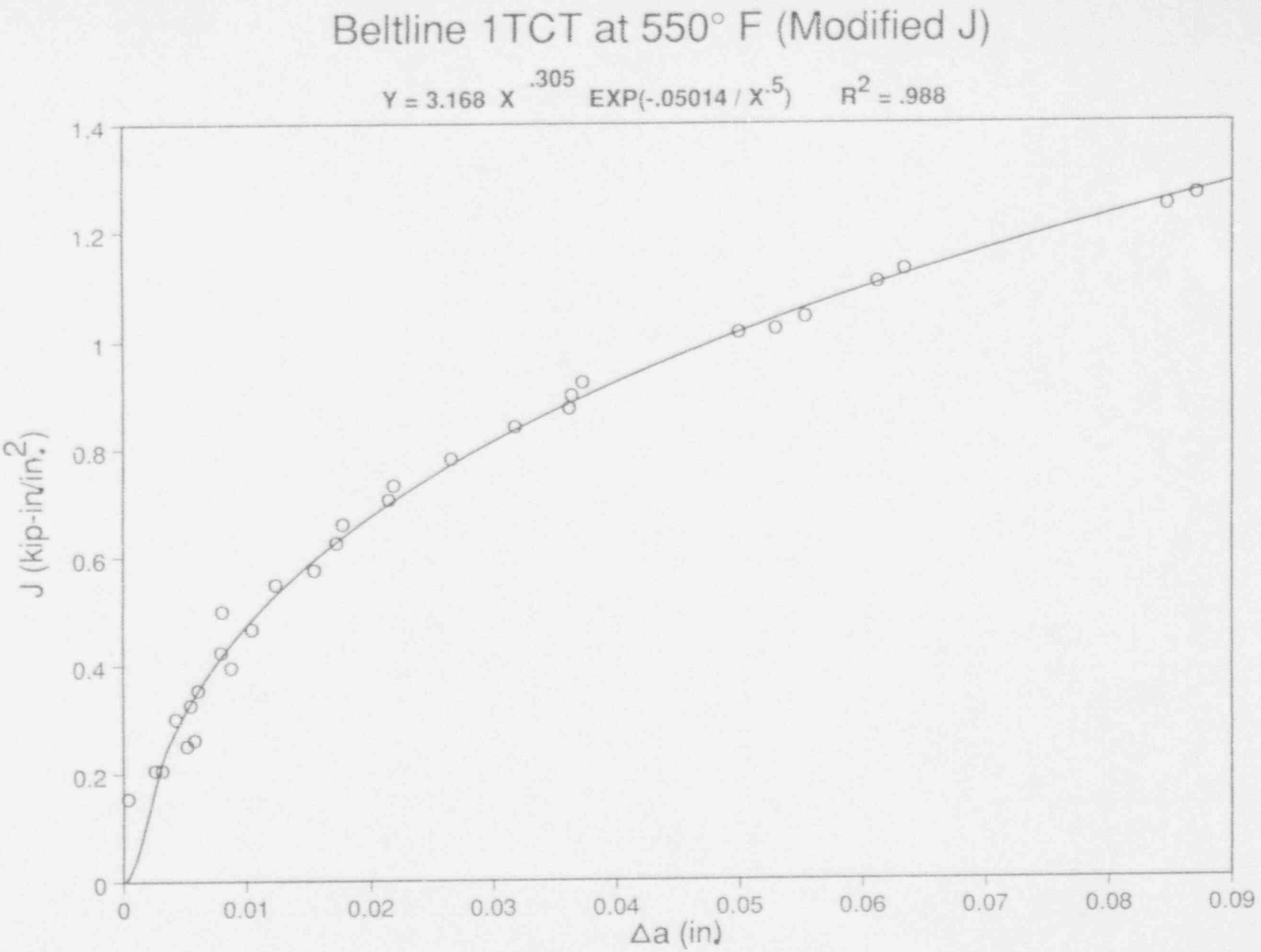
Beltline 1TCT at 550° F (Modified J)
Y = 3.168 X .305 EXP(-.05014 / X.5) R2 = .988
J (kip-in/in2)
Δa (in)
0
0.2
0.4
0.6
0.8
1
1.2
1.4
0.01
0.02
0.03
0.04
0.05
0.06
0.07
0.08
0.09

INTERNAL DISTRIBUTION

1. D. J. Alexander
2. B. R. Bass
3. J. Bryson
4. R. D. Cheverton
5-9. W. R. Corwin
10. D. F. Craig
11. T. L. Dickson
12. F. M. Haggag
13-15. S. K. Iskander
16. F. B. Kam
17. J. A. Keeney
18. W. McAfee
19-24. D. E. McCabe
25. J. G. Merkle
26-30. R. K. Nanstad
31. W. E. Pennell
32. C. E. Pugh
33. I. I. Siman Tov
34. R. E. Stoller
35-39. R. L. Swain
40. K. R. Thoms
41. J. A. Wang
42. ORNL Patent Section
43. Central Research Library
44. Document Reference Section
45-46. Laboratory Records Department
47. Laboratory Records (RC)
48-50. M&C Records Office

EXTERNAL DISTRIBUTION

51-52. ABB-Combustion Engineering, Department 487-4, Windsor, CT 60695

D. J. Ayres
S. T. Byrne

53-54. AEA-Technology-Harwell, Thermal Reactor Services, Oxfordshire OX11 ORA, United Kingdom

G. Gage
R. McElroy

55. ATI, Suite 160, 2010 Crow Canyon Place, San Ramon, CA 94583

W. L. Server

56. BABCOCK AND WILCOX, Research and Development Division, 1562 Beeson Street, Alliance, OH 44601

W. A. Van Der Sluys

57. BABCOCK AND WILCOX, 3315 Old Forest Road, Lynchburg, VA 24501

K. E. Moore

58. BETTIS ATOMIC POWER LABORATORY, Westinghouse Electric Corp., P.O. Box 79, West Mifflin, PA 15122

L. A. James

59. ELECTRIC POWER RESEARCH INSTITUTE, P.O. Box 10412, Palo Alto, CA 94303

R. Carter

60-61. Electricite de France, Les Renardieres Research Center, B.P. No. 1, F-77250 Moret-Sur-Long, France

M. Bethmont

62-63. ENERGIA NUCLEARE DELLA ENERGIA ALTENATIVE (ENEA-DISP), Via Brancati, 00144 Roma, Italy

P. M. Pietro
A. Pini

64. Framatome, Tour Fiat Cedex 16, 92084 Paris la Defense, France

B. Houssin

65. FRAUENHOFER-INSTITUT FUER WERKSTOFFMECHANIK, Woehlerstr. 11, D 7800 Freiburg, Germany

W. Boehme

66. Grove Engineering Inc., Suite 218, 9040 Executive Park Drive, Knoxville, TN 37923

W. A. Pavinich

67. HANFORD ENGINEERING DEVELOPMENT LABORATORY, P.O. Box 1970, Richland, WA 99352

M. L. Hamilton

68. IMATRON VOIMA, Mechanical Department, P.O. Box 138, SS 00101, Helsinki 10, Finland

R. Ahlstrand

69. IMPERIAL COLLEGE, Mechanical Engineering Department, Exhibition Road, London, SW7 2AZ England

H. J. Macgillivray

70. MITSUBISHI HEAVY INDUSTRIES, LTD., Takasago Research and development Center, 2-1-1 Shinhama, ARAI-CHO, Takasago, 676 Japan

Y. Urabe

71. NATIONAL INSTITUTE OF STANDARDS, Department of Commerce, Office of NonDestructive Evaluation, Gaithersburg, MD 20899

J. Gudas, Deputy Chief

72-75. NRC, RES/MEB, MS-T10-E10, Washington, DC 20555

A. Hiser
S. N. Malik
M. E. Mayfield
L. C. Shao

76-77. SOUTHWEST RESEARCH INSTITUTE, P.O. Drawer 28510, 6220 Culeebra Rd., San Antonio, TX 78284

S. J. Hudak
M. F. Kanninen

78-79. STAATL. MATERIALPRUFUNGSANSTALT, Pfaffenwalding 32, 7000 Stuttgart 80, Federal Republic of Germany

J. Fohl
R. Gillot

80. L. E. Steele, 7624 Highland St., Springfield, VA 22150-3931

81-82. TEXAS A&M UNIVERSITY, Department of Mechanical Engineering, College Station, TX 77843-3123

T. Anderson
R. Chona

83. TOYOHASHI UNIVERSITY OF TECHNOLOGY, 1-1 Tempaku-Cho, Toyohashi, Japan 441

H. Homma

84. TVFA TU VIENNA, Karlsplatz 13, 1040 Vienna, Austria

T. Varga

85-86. UNIVERSITY OF CALIFORNIA, Department of Chemical and Nuclear Engineering, Ward Memorial Drive, Santa Barbara, CA 93106

G. E. Lucas
G. R. Odette

87-88. UNIVERSITY OF MARYLAND, Mechanical Engineering Department, College Park, MD 20742

W. L. Fourney
G. R. Irwin

89. UNIVERSITY OF TENNESSEE, Engineering Science and Mechanics, 310 Perkins Hall, Knoxville, TN 37996-2030

J. D. Landes

90. VTT, Technical Research Centre of Finland, Kemistintie 3, Box 2G, Espoo 02750, Finland

K. Wallin

91. WASHINGTON STATE UNIVERSITY, Mechanical and Materials Engineering Department, Pullman, WA 99164

R. G. Hogland

92. E. T. Wessel, Lake Region Mobile Home Village, 312 Wolverine Lane, Haines City, FL 33844

93-94. WESTINGHOUSE ELECTRIC CORP., P.O. Box 355, Pittsburgh, PA 15230

W. Bamford
T. Mager

95. WESTINGHOUSE R & D CENTER, 1310 Beulah Rd., Pittsburgh, PA 15325

R. G. Lott

96. Sumio Yukawa, 4925 Valkyrie Drive, Boulder, CO 80301

97. DOE, OAK RIDGE OPERATIONS OFFICE, Oak Ridge, TN 37831-6269

Office of Deputy Assistant Manager for Energy Research and Development

98-99. DOE, OFFICE OF SCIENTIFIC AND TECHNICAL INFORMATION, P.O. Box 62, Oak Ridge, TN 37831

100-218. Given distribution as shown in category RF (NTIS-10)

NRC FORM 335 (2-89) NRCM 1102, 3201, 3202

U.S. NUCLEAR REGULATORY COMMISSION

BIBLIOGRAPHIC DATA SHEET

(See instructions on the reverse)

1. REPORT NUMBER (Assigned by NRC, Add Vol., Supp., Rev., and Addendum Numbers, if any.)

NUREG/CR-6249
ORNL/TM-12777

2. TITLE AND SUBTITLE

Unirradiated Material Properties of Midland Weld WF-70

3. DATE REPORT PUBLISHED

MONTH: October YEAR: 1994

4. FIN OR GRANT NUMBER

L1098

5. AUTHOR(S)

D. E. McCabe, R. K. Nanstad, S. K. Iskander, R. L. Swain

6. TYPE OF REPORT

Technical

7. PERIOD COVERED *(Inclusive Dates)*

8. PERFORMING ORGANIZATION – NAME AND ADDRESS *(If NRC, provide Division, Office or Region, U.S. Nuclear Regulatory Commission, and mailing address; if contractor, provide name and mailing address.)*

Oak Ridge National Laboratory
Oak Ridge, TN 37831-6151

9. SPONSORING ORGANIZATION – NAME AND ADDRESS *(If NRC, type "Same as above"; if contractor, provide NRC Division, Office or Region, U.S. Nuclear Regulatory Commission, and mailing address.)*

Division of Engineering
Office of Nuclear Regulatory Research
U. S. Nuclear Regulatory Commission
Washington, D.C. 20555-0001

10. SUPPLEMENTARY NOTES

11. ABSTRACT *(200 words or less)*

Weld metal, designated WF-70, taken from the nozzle course and beltline welds of the Midland Reactor, Unit 1, has been given a preliminary evaluation using the conventional Charpy V-notch (CVN), drop-weight (DWT), and chemical analyses. There was a significant difference in copper content, nominally 0.25% versus 0.40%. Because the objective of this study was to evaluate the before-and-after irradiation properties, these are regarded as different materials. This report summarizes material characterization results and presents the results of fracture mechanics tests on the unirradiated material to establish baseline transition temperature and J-R curves. Tensile properties were also determined. Reference nil-ductility temperatures, RT_{NDT}, determined from CVN transition curves (RT_{NDT} method specific to low upper-shelf energy materials) varied from −20 to +37°C (−4 to 99°F) at various locations in the beltline weld. Reference temperatures using a fracture mechanics-based transition temperature model were −60°C (−76°F) for the beltline weld and −33°C (−27°F) for the nozzle weld. Tensile tests indicated the nozzle weld had higher strength than the beltline weld. J-R curves were developed at 21, 50, and 288°C (70, 32, and 550°F). The predicted J-R curves matched the experimental J-R curves reasonably well. Crack-arrest tests were conducted, but the specimens failed to develop American Society for Testing and Materials valid data in all but one test. More experimentation and test method development are recommended. Five experimental objectives to be accomplished from the testing of irradiated material were identified.

12. KEY WORDS/DESCRIPTORS *(List words or phrases that will assist researchers in locating the report.)*

Charpy V-notch, Fracture toughness, tensile, copper content, nil-ductility transition, upper-shelf energy, crack arrest, reactor pressure vessel, weld, drop-weight, reference temperature

13. AVAILABILITY STATEMENT

Unlimited

14. SECURITY CLASSIFICATION

(This Page) Unclassified

(This Report) Unclassified

15. NUMBER OF PAGES

16. PRICE

Federal Recycling Program